(2)

EXPENDABLE AIR VEHICLES / HIGH ALTITUDE BALLOON TECHNOLOGY

28 February 1989

CHR/89-1909

Sponsored By:

Defense Advanced Research Projects Agency (DoD)
Defense Small Business Innovation Research Program
ARPA Order No. 5916, Amendment 9

Issued by U.S. Army Missile Command
Under Contract Number:

DAAH01-88-C-0581

Prepared By:

Coleman Research Corporation
Robert L. Hawkins, Principal Investigator
401 Wynn Drive
Huntsville, AL 35805-1962
(205) 837-6000

Contract Effective: **14 July 1988**
Contract Expires: **28 February 1989**

APPROVED FOR PUBLIC RELEASE; DISTRIBUTION UNLIMITED.

Coleman Research Corporation

HIGH TECHNOLOGY AEROSPACE SYSTEMS DESIGN

ORLANDO HUNTSVILLE WASHINGTON, D.C. EL PASO

COLEMAN RESEARCH CORPORATION

Headquarters

5950 Lakehurst Drive
Orlando, FL 32819
(407) 352–3700

Advanced Systems Division

401 Wynn Drive, NW
Huntsville, AL 35805
(205) 837–6000

Production Systems Division

401 Wynn Drive, NW
Huntsville, AL 35805
(205) 837–6000

Washington Division

8330 Boone Boulevard, Suite 750
Vienna, VA 22180
(703) 821–8181

Southwest Division

5G Butterfield Trail Boulevard
El Paso, TX 79906
(915) 772–4444

SECURITY CLASSIFICATION OF THIS PAGE

REPORT DOCUMENTATION PAGE

Form Approved
OMB No. 0704-0188

1a. REPORT SECURITY CLASSIFICATION Unclassified	1b. RESTRICTIVE MARKINGS N/A
2a. SECURITY CLASSIFICATION AUTHORITY	3. DISTRIBUTION/AVAILABILITY OF REPORT Approved for public release; distribution unlimited.
2b. DECLASSIFICATION/DOWNGRADING SCHEDULE	
4. PERFORMING ORGANIZATION REPORT NUMBER(S) CHR/89-1909	5. MONITORING ORGANIZATION REPORT NUMBER(S)
6a. NAME OF PERFORMING ORGANIZATION Coleman Research Corporation 6b. OFFICE SYMBOL (If applicable)	7a. NAME OF MONITORING ORGANIZATION U.S. Army Missile Command
6c. ADDRESS (City, State, and ZIP Code) 401 Wynn Drive Huntsville, AL 35805-1962	7b. ADDRESS (City, State, and ZIP Code) Redstone Arsenal, AL 35898-5280
8a. NAME OF FUNDING/SPONSORING ORGANIZATION U.S. Army Missile Command 8b. OFFICE SYMBOL (If applicable) AMSMI-RD-DP-TT	9. PROCUREMENT INSTRUMENT IDENTIFICATION NUMBER
8c. ADDRESS (City, State, and ZIP Code) Redstone Arsenal, AL 35898-5280	10. SOURCE OF FUNDING NUMBERS PROGRAM ELEMENT NO. / PROJECT NO. / TASK NO / WORK UNIT ACCESSION NO.

11. TITLE (Include Security Classification)
Expendable Air Vehicles/High Altitude Balloon Technology (U)

12. PERSONAL AUTHOR(S)
Robert L. Hawkins

13a. TYPE OF REPORT	13b. TIME COVERED	14. DATE OF REPORT (Year, Month, Day)	15. PAGE COUNT
Final Technical Report	FROM 13/7/88 TO 28/2/89	1989 February 28	

16. SUPPLEMENTARY NOTATION

17. COSATI CODES			18. SUBJECT TERMS (Continue on reverse if necessary and identify by block number)
FIELD	GROUP	SUB-GROUP	

19. ABSTRACT (Continue on reverse if necessary and identify by block number)

Coleman Research Corporation demonstrates a capability to produce drift patterns for high-altitude zero-pressure and super-pressure balloons. A simplified balloon dynamics model and a highly detailed, statistical wind model are integrated into a proprietary flight simulation framework to enable the production of balloon drift patterns. The worldwide, time-dependent wind model in conjunction with the data-configurable balloon model allow the production and analysis of drift patterns for balloons launched from any point on the earth's surface at any time of year. Sample drift patterns are produced for a zero-pressure balloon floating at 70,000 feet for 24 hours and for a super-pressure balloon floating at 120,000 feet for one year.

20. DISTRIBUTION/AVAILABILITY OF ABSTRACT ☐ UNCLASSIFIED/UNLIMITED ☐ SAME AS RPT. ☐ DTIC USERS	21. ABSTRACT SECURITY CLASSIFICATION
22a. NAME OF RESPONSIBLE INDIVIDUAL Dr. Ralph Norman	22b. TELEPHONE (Include Area Code) (205) 876-2541 22c. OFFICE SYMBOL AMSMI-RD-DP-TT

DD Form 1473, JUN 86 *Previous editions are obsolete.* SECURITY CLASSIFICATION OF THIS PAGE

EXPENDABLE AIR VEHICLES/HIGH ALTITUDE BALLOON TECHNOLOGY
(BALLOON DRIFT PATTERN SIMULATION)
CHR/89-1909

28 February 1989

In accordance with Contract Number DAAH01-88-C-0581

Prepared for:

U.S. Army Missile Command
ATTN: AMSMI-RD-DP-TT, Dr. Norman
Redstone Arsenal, AL 35898-5244

Prepared by:

Coleman Research Corporation
401 Wynn Drive, N.W.
Huntsville, AL 35805

CERTIFICATION OF TECHNICAL DATA CONFORMITY

The Contractor, Coleman Research Corporation, hereby certifies that, to the best of its knowledge and belief, the technical data delivered herewith under Contract No. DAAH01-88-C-0581 is complete, accurate, and complies with all requirements of the contract.

Date 28 February 1989

Name and Title of Certifying Official:

Name Michael C Bateman

Title Vice President, System Technologies

TABLE OF CONTENTS

1.0 INTRODUCTION

The Defense Advanced Research Projects Agency (DARPA) is interested in exploiting balloon-borne communication and surveillance capabilities for military applications. Balloons offer several unique capabilities when high-altitude balloon technologies are integrated with payloads employing the power-efficient, light-weight electronic technologies available today. In order to establish communication and surveillance systems design requirements and deployment schedules, DARPA must analyze upper-atmosphere drift pattern simulation results for a variety of balloon payload concepts.

Coleman Research Corporation (CRC), in support of DARPA through a Small Business Innovative Research (SBIR) Phase I effort, has demonstrated the technical feasibility of predicting high-altitude balloon drift patterns using a digital computer simulation. CRC realized this ultimate goal by completing each of four contract objectives: performing a literature survey, developing and integrating atmosphere and balloon models into a Balloon Drift Pattern Simulation (BDPS), developing drift pattern output formats, and exercising the BDPS to produce and analyze balloon drift patterns. Drift patterns were produced for two missions which were specified by DARPA. The first mission employs a zero-pressure balloon which floats at an altitude of 70,000 feet over 24 hours. The second mission uses a super-pressure balloon which floats at 120,000 feet for a one-year period.

The schedule which CRC followed during this six-month effort is shown in Figure 1.0-1. This figure shows the sequence of performance of the various tasks. The overlapping schedule of some of the tasks indicates that mutual dependencies of those tasks required that those activities be performed in parallel.

CRC communicated throughout the contract performance period with DARPA personnel and with DARPA-appointed contacts. Through this communication, several technical guidelines were received.

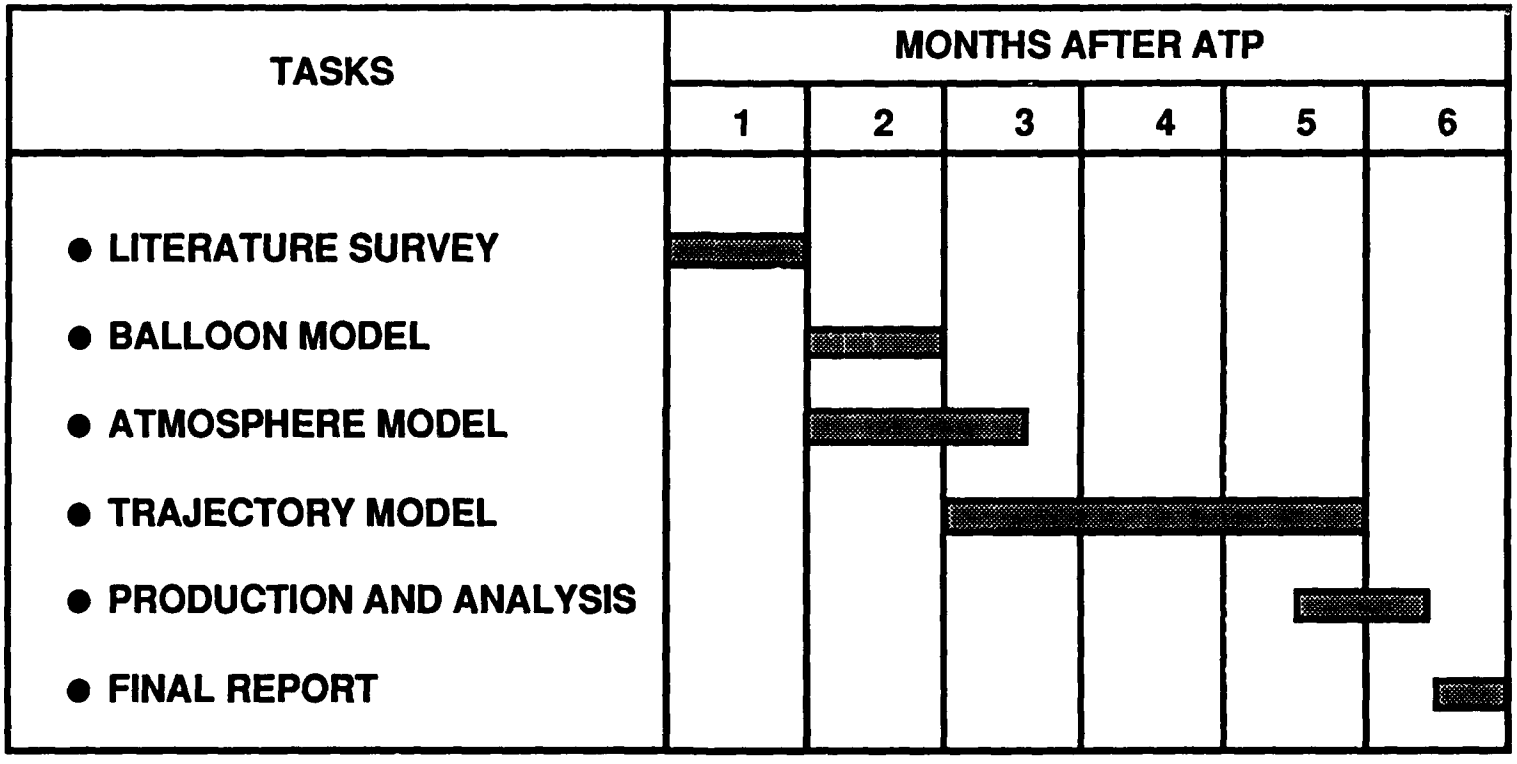

Figure 1.0–1. Task Schedule

The primary sources of information were Lt. Cdr. Larry Epley and Lt. Cdr. Ted Kral, both of the Naval Technology Office of DARPA in Arlington, Virginia, and Les Reading, an employee of Scientific Research Laboratory in Santa Maria, California. Lt. Cdr. Epley described the U.S. Navy's mission for using the balloons and requested that CRC model balloon ascent and descent in addition to the constant-altitude drift modeling originally proposed by CRC. Lt. Cdr. Epley also requested that CRC concentrate on the 24-hour, zero-pressure-balloon mission at the expense of the 1-year, super-pressure-balloon mission. Lt. Cdr. Epley and Les Reading jointly approved output formats. Lt. Cdr. Kral specified six launch sites to be used in the production of 24-hour drift patterns and one launch site for the production of a 1-year drift pattern. Finally, Les Reading provided CRC with some zero-pressure balloon design and performance information.

2.0 TECHNICAL APPROACH

2.1 LITERATURE SURVEY

CRC used several resources in surveying the available literature on balloon and atmospheric modeling. In addition to personnel at DARPA, CRC initiated contacts with engineers at NASA's Balloon Projects Branch at NASA Goddard's Wallops Island Flight Facility, researchers at Texas A & M University, and staff at the National Scientific Balloon Facility (NSBF) in Palestine, Texas. These contacts provided information which guided CRC to specific research reports which had some relevance to BDPS design and construction.

Having identified specific reports for collection, CRC utilized the Redstone Scientific Information Center (RSIC) in Huntsville, Alabama. Many of the pertinent documents were found to be readily available. Other documents were requested either through RSIC or through the previously mentioned contacts. As is common with surveys of this nature, the specific documents which CRC set out to find referenced many other documents, some of which also proved to be useful. In addition to chaining through technical journals, CRC also requested RSIC to perform keyword searches of on-line literature databases.

A number of scientific ballooning reports provided CRC with background information for BDPS design, construction, and operation. The single most useful volume which served this purpose was the Scientific Ballooning Handbook [ref. 1]. This work contains discussions of the history of ballooning, the physics of balloon flight, balloon design, lifting gas selection, and operational considerations.

Kreith [ref. 2] provides a detailed perspective on the thermal design factors which affect a scientific balloon's design and performance. He presents an analysis of the energy balance for the balloon system by looking first at the kinematics of the

balloon system, then at the thermodynamic interaction between the balloon and the atmosphere, and finally at the interaction of the balloon fabric and the lifting gas.

Carlson and Horn developed a balloon model which incorporates the dynamic and thermodynamic aspects of high-altitude balloon flight. Their work is presented in two volumes, the first of which describes their analytical approach [ref 3]. The second document [ref. 4] provides the details of implementation of the model, including FORTRAN source code and sample output from execution of the program. The source code contained in the latter of the two documents proved to be very helpful during the development of BDPS because it provided pertinent modeling examples. It should be noted that the NSBF and NASA's Balloon Projects Branch both report that they currently use this program (with minor modifications) for their in-house simulation purposes.

A particularly informative report by Dwyer [ref. 5] was discovered through one of the on-line searches performed by RSIC. Dwyer categorizes and critiques existing aerodynamic-thermodynamic models for predicting the vertical motion of zero pressure balloons. The report identifies deficiencies of some of the existing modeling approaches and proposes corrections and/or improvements. This report is an excellent, in-depth, technical review of balloon modeling practices. However, the factors discussed in the report far exceed the level of detail required in the present effort to develop a balloon drift pattern simulation.

The flight simulation models and programs surveyed model the vertical motion of scientific balloons yet none were found which also address the lateral motion of the balloon during ascent, float, or descent. This is likely attributable to the practical difficulty of incorporating a reliable and useful wind model. Also, since CRC was unable to locate any data or reference to data, it is reasonable to assume that only in rare cases is a

balloon subjected to low-speed wind tunnel testing to formulate accurate representations of a balloon's response to horizontal air flow. On the other hand, a balloon's vertical motion can be understood more readily since the vertical component of motion is more repeatable during tests and actual flights. This is the apparent explanation for the presence of detailed, validated models of a balloon's vertical motion and for the absence of more comprehensive, multi-dimensional balloon flight performance models.

The search for an atmospheric model for the simulation of winds in BDPS led to a single candidate, NASA's Global Reference Atmosphere Model (GRAM). GRAM is an empirical FORTRAN computer simulation of the earth's atmosphere. It was developed by Georgia Tech under contract to NASA's Marshall Space Flight Center. Dale [ref. 6] summarizes the capabilities and operation of GRAM. The features which are most significant to BDPS development are that GRAM provides a worldwide, 12-month database of atmospheric properties including wind speed and wind azimuth. The atmospheric properties are provided in statistical form (mean values and standard deviations from the mean) in order to best represent the actual data collected over several decades. NASA's most significant use of GRAM was in the aerothermal design of the Space Shuttle Transportation System where atmospheric reentry heating issues had to be resolved.

Previously, CRC had acquired GRAM and had become familiar with its operation. This factor, added to GRAM's suitability to the BDPS mission, made it an obvious choice for inclusion in BDPS.

2.2 MODEL DEVELOPMENT AND INTEGRATION

As shown in the Figure 1.0-1 schedule, the majority of effort for this contract was focused on modeling tasks. First, atmosphere models and balloon models were implemented. Then, those models were integrated with a vehicle flight dynamics program to develop the BDPS capability.

2.2.1 Atmospheric Model

GRAM is a combination of different empirical atmosphere models corresponding to three different altitude regimes. Figure 2.2.1-1 shows these regimes and the models used. Between 0 and 25 kilometers atmospheric pressure, density and temperature are simulated by the 4-Dimensional World-Wide Atmosphere Model developed by Allied Research Associates under NASA sponsorship. The 4-D model accesses large data files containing empirically determined atmospheric parameter profiles for a grid of world-wide locations. A modified version of the latitude-dependent model of G. V. Groves is used for altitudes between 30 and 115 kilometers. This model was modified to incorporate longitudinal variations in pressure, density, and temperature in addition to the latitudinal variations. For altitudes above 90 kilometers, the model of L. G. Jacchia is used to compute the thermospheric-exospheric values of atmospheric pressure, density, and temperature. Interpolation between the 4-D and the Groves values is performed between 25 and 30 kilometers, and a fairing technique is used between the Groves and the Jacchia models.

Two different wind models are used in GRAM. The geostrophic wind model is applicable for altitudes between 0 and 25 kilometers and above 90 kilometers. This model uses finite differencing of pressure values to estimate horizontal pressure gradients which are then used to compute wind velocities. The wind speed model for the middle atmosphere from 25 to 90 kilometer is the spherical harmonic wind model based on the spherical harmonic equation which is a function of latitude, longitude, month, and altitude and whose coefficients are fitted to measured data and vary with month and altitude. Smooth fairing between spherical harmonic winds and geostrophic winds is performed between 20 and 25 kilometers and between 90 and 95 kilometers. The GRAM wind model also computes values for mean vertical winds and thermal wind shear. The mean vertical winds are typically of the order of a centimeter/second or less and represent the large-scale mean vertical winds characteristic of

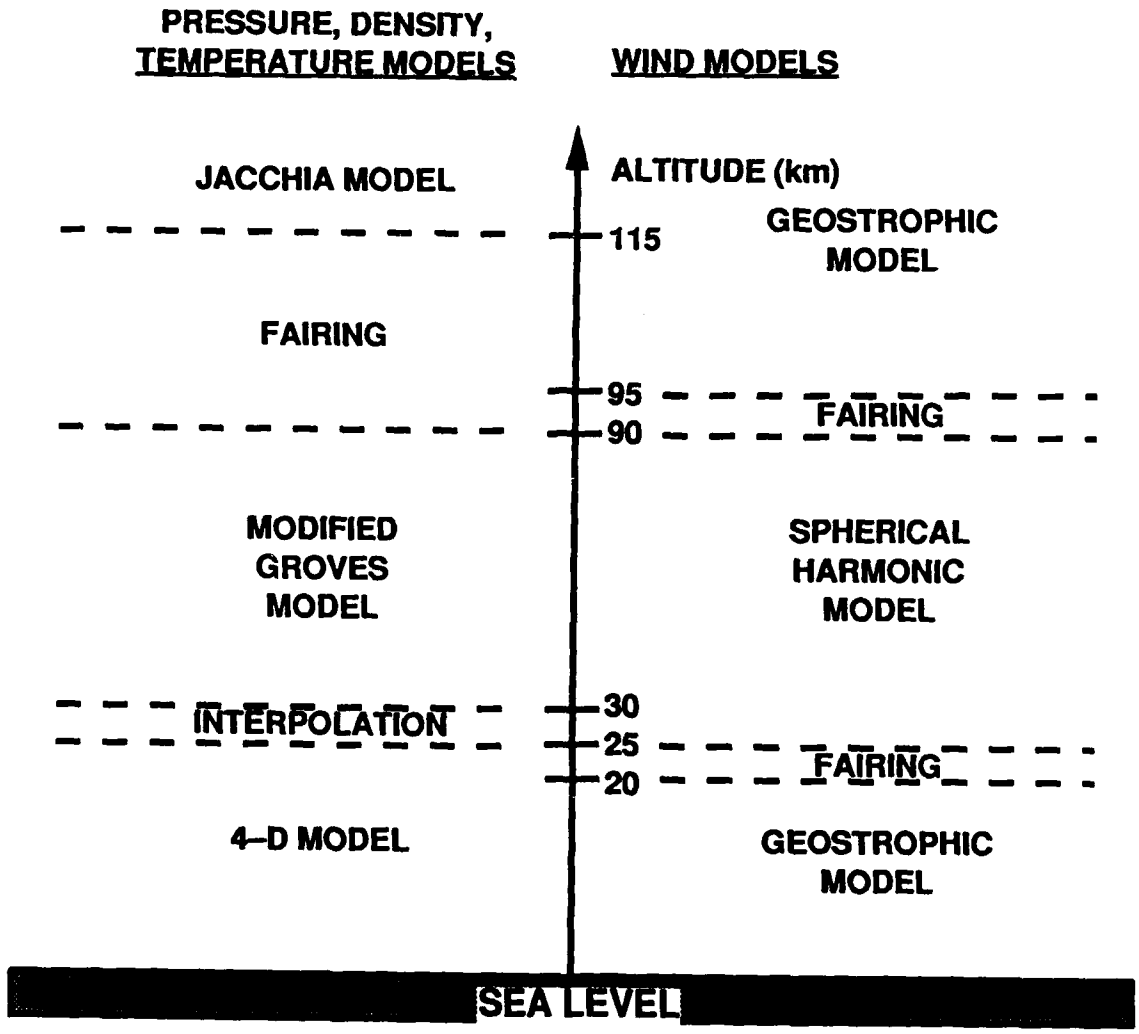

Figure 2.2.1–1. Simulation Models and Altitude Regimes in GRAM

mean meridional circulation. Wind shear values are calculated for any altitude below 700 kilometers but are reliable only below 90 kilometers.

Figure 2.2.1-2 shows a sample wind profile provided by GRAM. The figure shows the east wind component and the north wind component at a latitude and longitude corresponding to Wallops Island, Virginia. The January database was used by GRAM to produce the data shown in this figure. The graphs show the mean wind velocity in each direction along with the mean $\pm 3\sigma$ values. The mean $\pm 3\sigma$ curves are significant because 99.7% of the wind speed values will fall within those bounds.

2.2.2 Balloon Model

CRC decided that a single, simplified model could be developed to model both zero-pressure and super-pressure balloon aspects which influence a balloon's drift pattern. The requirements imposed on the balloon model developed were that it be completely configurable through input data rather than through coding changes and that it provide all the balloon-specific parameters necessary for drift pattern production to the vehicle flight dynamics portion of the BDPS. Figure 2.2.2-1 shows a top-level flowchart of the balloon model, and the actual FORTRAN source code is provided as Appendix A. As shown in the figure, the only modeling difference in the treatment of the two types of balloons is that a zero-pressure balloon will expel excess gas while a super-pressure balloon retains the excess gas, causing an internal pressure greater than the current ambient atmospheric pressure.

By making the balloon model data-configurable, the source code edit-compile-link cycles are confined to code development. This feature enhances the usefulness of the balloon model for actual production of drift patterns since no parameters are "hard-wired" into the source code. Table 2.2.2-1 lists the input values required to configure a balloon with this model. The appropriate units for the input values are also shown in the table.

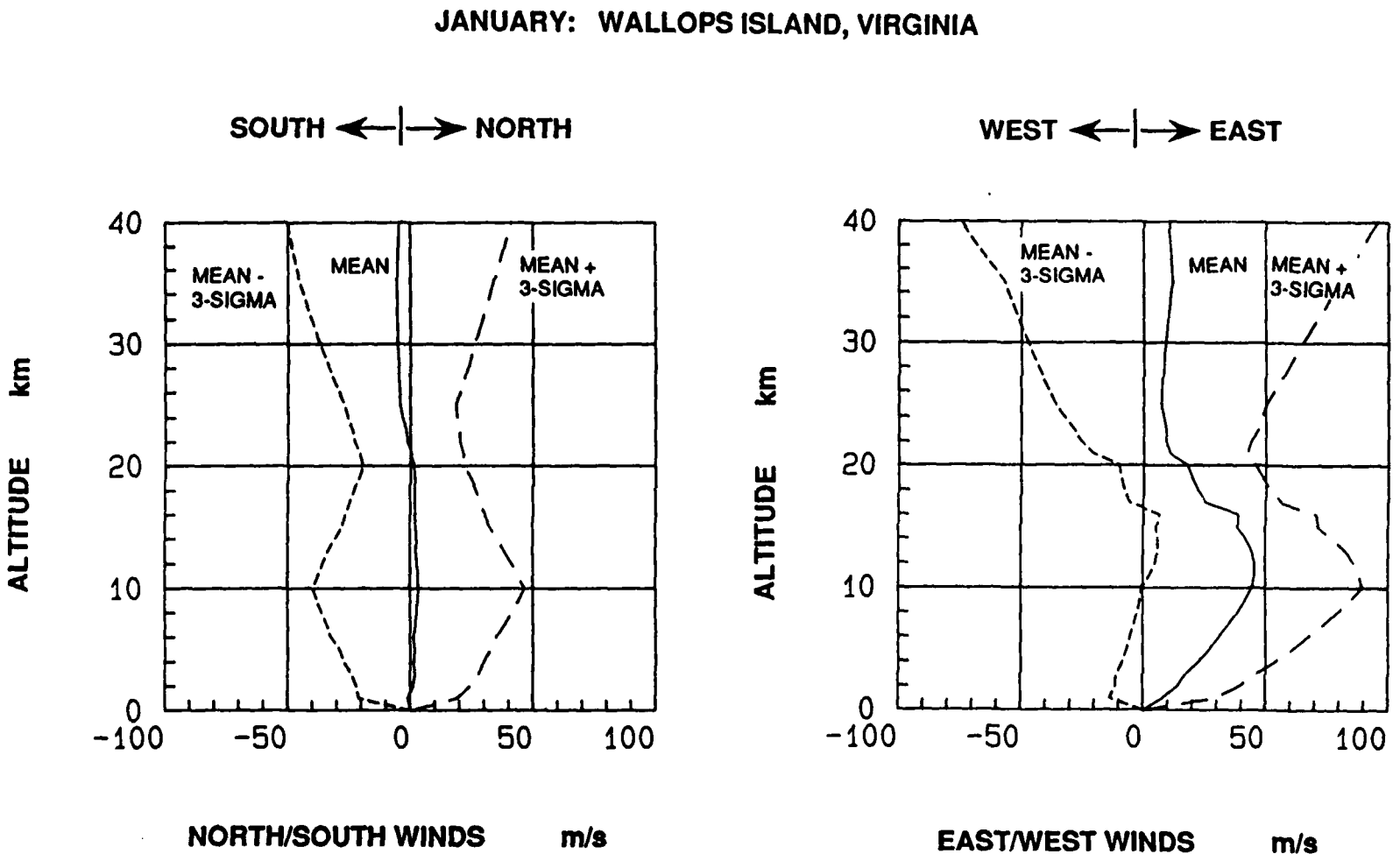

Figure 2.2.1–2. Sample GRAM Wind Profile

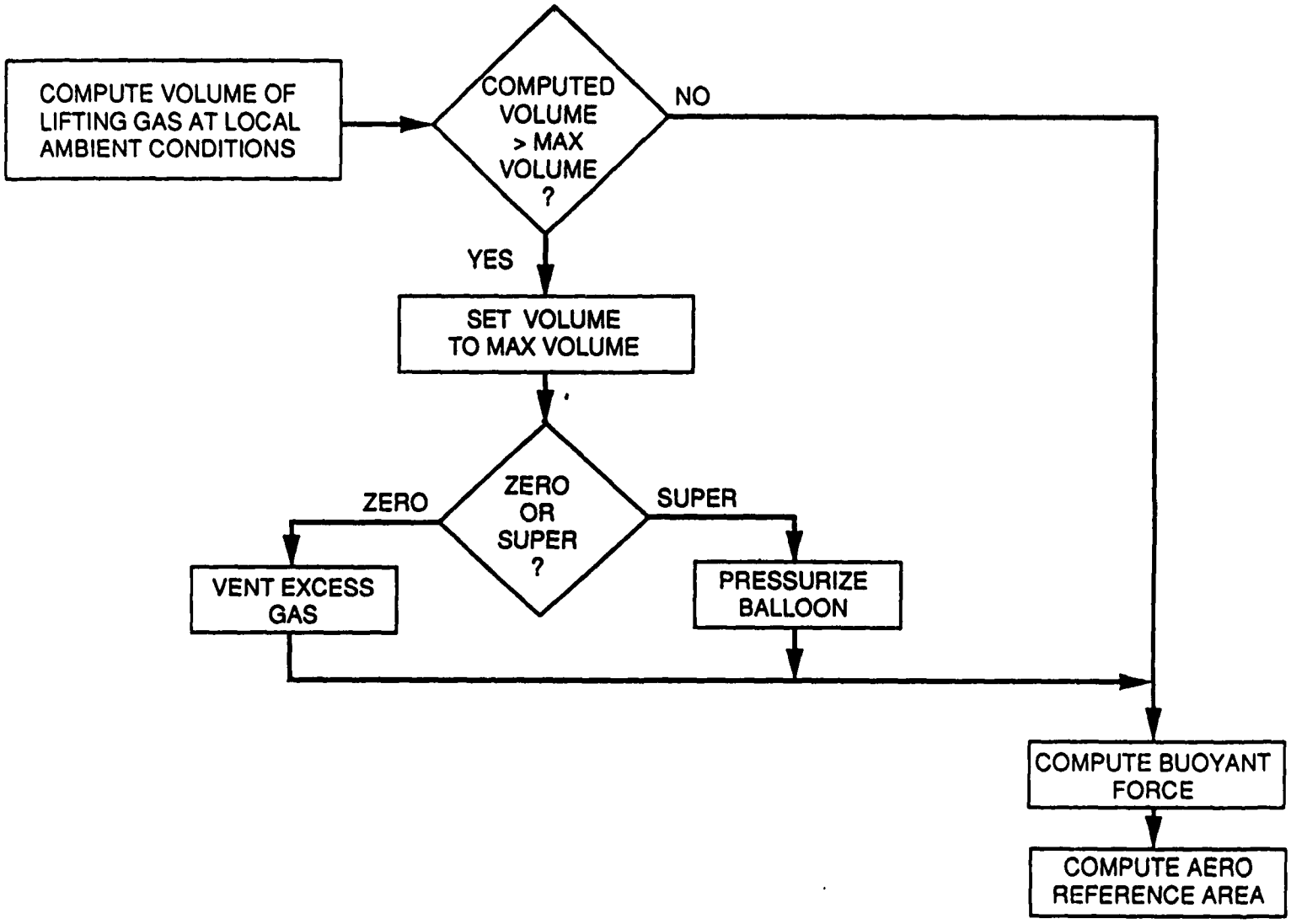

Figure 2.2.1–1. Simulation Models and Altitude Regimes in GRAM

Table 2.2.2-1. Balloon Model Input Data

Parameter	Units
Type of balloon (zero- or super-pressure)	-
Gas constant of lifting gas	$\frac{\text{meter}^2}{\text{second}^2 \cdot {}^\circ\text{Kelvin}}$
Weight of lifting gas	newton
Weight of payload and balloon	newton
Maximum diameter of balloon	meter
Drag coefficient	-

The model imposes spherical geometry on the balloons. The "maximum diameter" input parameter in Table 2.2.2-1 is used as a spherical diameter when determining if either type of balloon is fully inflated. Also, the aerodynamic reference area for fully or partially inflated balloons is calculated by using the assumption that the balloon's shape is always approximately spherical. Dwyer [ref. 5] dwells on the point that the shape of a partially inflated balloon must be treated carefully if a simulation is to attain fidelity with the actual behavior of a balloon.

The balloon model provides three essential output quantities for use in the vehicle flight dynamics program. As discussed above, a reference area is calculated and serves as the area upon which the aerodynamic drag calculation is based. Also, the model provides the magnitude of the buoyant force which is equal to the weight of the air displaced by the balloon. Finally, the model reports the current weight of lifting gas in the balloon which can only change if a zero-pressure balloon expels excess gas as it enters its float altitude.

In general, CRC recognizes that the thermodynamic fidelity of the balloon model described in this report suffers from comparison with highly detailed models such as those of Kreith [ref. 2] or Carlson and Horn [ref. 3], but the effort required to increase the fidelity of the present model would not necessarily be rewarded by significant differences in the resulting simulated drift patterns. For example, the addition of modeling the thermal stratification of the lifting gas would not be expected to cause a noticeable difference in the distance covered by a drifting balloon over several hours.

2.2.3 Balloon Flight Dynamics/Kinematics Model

CRC's proprietary Multiple Degree of Freedom (MDOF) simulation system provided the trajectory simulation framework required to demonstrate the BDPS capability. MDOF is a highly versatile FORTRAN computer program written by missile design and control system engineers as a tool for analyzing missile flight and engagement performance. It is designed to provide rapid synthesis of a wide variety of air vehicle configurations while allowing direct growth of simulation fidelity with vehicle design maturity. MDOF's modular structure and program control features provide the user with the essential elements of all flight simulations: input/output, equations of motion, executive control/sequencing, integration, and basic configuration modules.

2.2.4 Balloon Drift Pattern Simulation (BDPS) Integration

The integration of the balloon model into the MDOF framework was simple and straightforward. All input and output values were passed to and from the routine through the respective common blocks. In addition to the three main outputs discussed above, the balloon model also made available calculations of free lift percentage and internal balloon pressure. Once the calculations were made, those parameters could easily be added or deleted from the output files as desired by the user.

CRC decided to execute GRAM off-line and reduce its output to tabular wind data which could then be inserted into an MDOF data file. This allows for a single wind profile (wind speed and wind azimuth, each as a function of altitude) to be generated and then used for the entire BDPS execution. The wind profile for each 24-hour flight was generated for the balloon's launch position. The use of a single wind profile throughout a 24-hour flight introduced deviations in wind speed potentially as high as 15% when comparing the wind speed value taken from the input profile to the value which GRAM would have reported for the balloon's current position. An alternative approach would have been to patch the entire GRAM model directly into MDOF. However, either the combined program would be terribly inefficient with GRAM having to re-initialize itself during each MDOF execution step, or GRAM would have to be completely restructured and distributed throughout the MDOF code. Neither of these options were feasible under the SBIR Phase I time and funding constraints. A sample profile as used by BDPS is shown in Figure 2.2.4-1, where the wind speed values have been calculated by a root-sum-square combination of the east and north wind components shown previously in Figure 2.2.1-2.

The BDPS data flow is summarized in Figure 2.2.4-2. Balloon design data is combined with information about the balloon's intended mission. That data is used to build an input data file for MDOF and provides location data for creating a wind profile with GRAM. The GRAM wind profile is then inserted into the MDOF input data file, and MDOF is executed with the integrated balloon model. Depending on what variables were requested through the input file, certain variables are made available for display using CRC's proprietary PlotPlus graphics tool. Among other output options, PlotPlus may be used to produce balloon drift patterns.

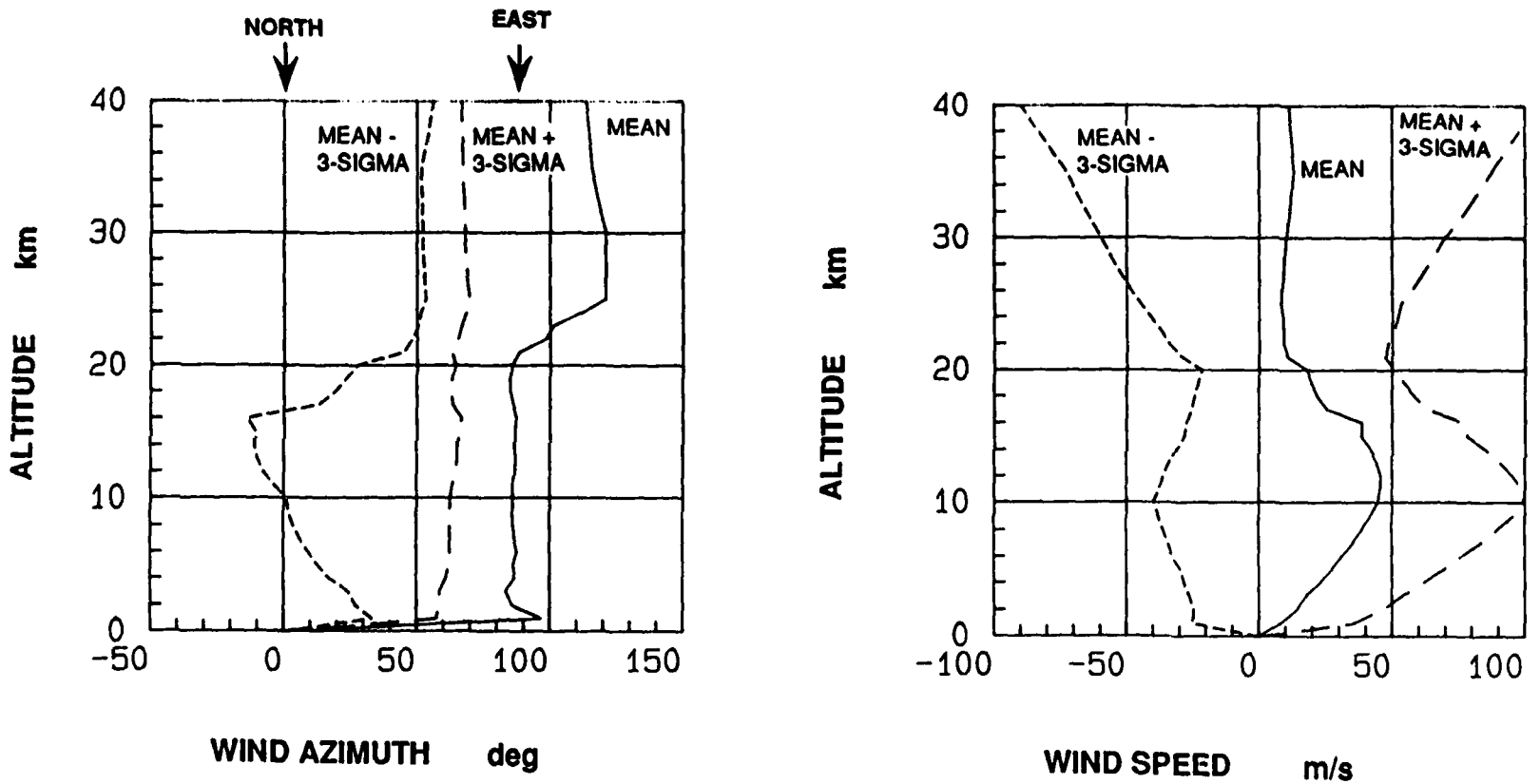

Figure 2.2.4–1. Sample BDPS Wind Profile

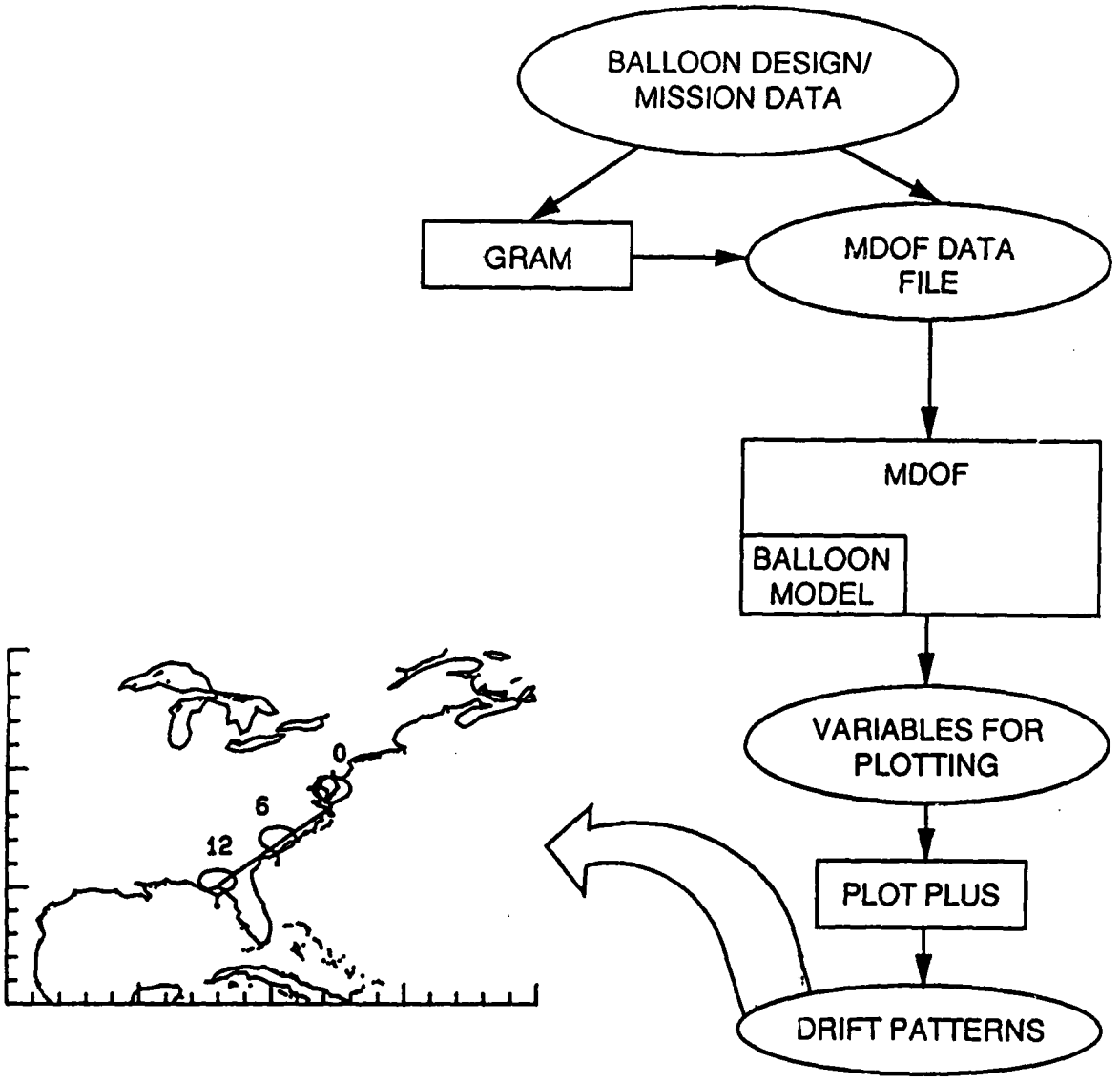

Figure 2.2.4–2. Data Flow for Drift Pattern Production

2.2.5 Output Format Development

After establishing contact with Lt. Cdr. Epley, CRC discussed DARPA's needs and developed sample output formats which were sent to Lt. Cdr. Epley and to Les Reading. The formats received approval and are used in this report to present the results of demonstrating the BDPS capability.

The primary output format requested by DARPA was a plot showing the latitude and longitude of a balloon with major land masses also visible for reference. Other plots of interest to DARPA included an ascent velocity history and a plot of the balloon's altitude versus the ground range from the balloon's launch point. Samples of these two output formats are shown in Figures 2.2.5-1 and 2.2.5-2.

2.3 DRIFT PATTERN PRODUCTION AND ANALYSIS

The data used to configure the zero-pressure balloon shown in six sample flights was primarily obtained from Les Reading. Specifically, he provided the weight of the balloon fabric and payload, the approximate dimensions of the fully inflated balloon, the approximate amount of lifting gas used to launch the balloon, and the type of lifting gas. He also provided CRC with estimates of the initial and final ascent velocity that he had observed during balloon flight tests.

CRC obtained an estimate of the balloon drag coefficient from Hoerner [ref. 7]. The coefficient value chosen was based on the balloon description given CRC by Les Reading, who described his design as a "pillow-shaped" rectangular balloon with the long axis oriented vertically. For an ascending balloon, such a shape could be most closely approximated by a circular cylinder in axial flow, which is catalogued by Hoerner as having a pressure drag coefficient of 0.8. This seems to be a reasonable choice since the use of this number produced simulated ascent velocity profiles which resembled those reported by Les Reading from flight tests. It should be noted, however, that the balloon model computes an aerodynamic reference area based on a spherical

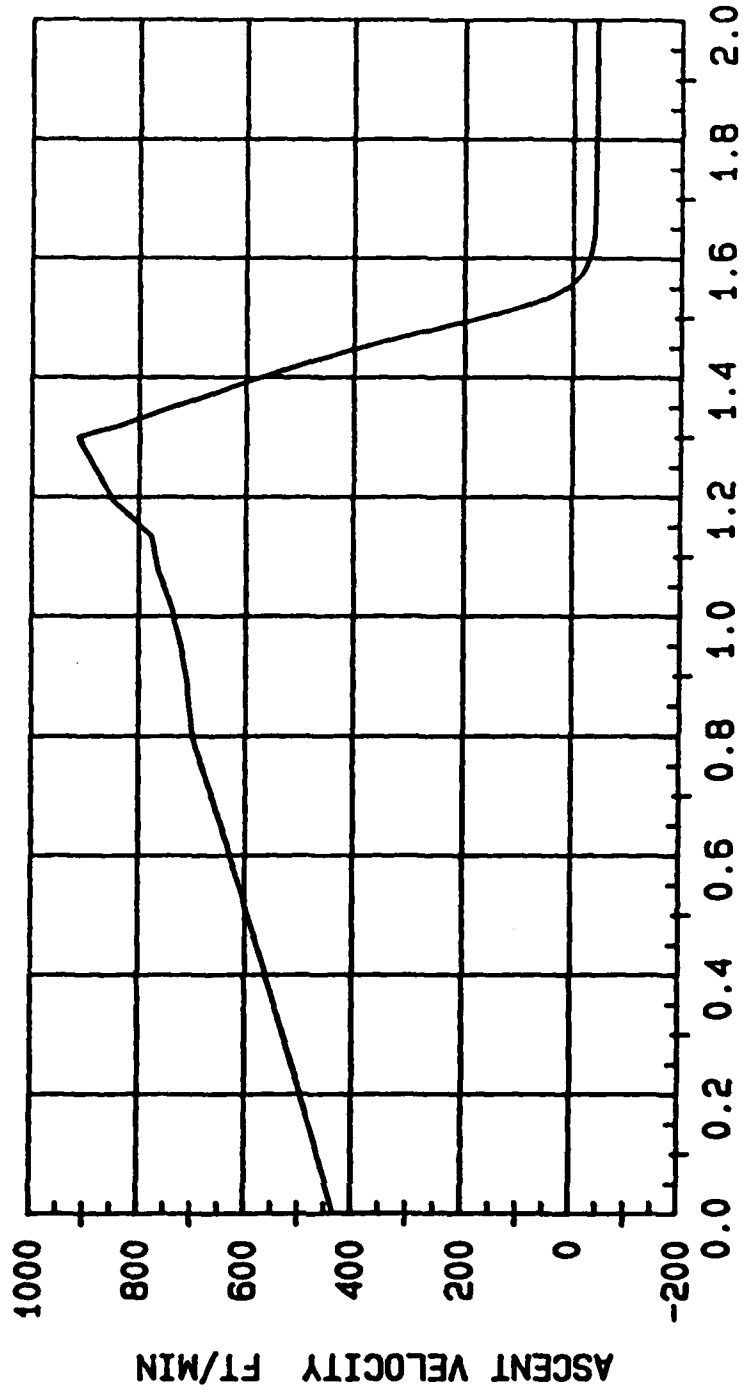

Figure 2.2.5–1. (U) Sample Output: Ascent Velocity History

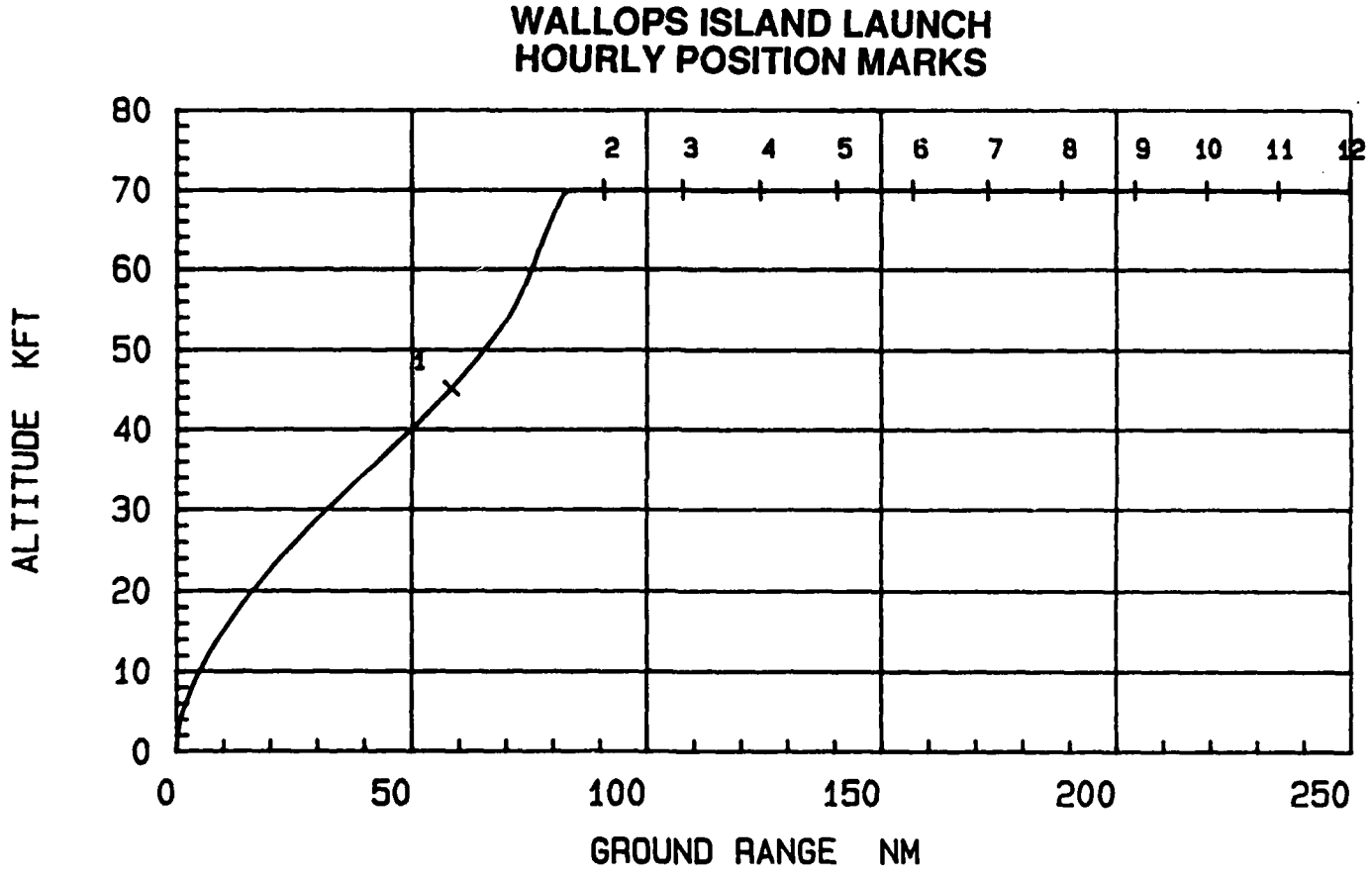

Figure 2.2.5–2. Sample Output: Balloon Altitude vs. Ground Range

volume, for which Hoerner reports a drag coefficient of 0.47. The apparent inconsistency between drag coefficients and reference areas serves to point out that the ascending balloon's shape and drag characteristics are not modeled to a high level of detail in this approach. In spite of this, the model produced results which track well with the reported flight test results. The simulated ascent rate and the flight test ascent rate are both shown in Figure 2.3-1.

Lt. Cdr. Kral identified launch sites to be used for both zero-pressure flights and for a super-pressure flight. The six sites from which zero-pressure balloon drift patterns are to originate are listed in Table 2.3-1. The latitude and longitude values for each location were estimated by CRC. The single location to be used for a super-pressure launch is also indicated in the table.

Table 2.3-1. Zero-Pressure Balloon Launch Sites

Description	Latitude	West Longitude
Wallops Island	37.9°	75.5°
Vandenberg AFB	35.7°	120.6°
Adak Island*	51.9°	176.6°
Indian Ocean	0.0°	295.0°
Mediterranean Sea	35.0°	344.0°
North of Puerto Rico	22.4°	65.0°

* Also used for super-pressure launch site

For each of the six launch locations listed in Table 2.3-1, four plots are presented. First, an overview chart shows the balloon drift pattern with respect to nearby land masses. Second, a magnified view of the latitude-longitude excursion is shown. The third plot for each launch shows the balloon's

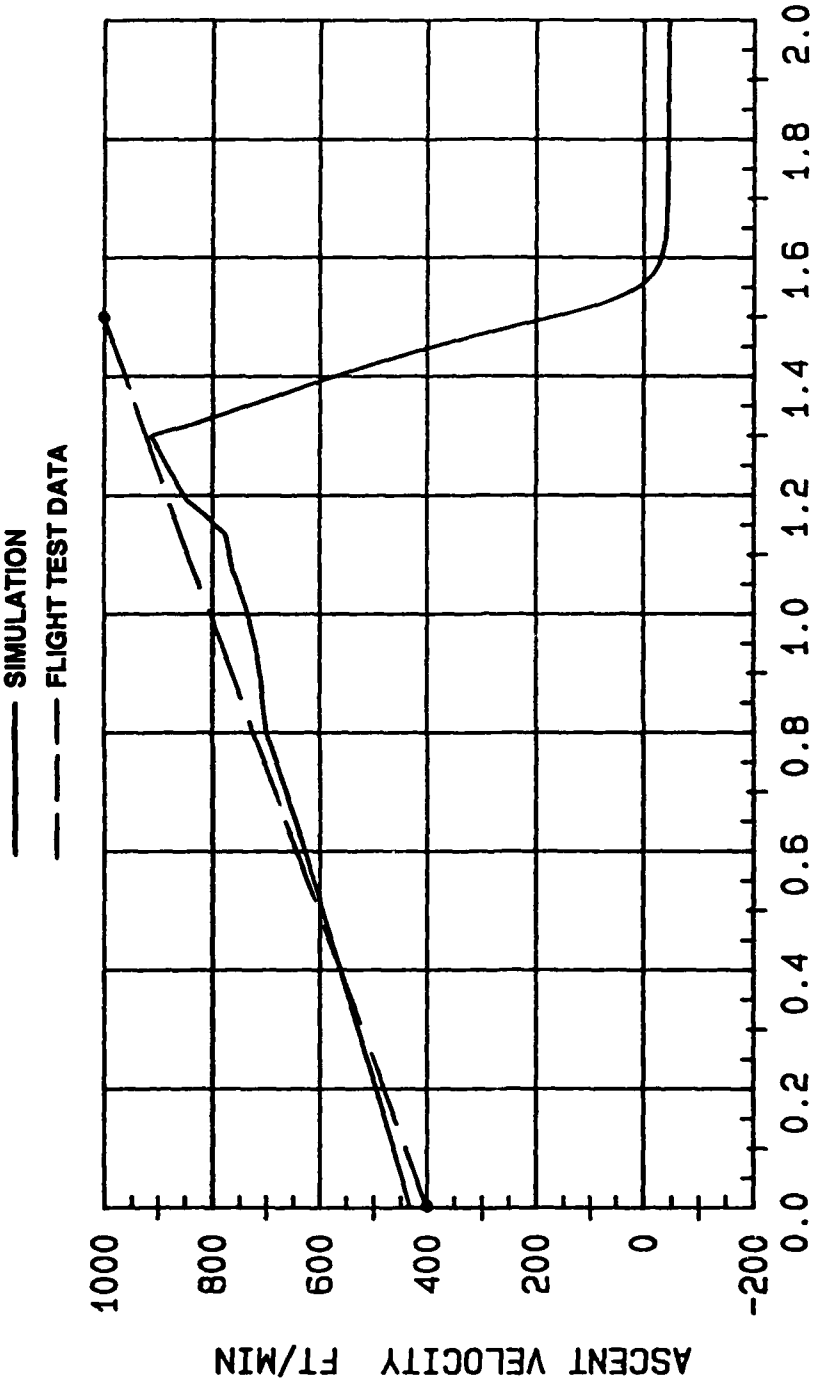

Figure 2.3–1. Comparison of Simulated Ascent Rate and Flight Test Ascent Rate

altitude as a function of its ground range. The fourth chart for each location shows the balloon's ascent velocity history during the time of ascent. The fifth and sixth charts for each launch site show the January speed and azimuth wind profiles which were used to generate that drift pattern. This series of plots can be found in Figures 2.3-2 through 2.3-37.

Figure 2.3-38 shows several 24-hour drift patterns for balloons launched from Wallops Island. For this figure, the BDPS was provided with several wind profiles which represent the statistical variations to be expected during January. Bounded by the drift patterns using the mean $\pm$ 3σ winds, the area over which the balloons drifted represents 99.7% of the area over which the balloons could conceivably drift for that 24-hour period in January.

For the Wallops Island launch site, four drift patterns were produced showing the effect of winds during different months of the year. Figure 2.3-39 shows the four drift patterns, produced using January, April, July, and October winds.

Figure 2.3-40 through 2.3-67 show the drift pattern of the super-pressure balloon launched from Adak Island and allowed to drift at 120,000 feet for one year. CRC was given latitude in the configuration specification of this balloon since the only available information was its design altitude and its 50-lb payload. The drift pattern was segmented among several pages for clarity of presentation.

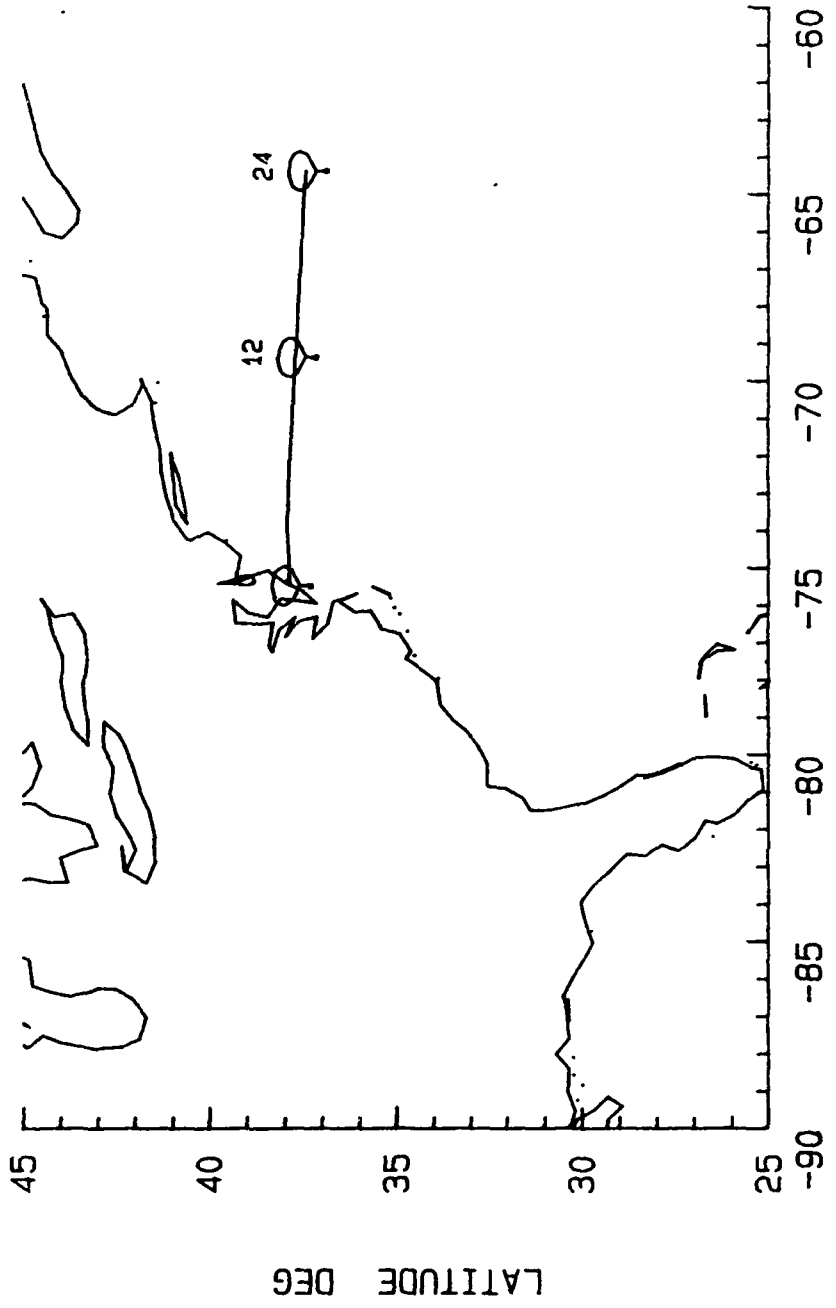

Figure 2.3–2. 24-Hour Drift Pattern for Wallops Island Flight

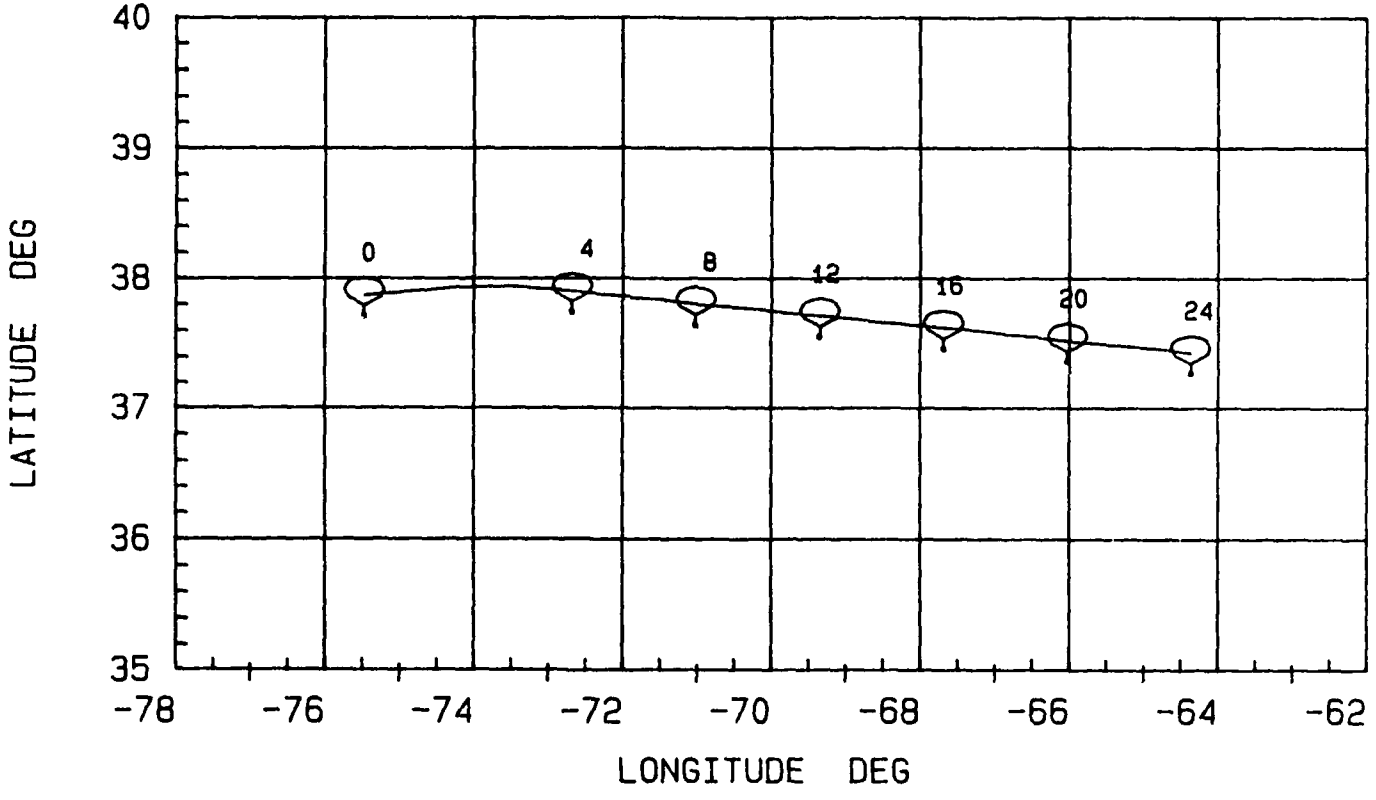

Figure 2.3–3. 24-Hour Drift Pattern for Wallops Island Flight

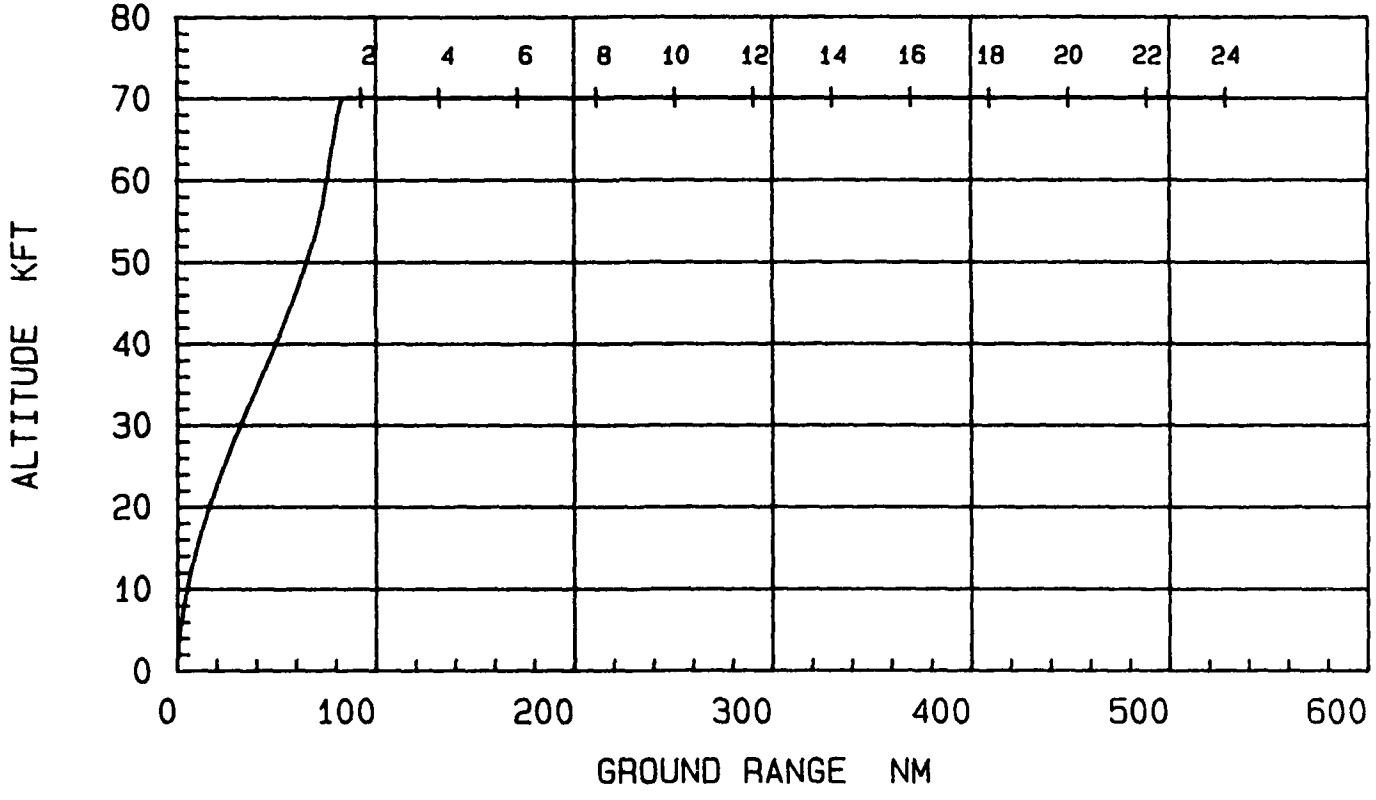

Figure 2.3–4. Altitude Versus Ground Range for 24-Hour Wallops Island Flight

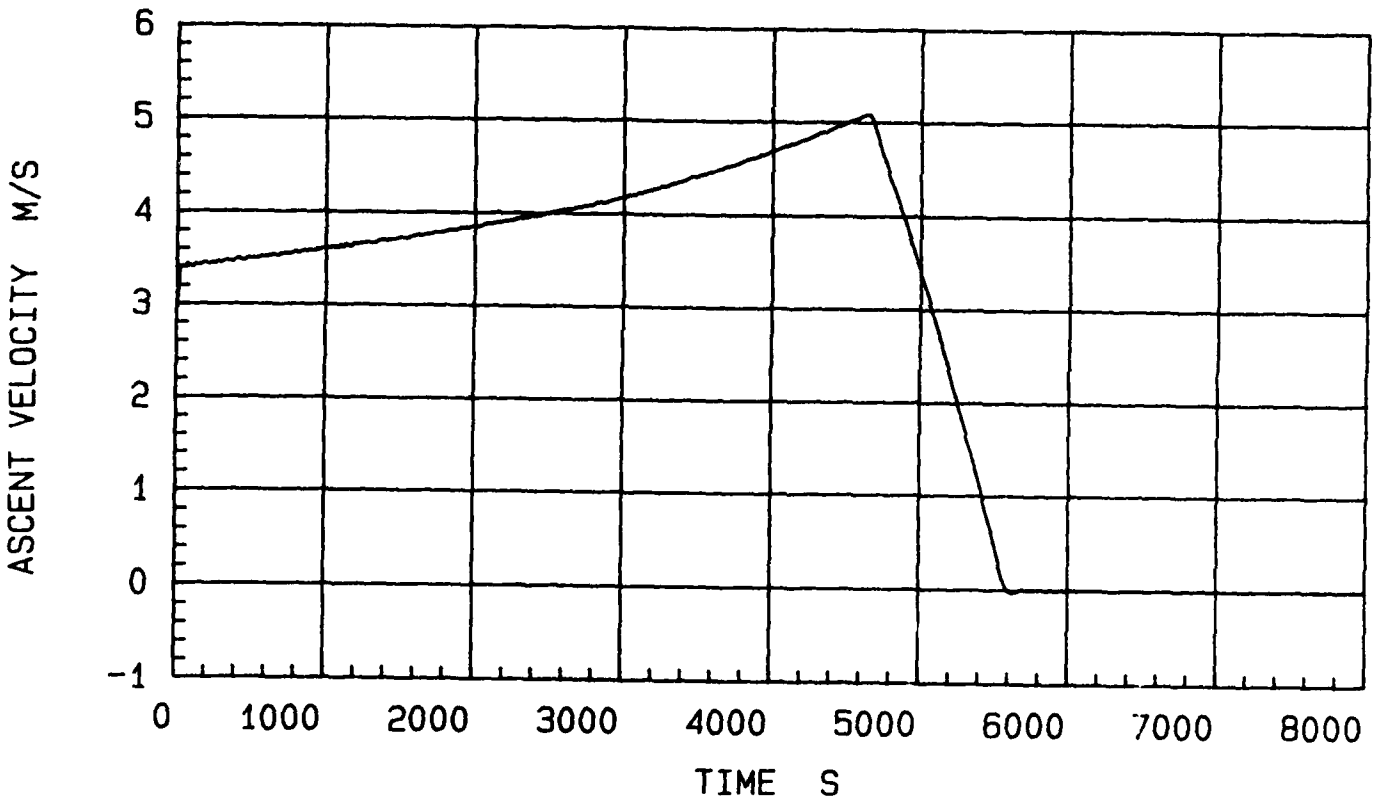

Figure 2.3–5. Ascent Velocity History for 24-Hour Wallops Island Flight

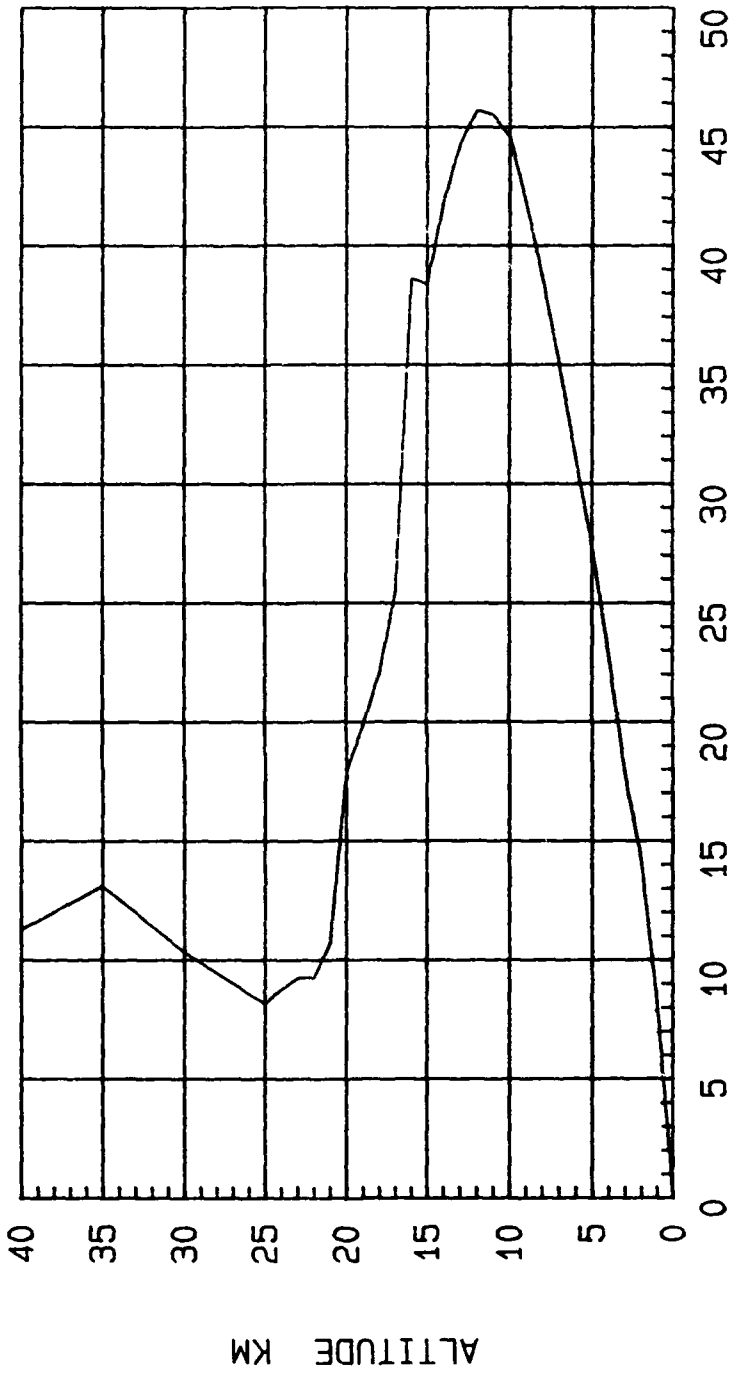

Figure 2.3–6. Wind Speed Profile at Wallops Island in January

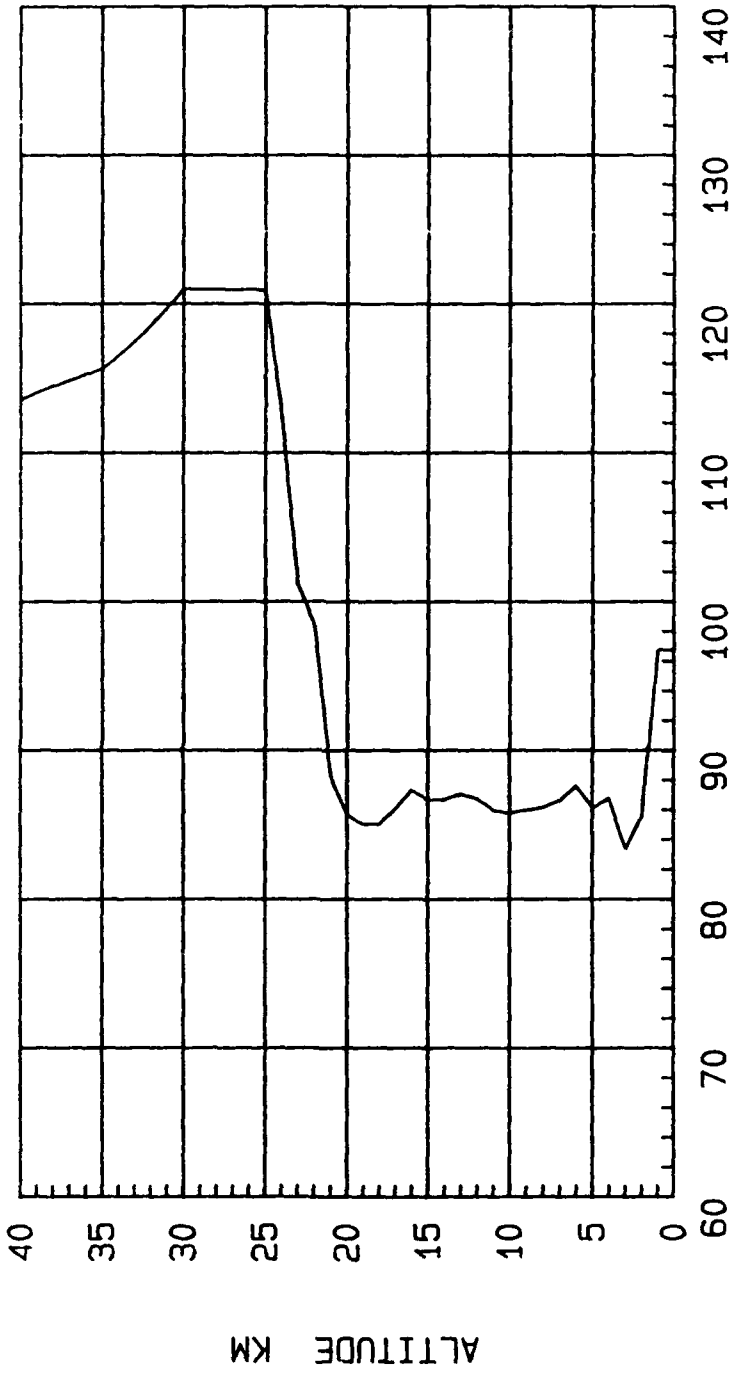

Figure 2.3–7. Wind Azimuth Profile at Wallops Island in January

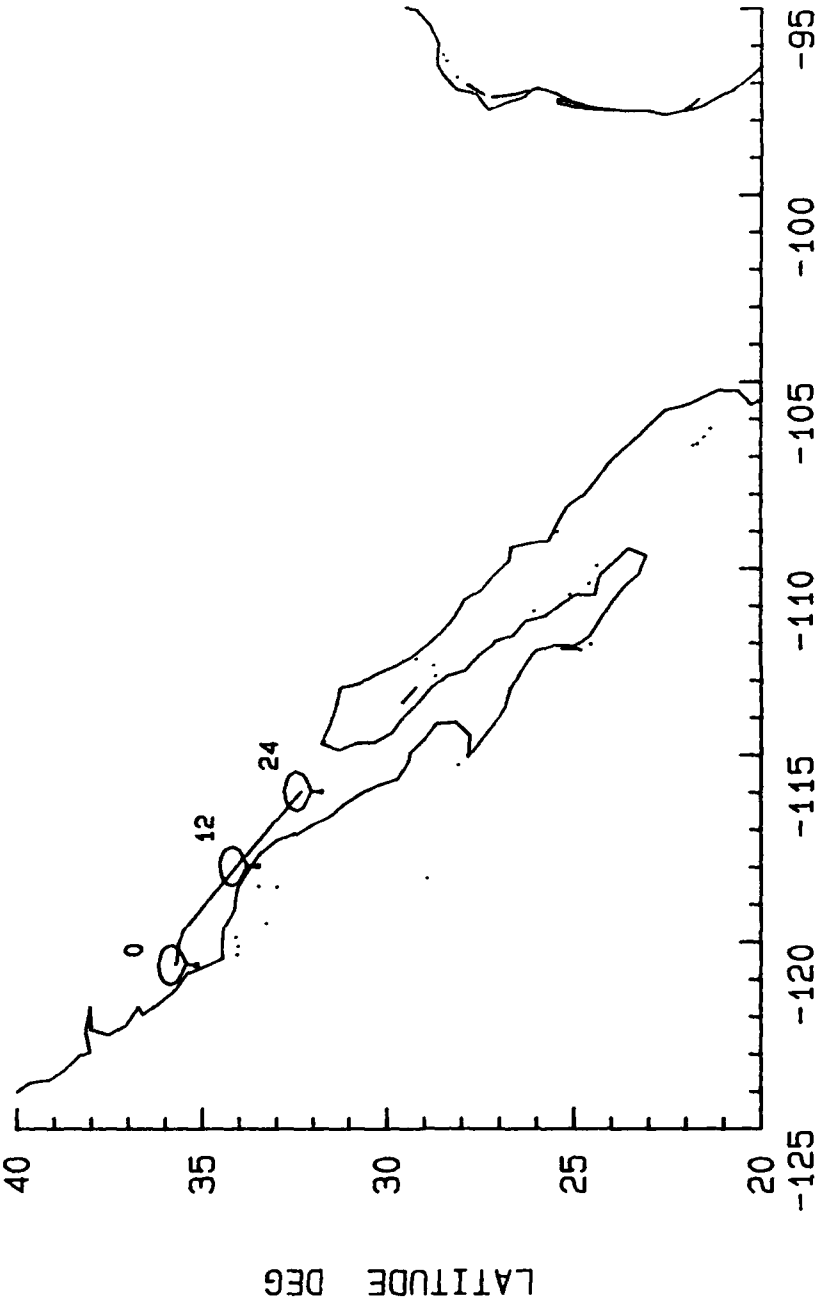

Figure 2.3–8. 24-Hour Drift Pattern for Vandenberg AFB Flight

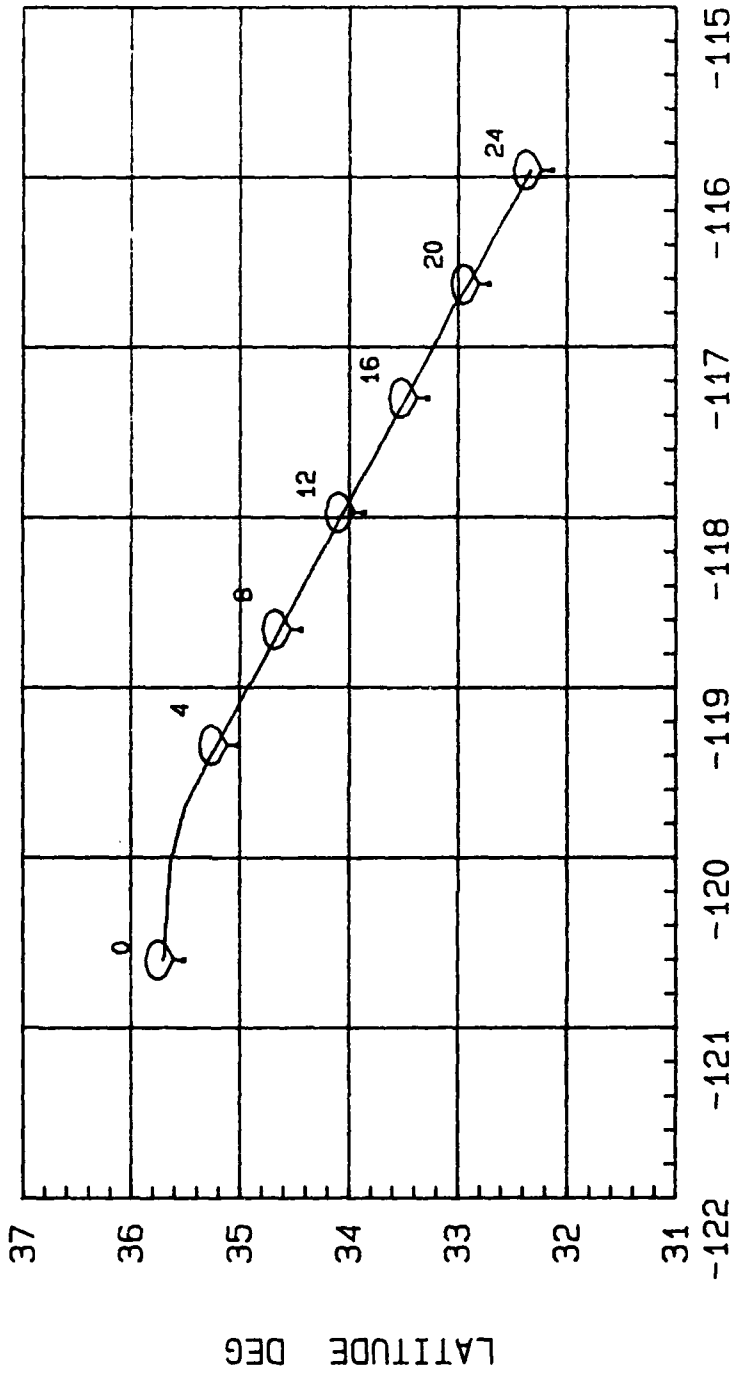

Figure 2.3–9. 24-Hour Drift Pattern for Vandenberg AFB Flight

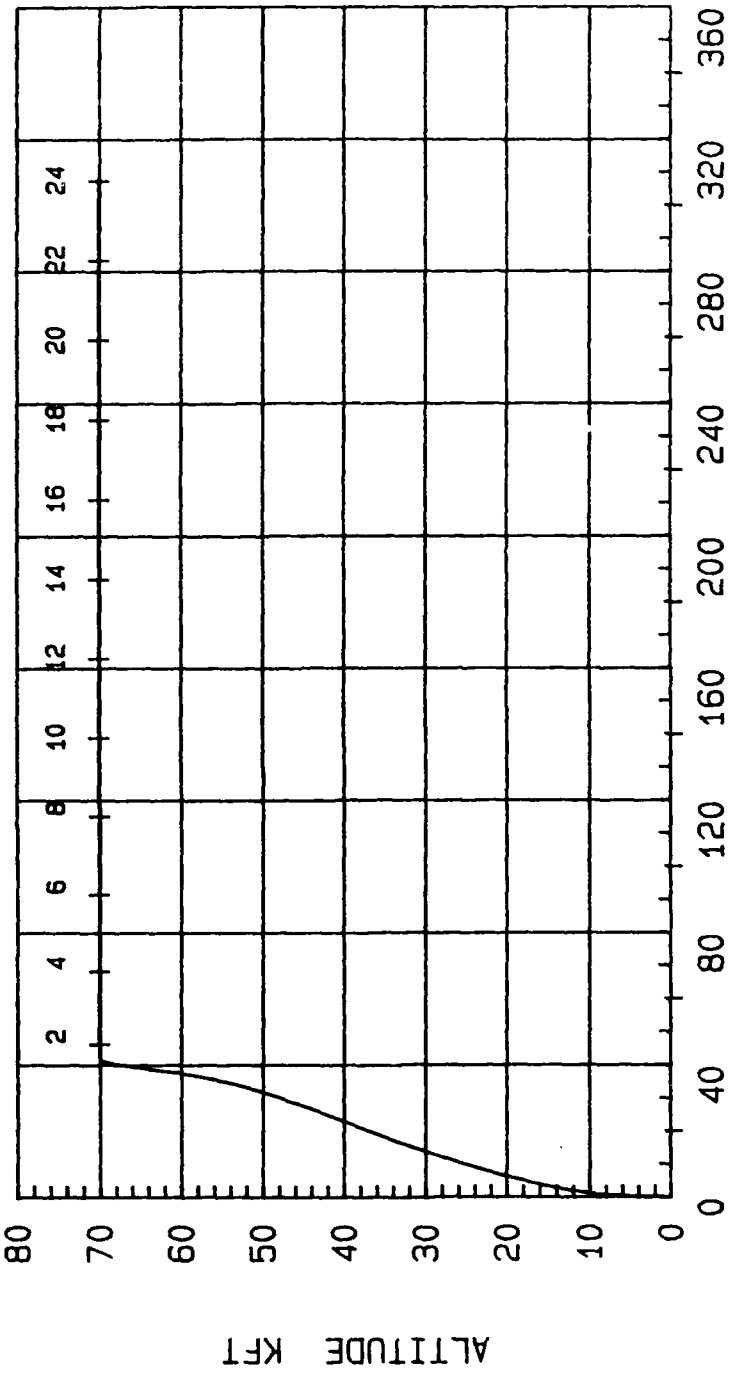

Figure 2.3–10. Altitude Versus Ground Range for 24-Hour Vandenberg AFB Flight

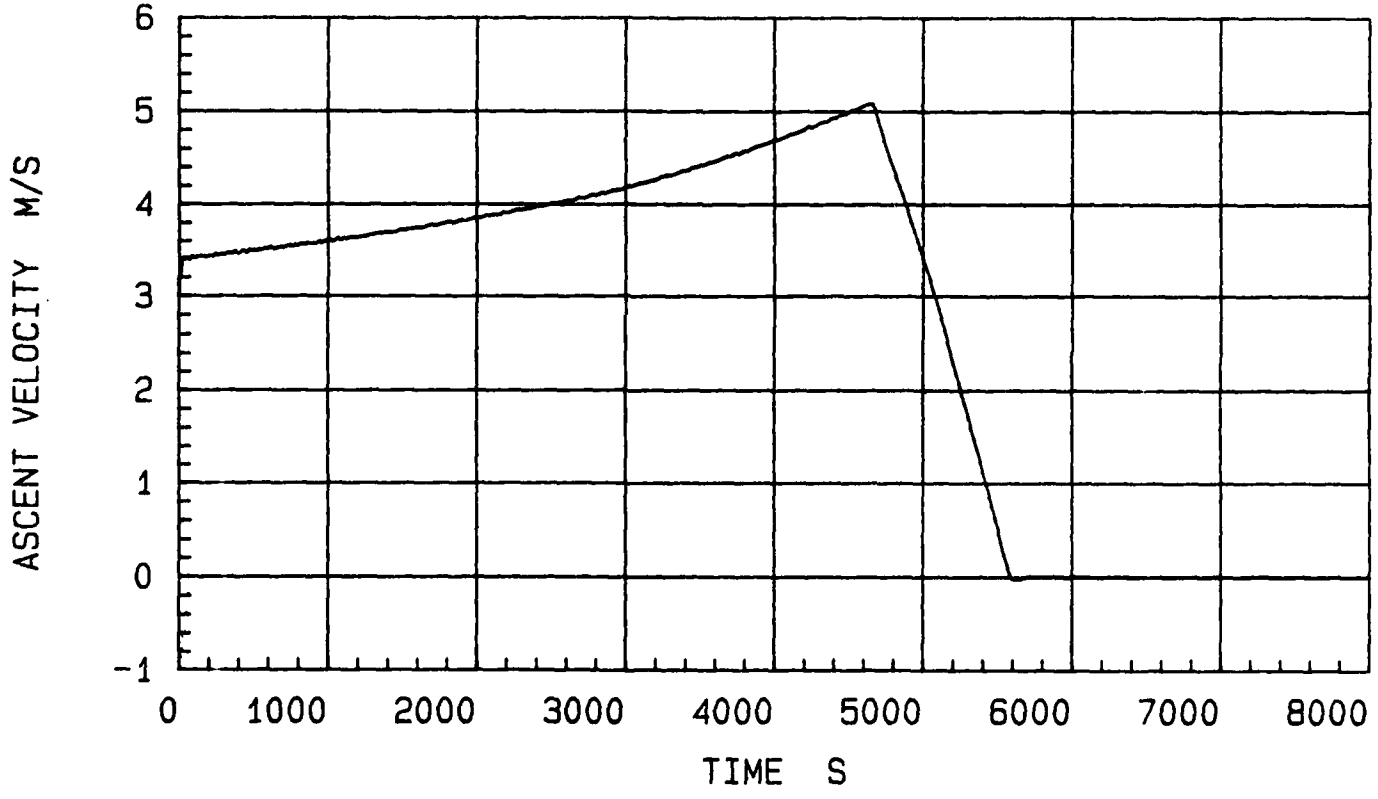

Figure 2.3–11. Ascent Velocity History for 24-Hour Vandenberg AFB Flight

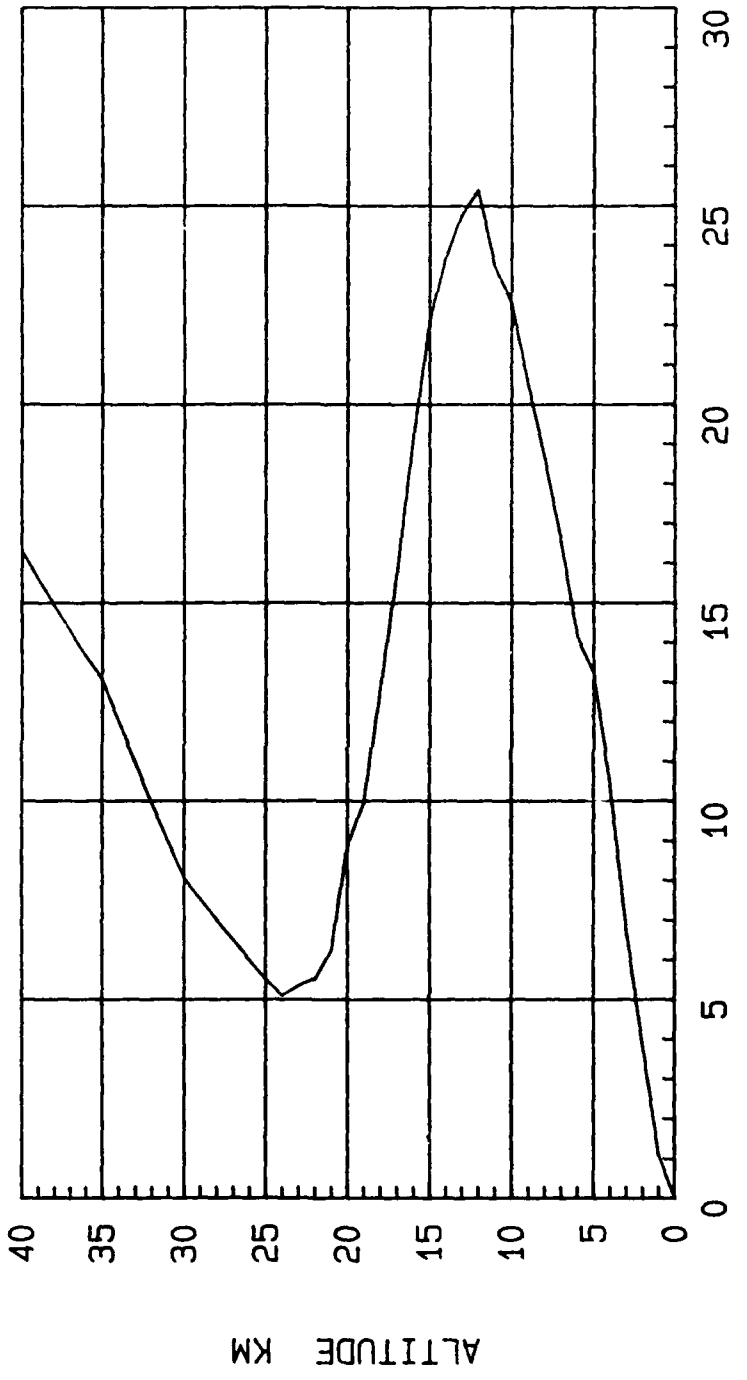

Figure 2.3–12. Wind Speed Profile at Vandenberg AFB in January

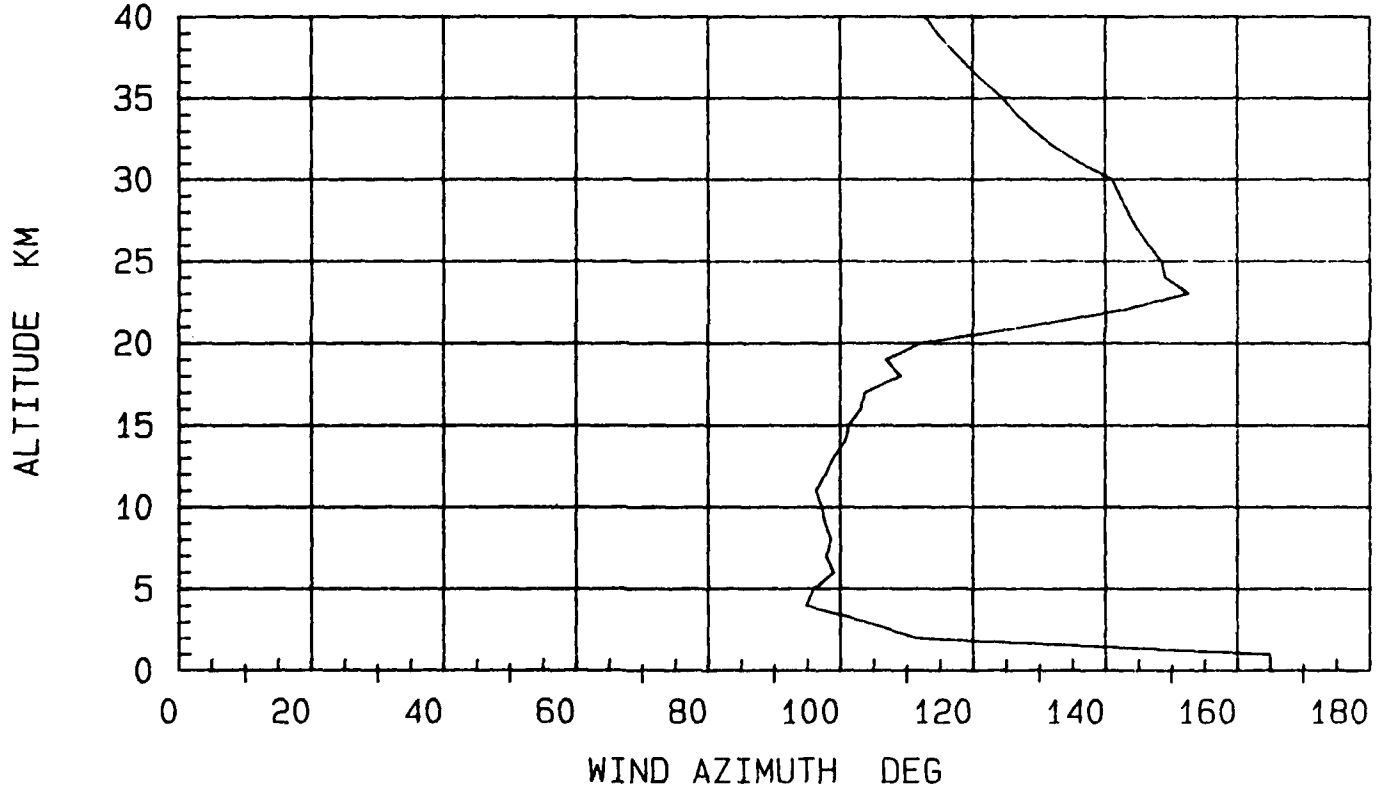

Figure 2.3–13. Wind Azimuth Profile at Vandenberg AFB in January

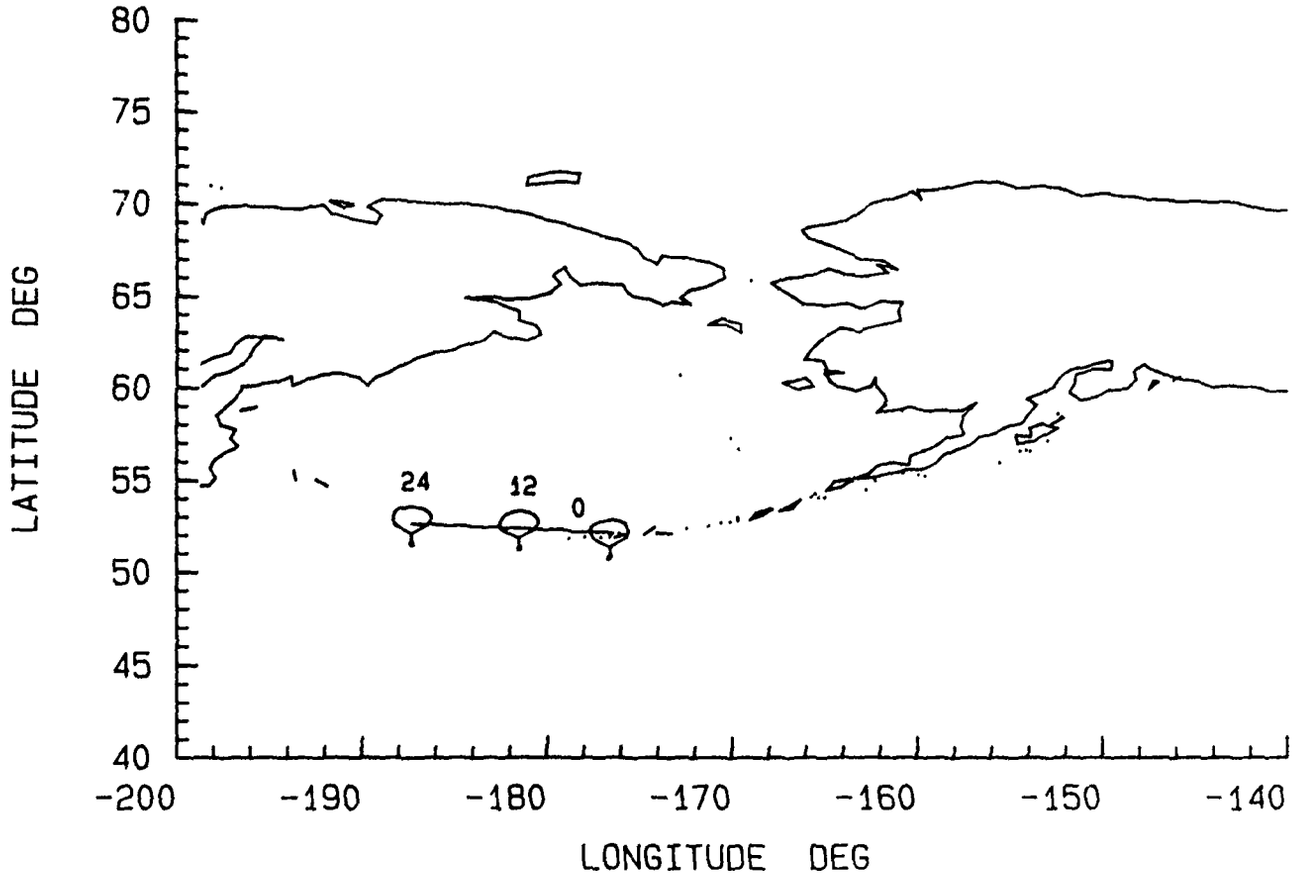

Figure 2.3–14. 24-Hour Drift Pattern for Adak Island Flight

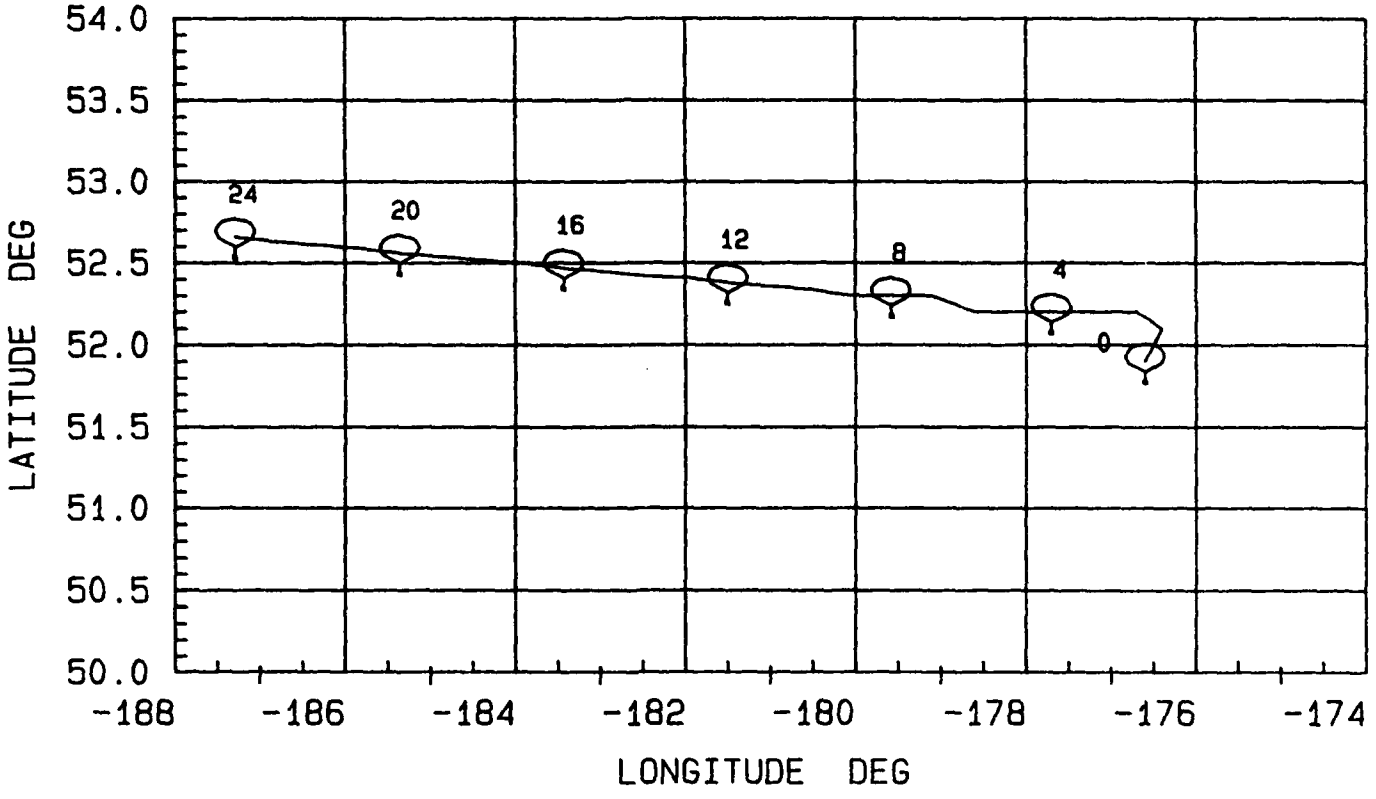

Figure 2.3–15. 24-Hour Drift Pattern for Adak Island Flight

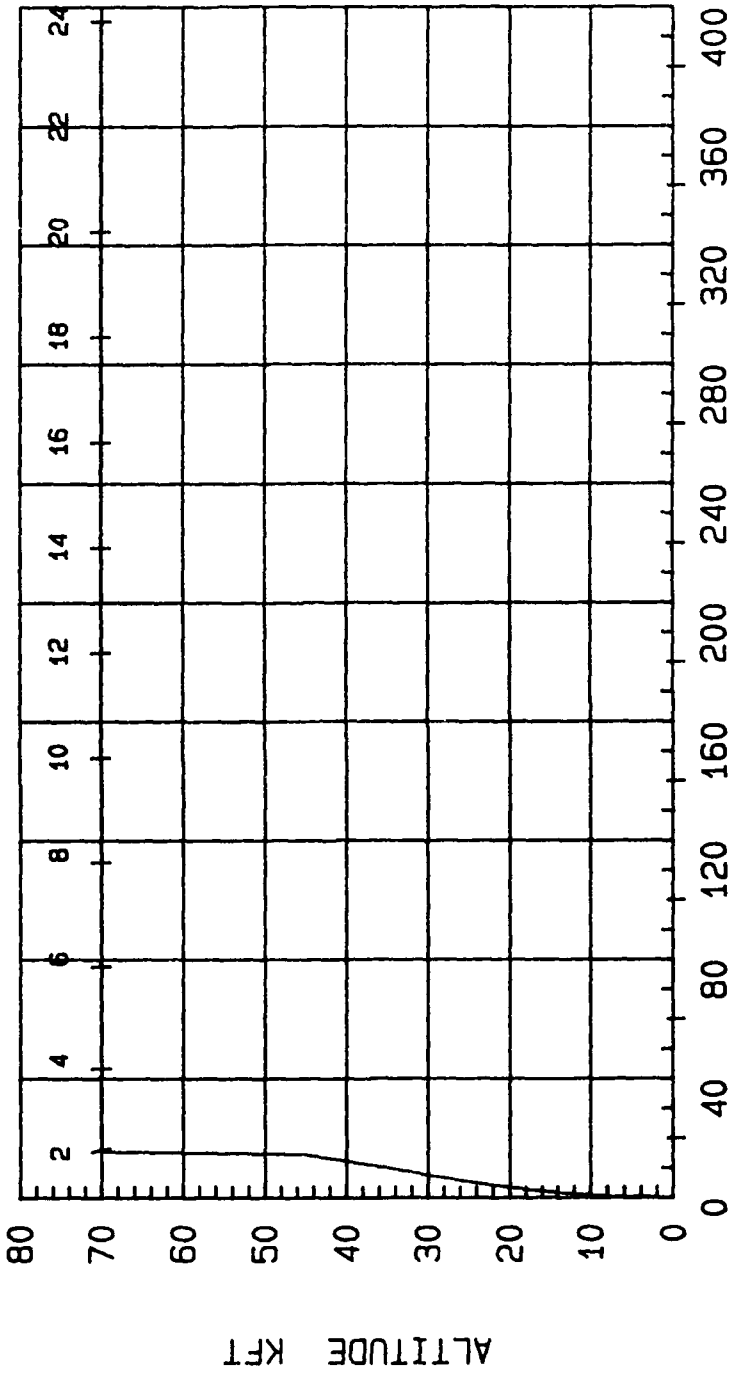

Figure 2.3–16. Altitude Versus Ground Range for 24-Hour Adak Island Flight

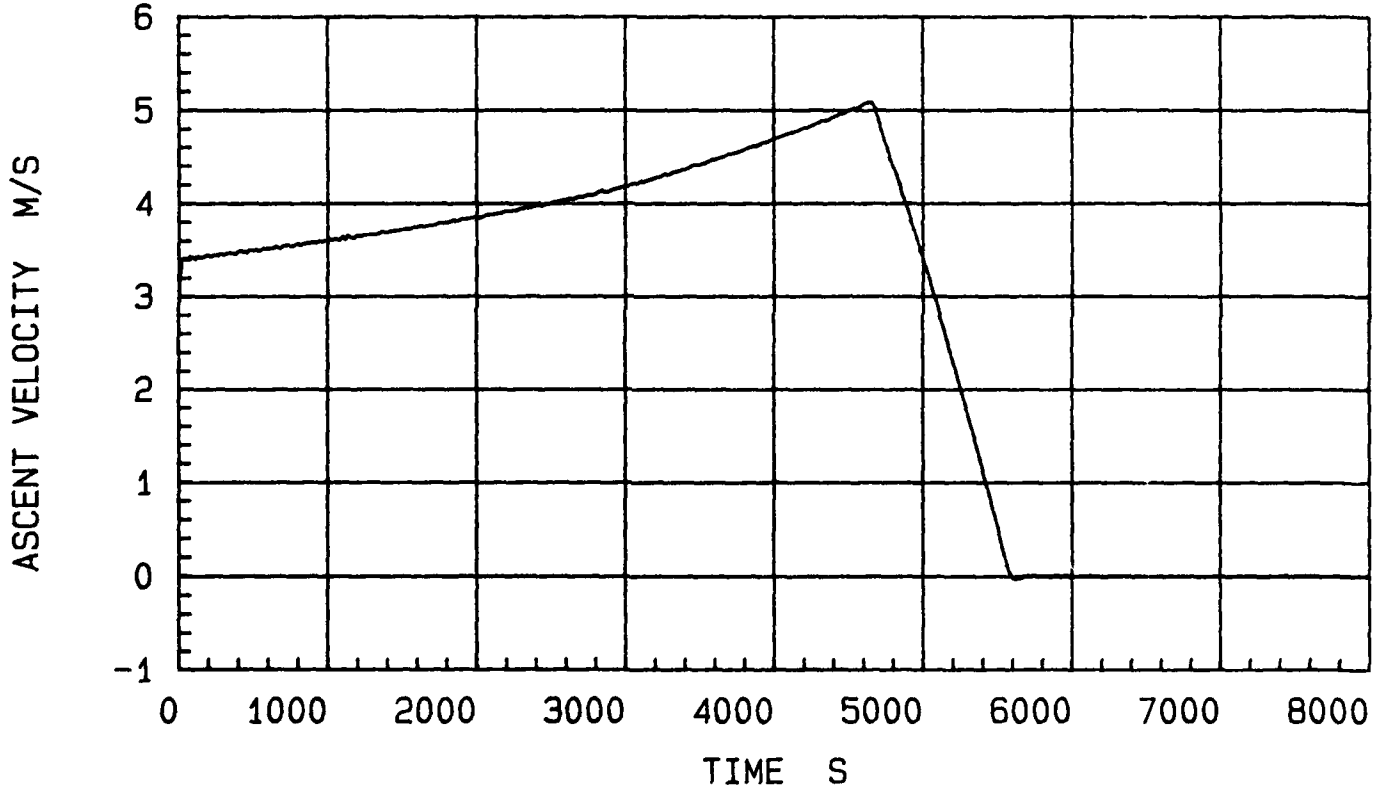

Figure 2.3–17. Ascent Velocity History for 24-Hour Adak Island Flight

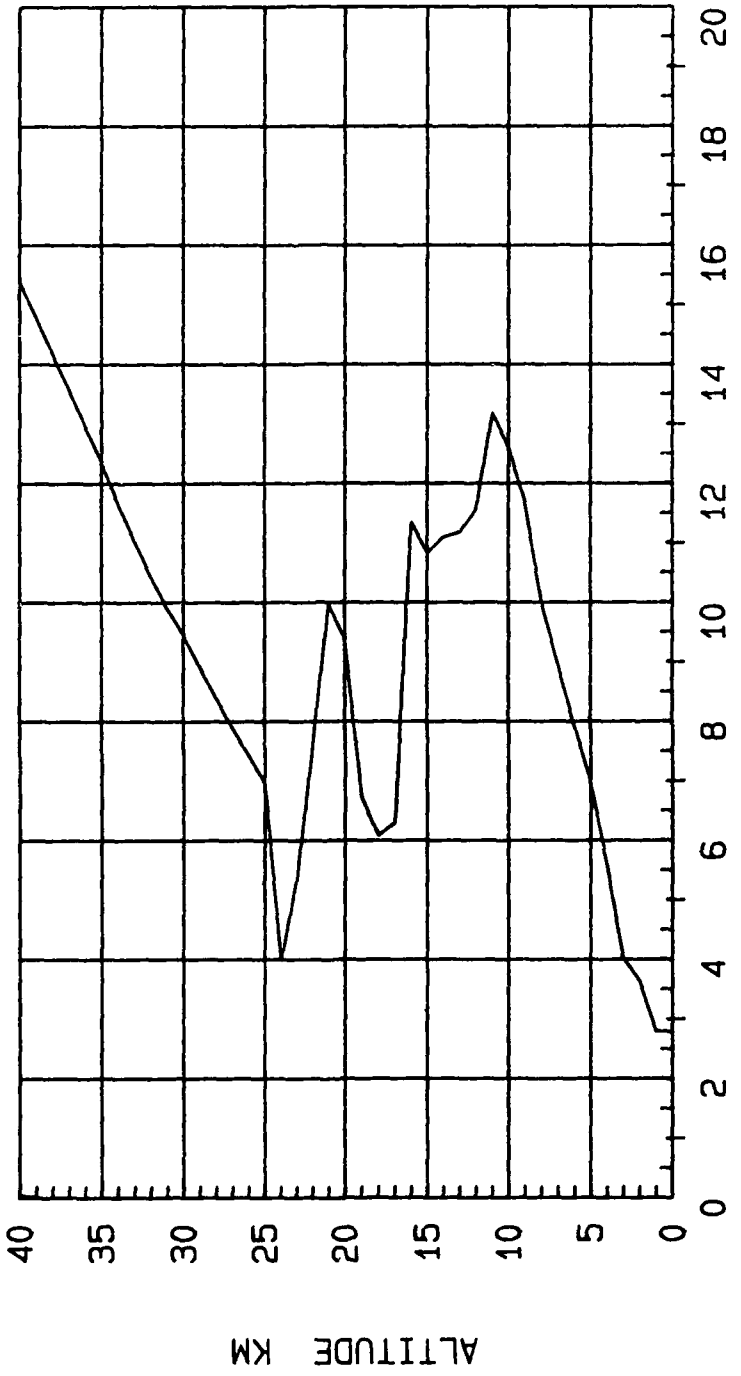

Figure 2.3–18. Wind Speed Profile at Adak Island in January

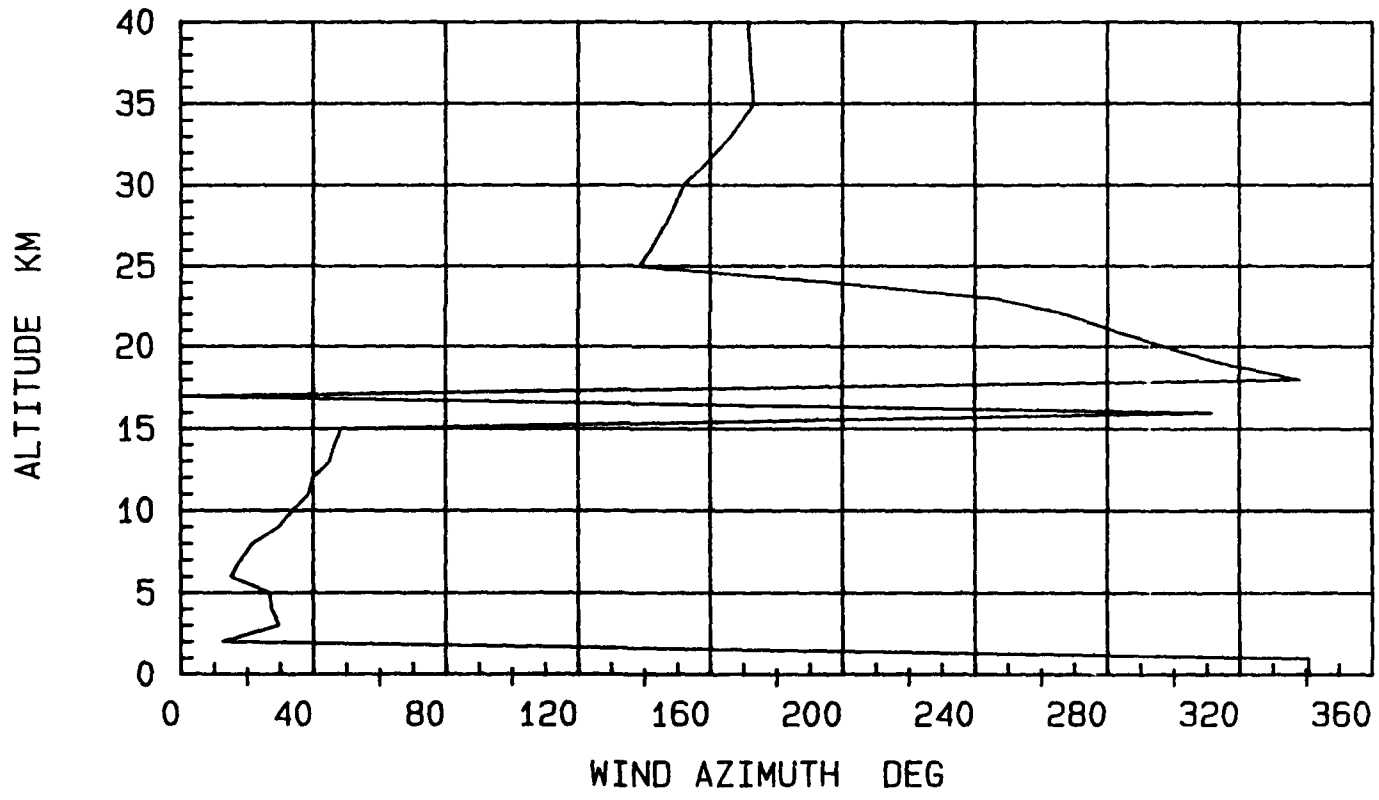

Figure 2.3–19. Wind Azimuth Profile at Adak Island in January

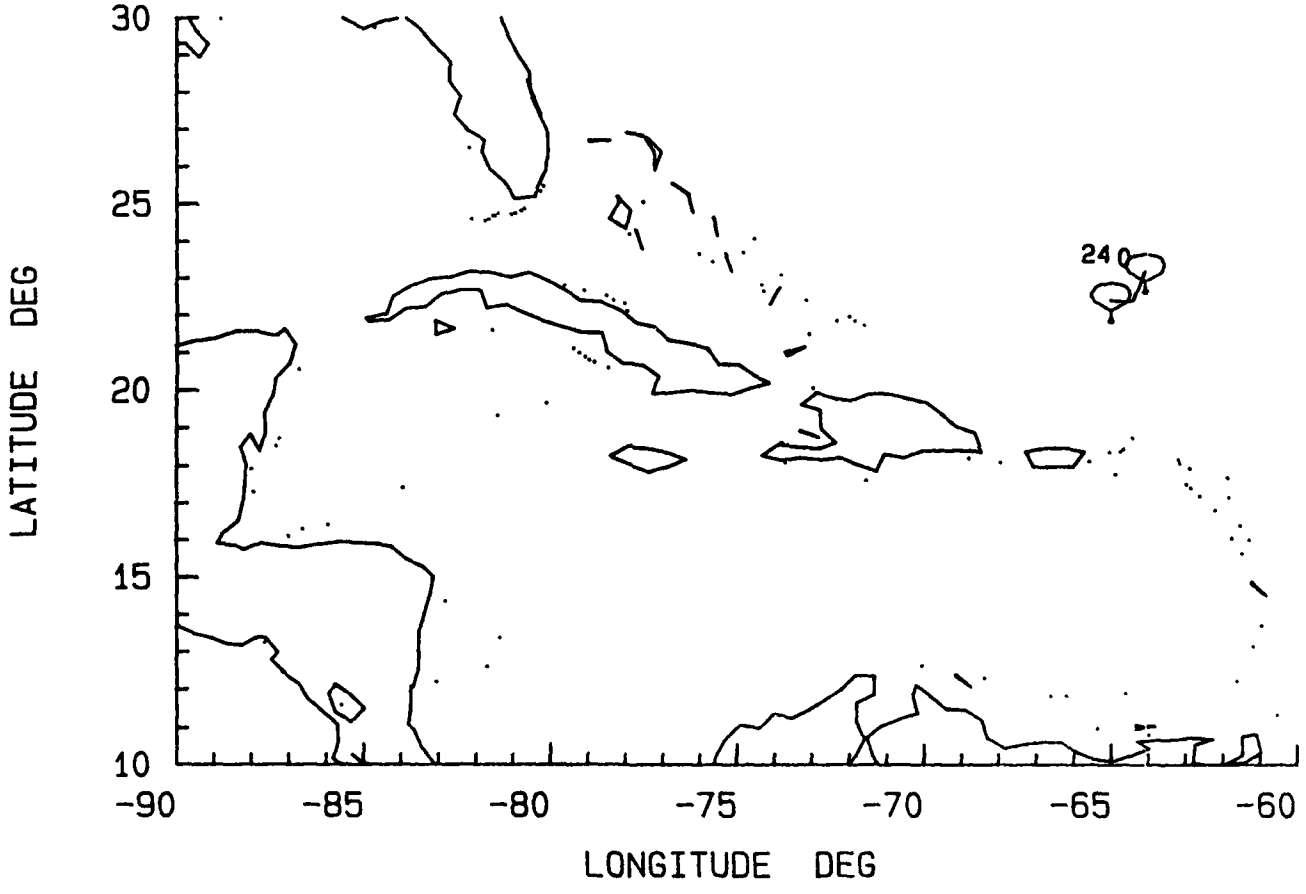

Figure 2.3–20. 24-Hour Drift Pattern for Flight North of Puerto Rico

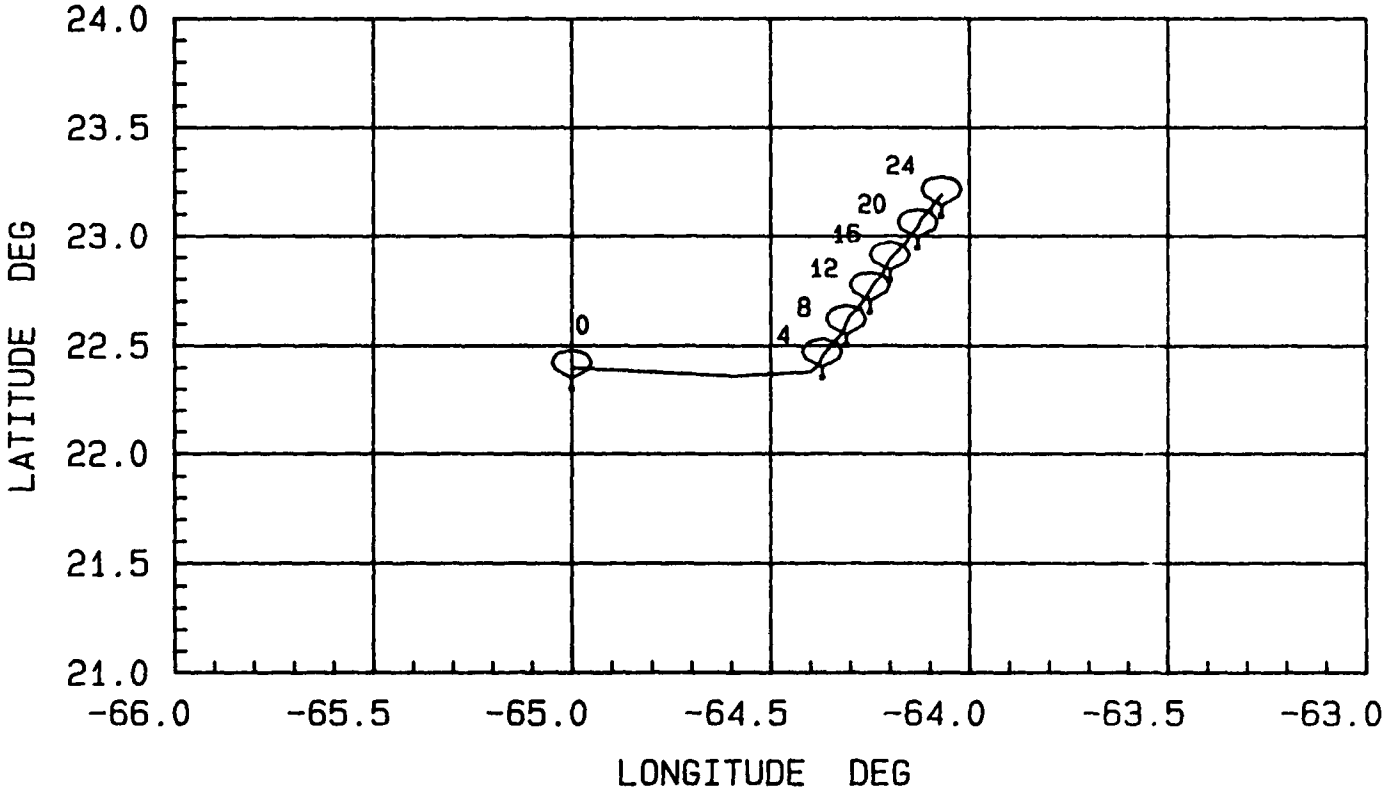

Figure 2.3–21. 24-Hour Drift Pattern for Flight North of Puerto Rico

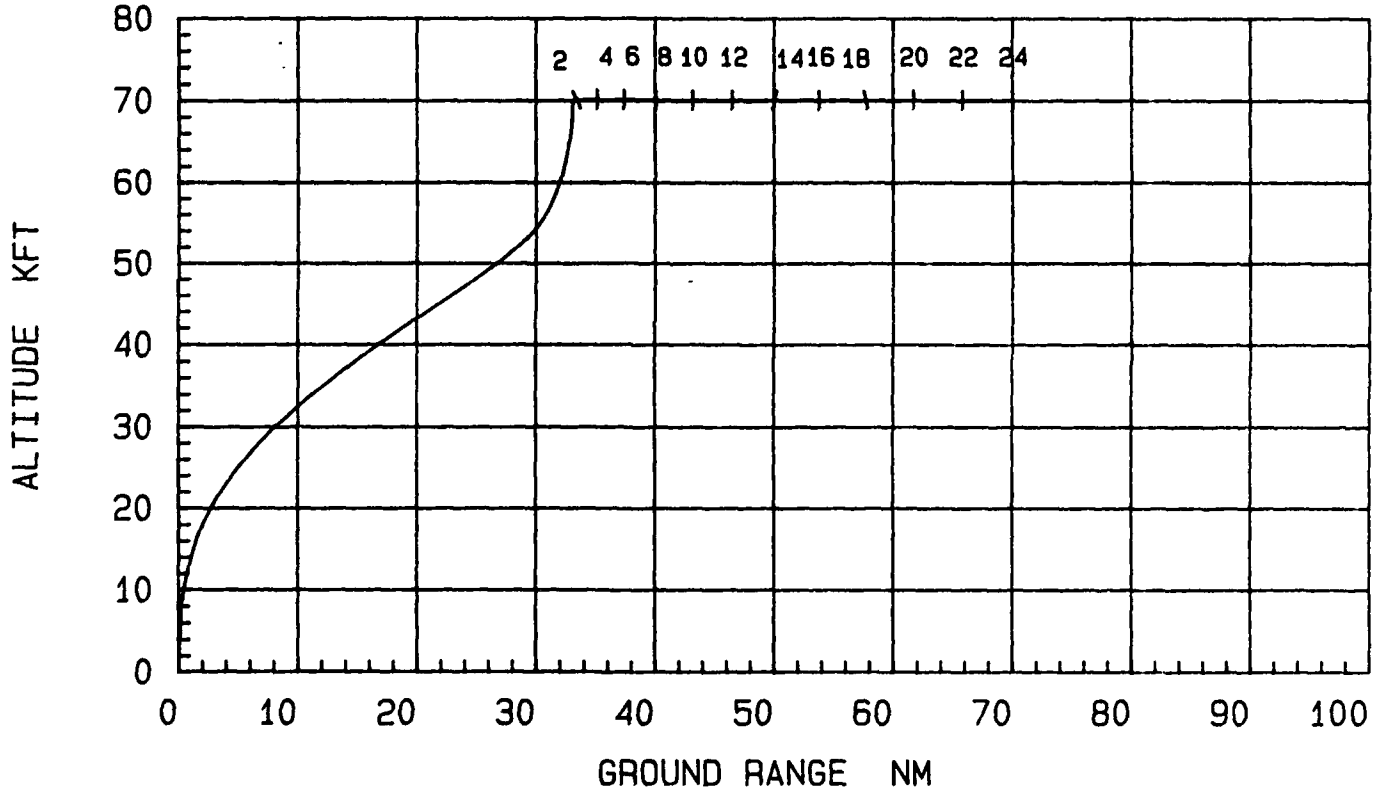

Figure 2.3–22. Altitude Versus Ground Range for 24-Hour Flight North of Puerto Rico

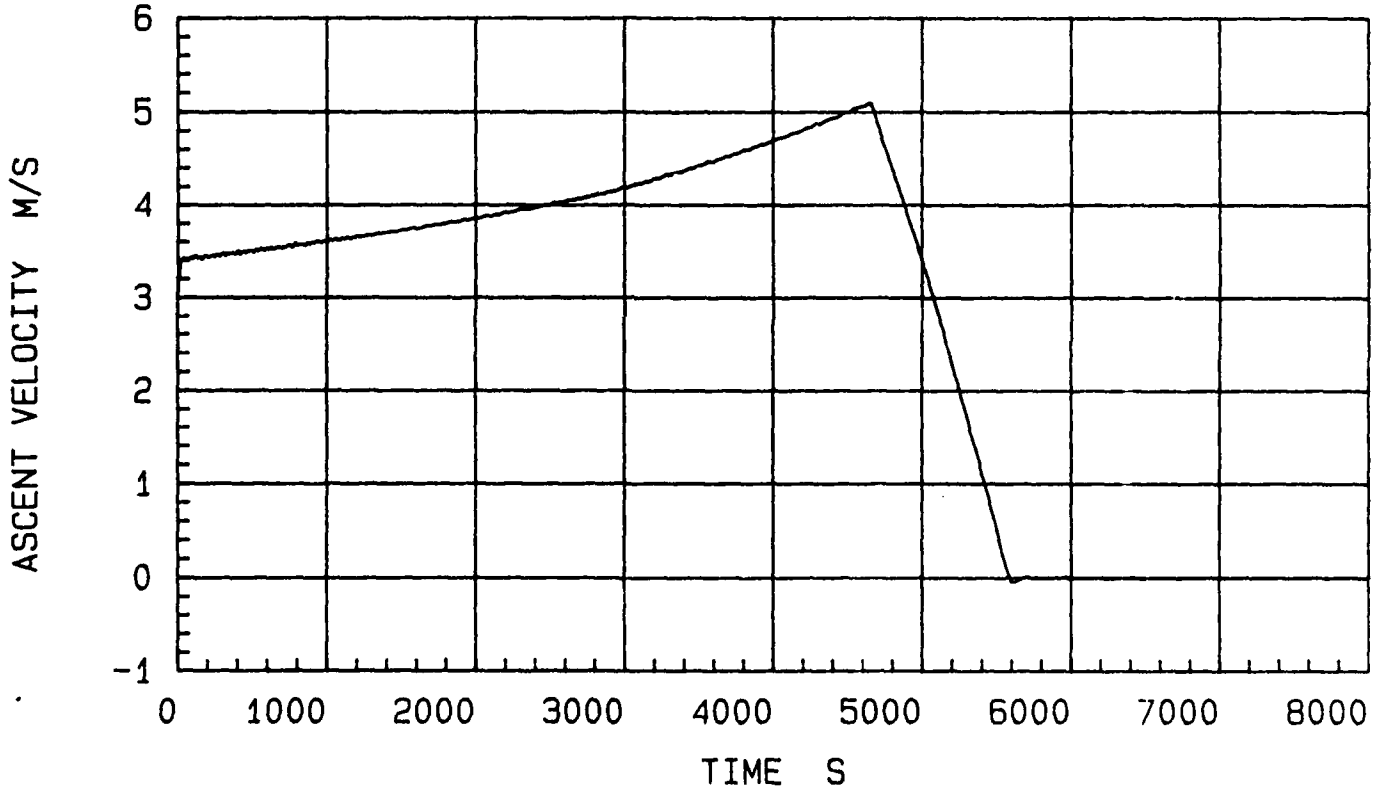

Figure 2.3–23. Ascent Velocity History for 24-Hour Flight North of Puerto Rico

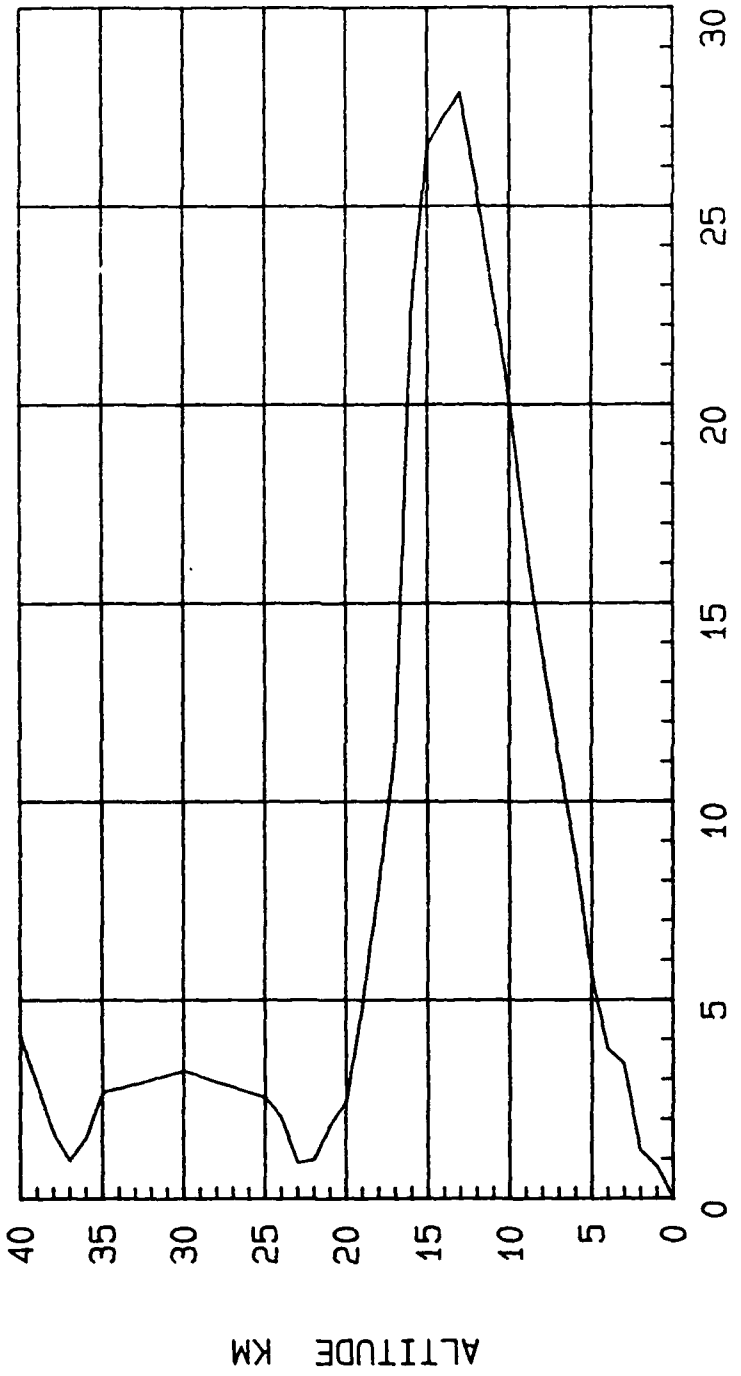

Figure 2.3–24. Wind Speed Profile North of Puerto Rico in January

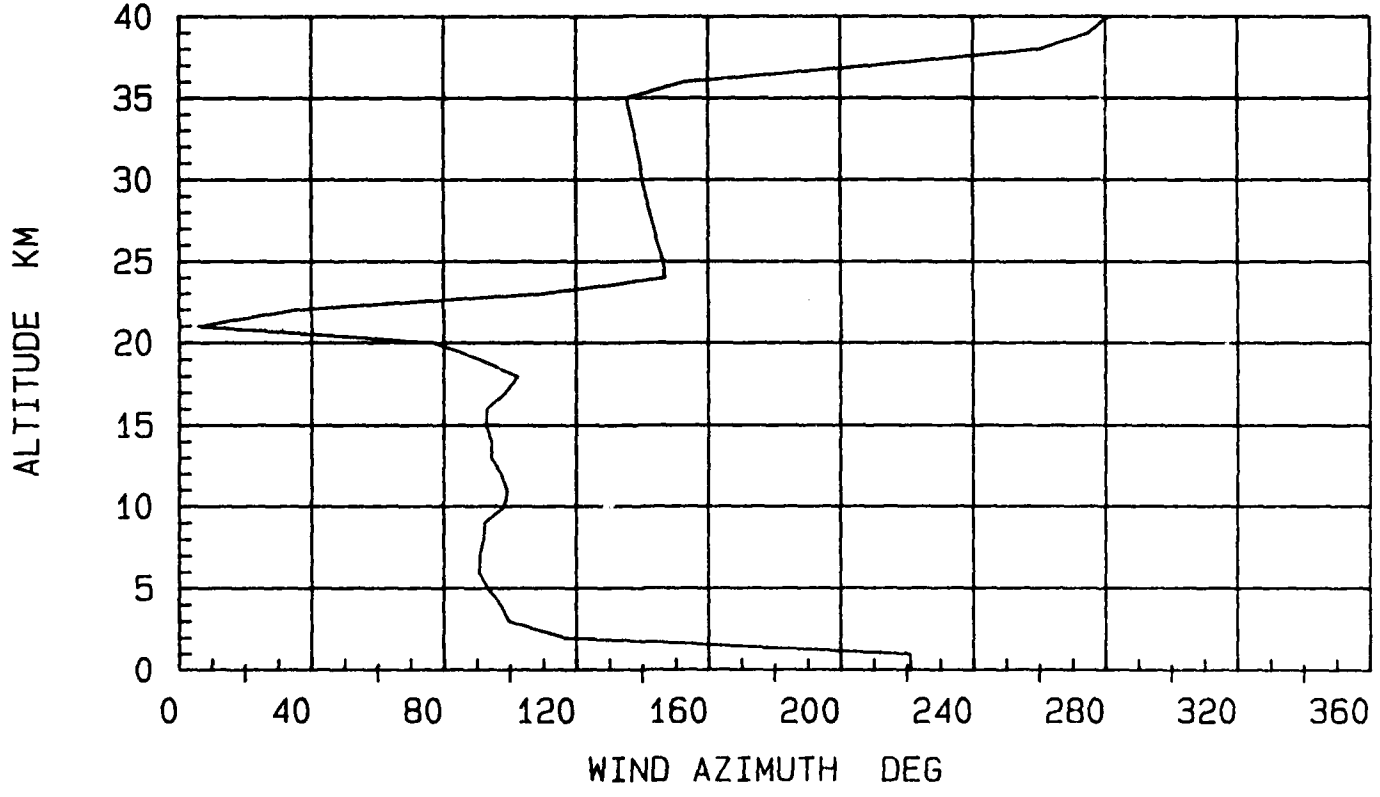

Figure 2.3–25. Wind Azimuth Profile North of Puerto Rico in January

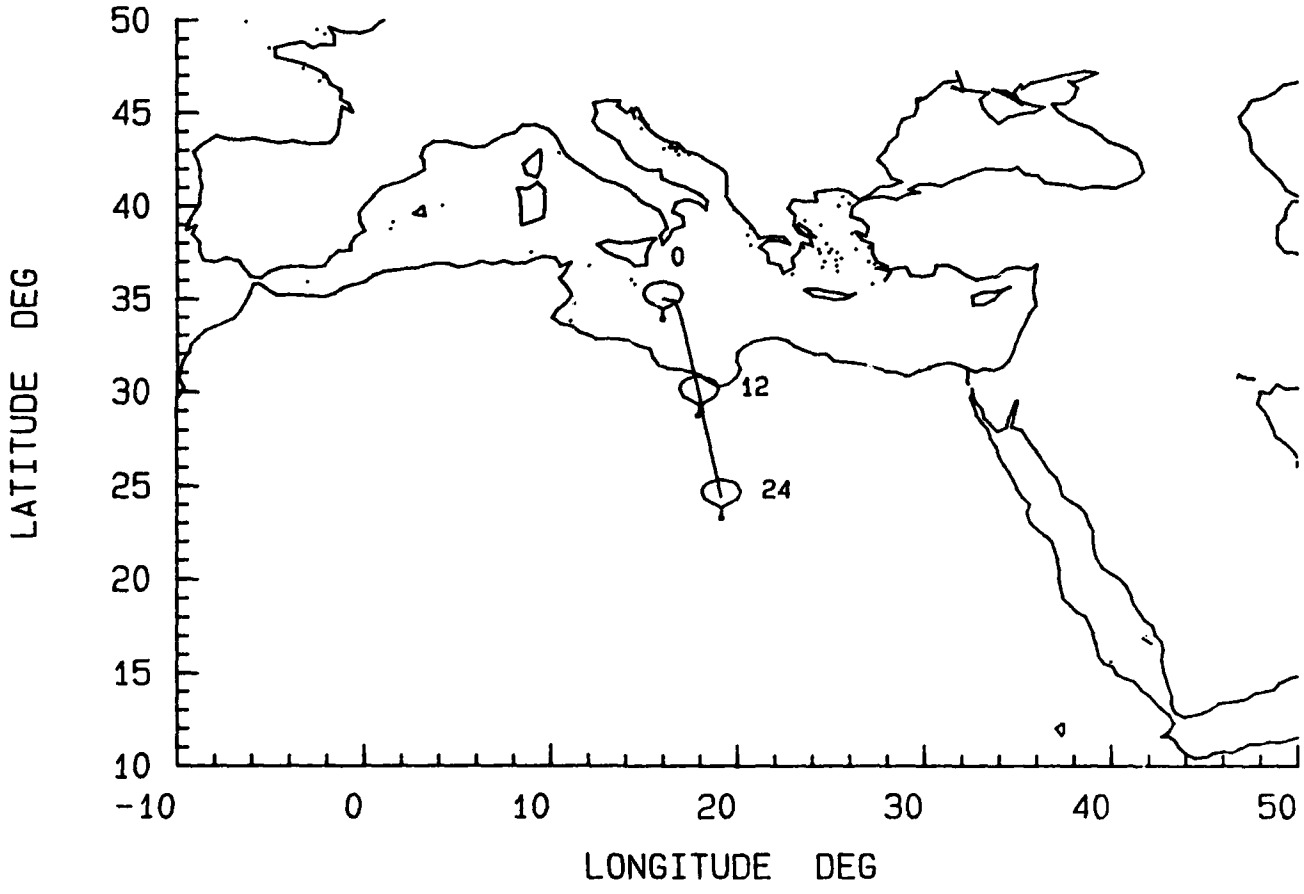

Figure 2.3–26. 24-Hour Drift Pattern for Mediterranean Sea Flight

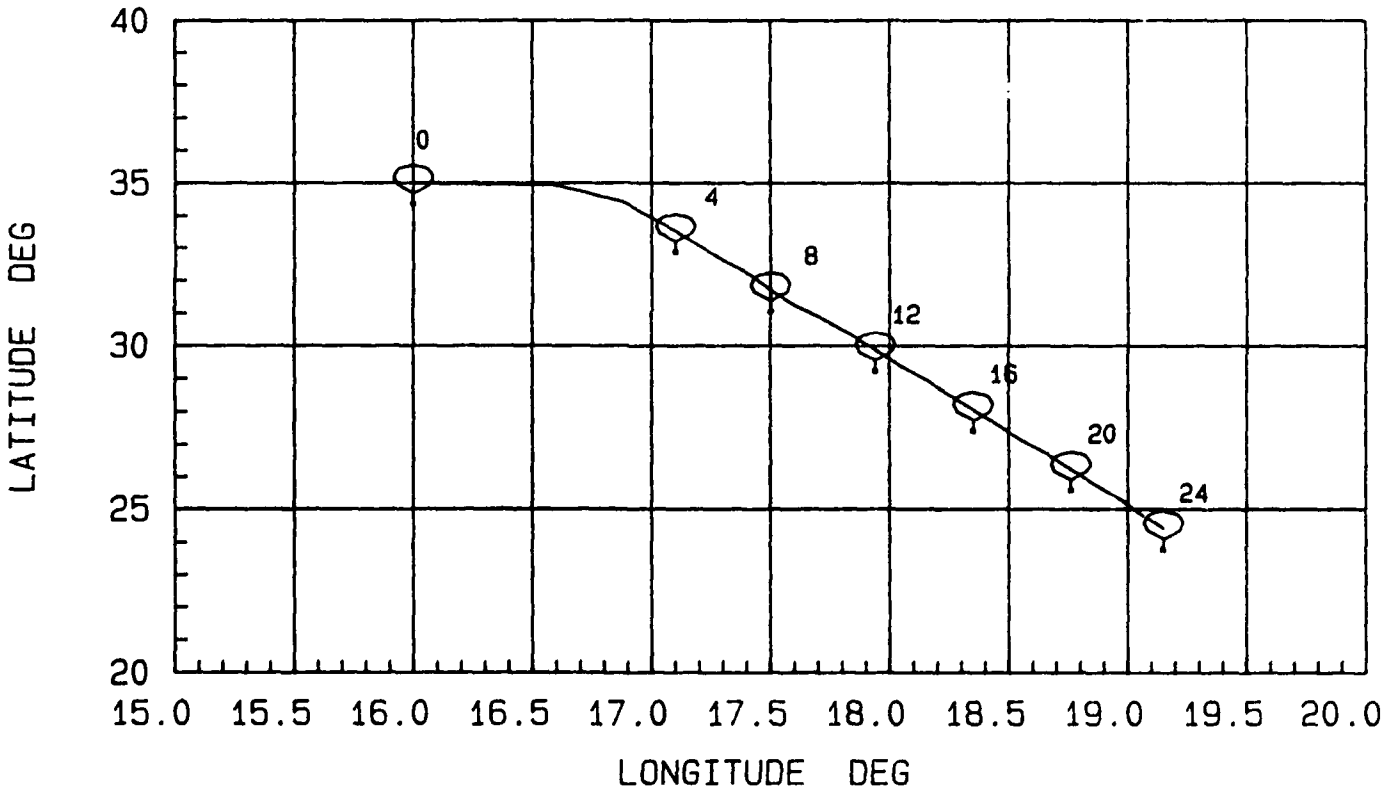

Figure 2.3–27. 24-Hour Drift Pattern for Mediterranean Flight

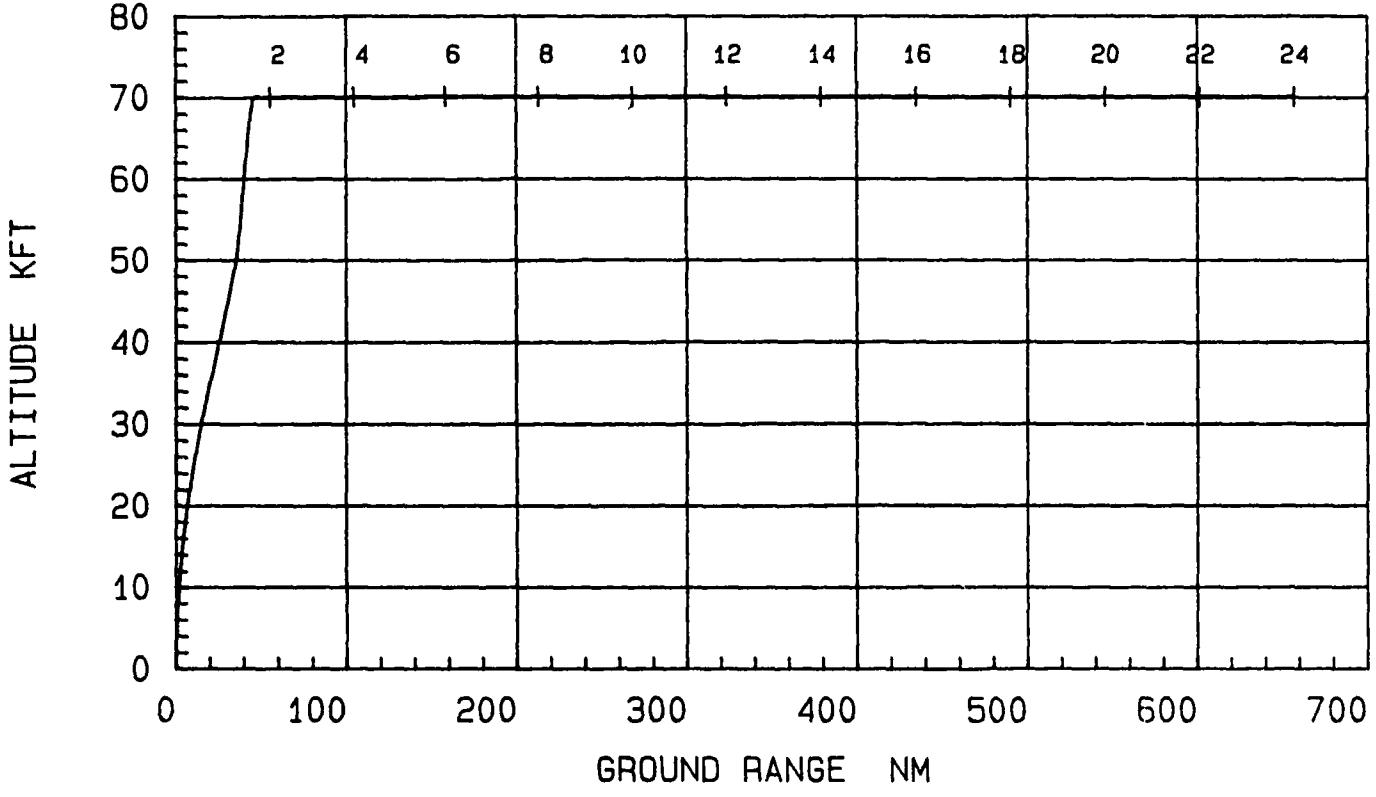

Figure 2.3–28. Altitude Versus Ground Range for 24-Hour Mediterranean Sea Flight

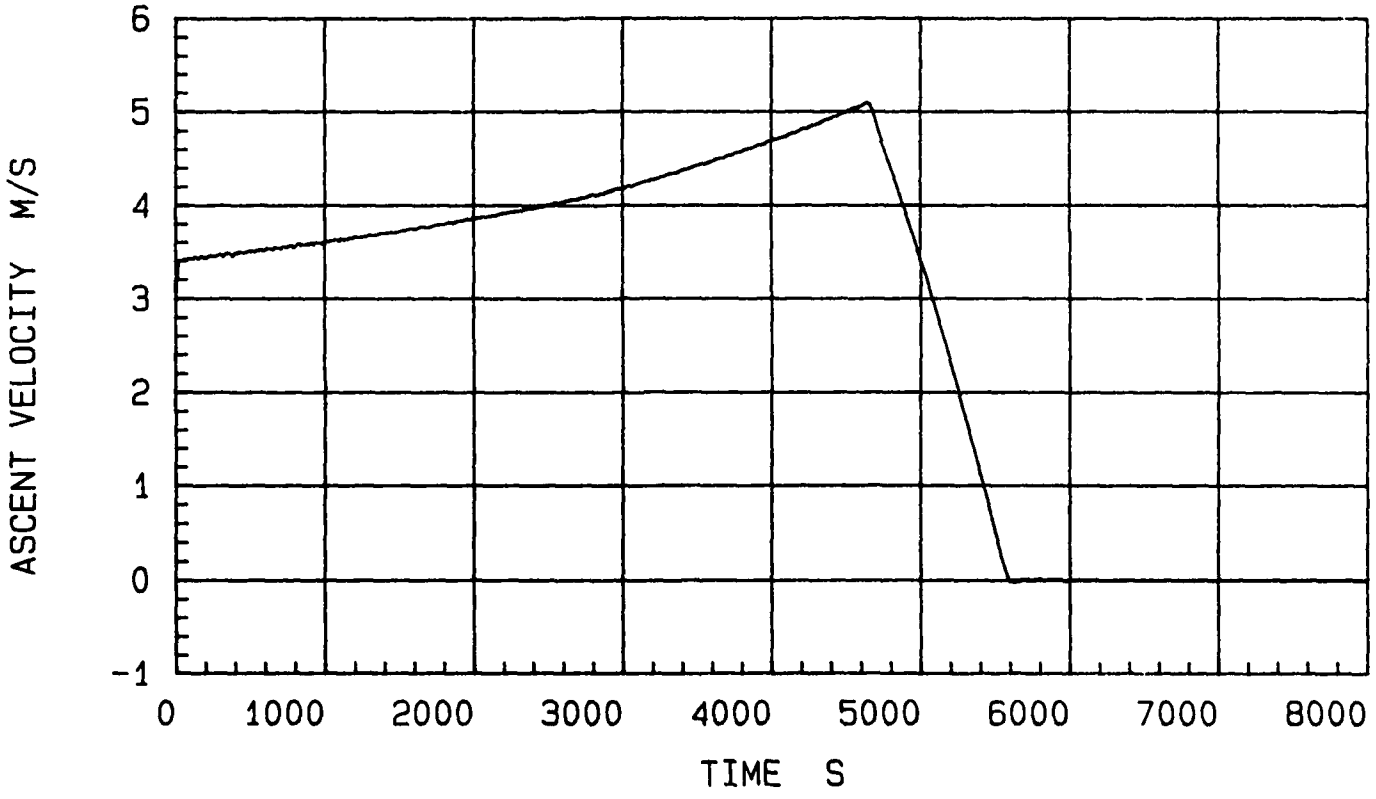

Figure 2.3–29. Ascent Velocity History for 24-Hour Mediterranean Sea Flight

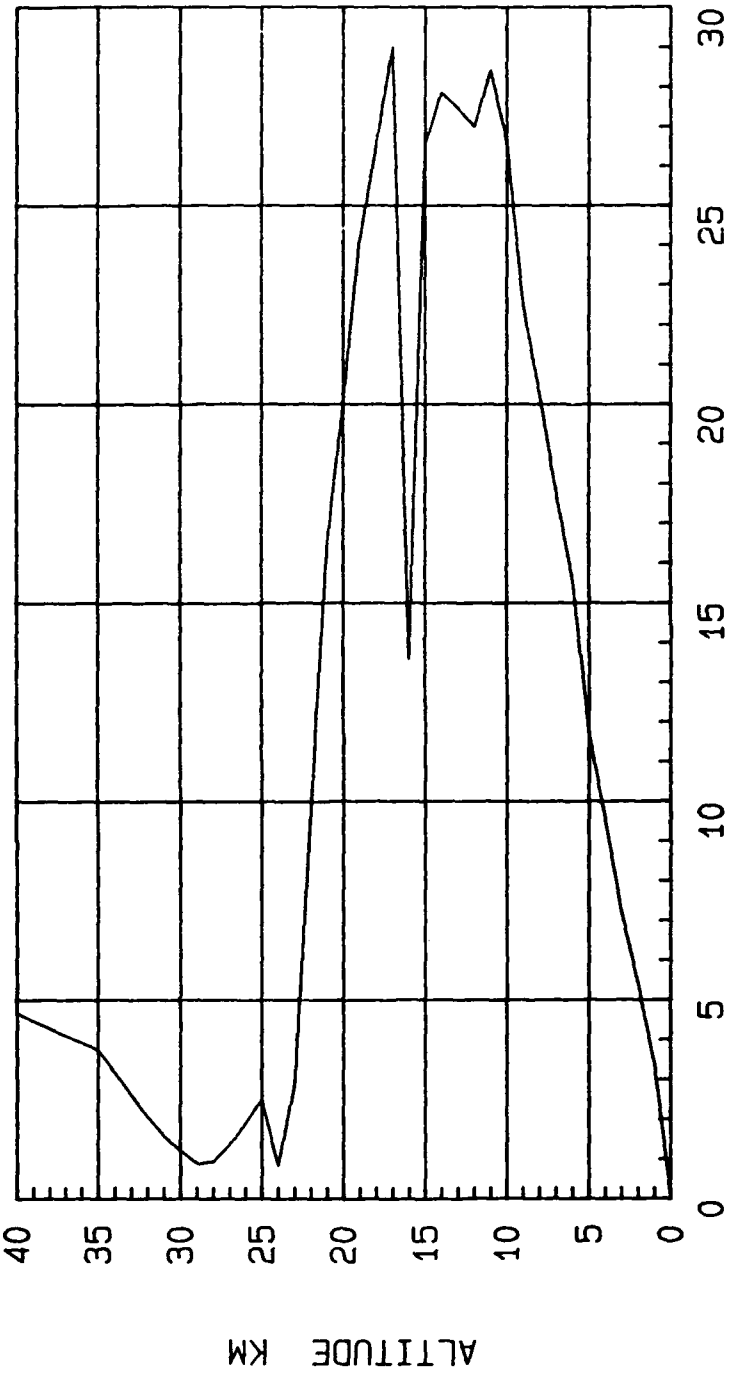

Figure 2.3–30. Wind Speed Profile in Mediterranean Sea in January

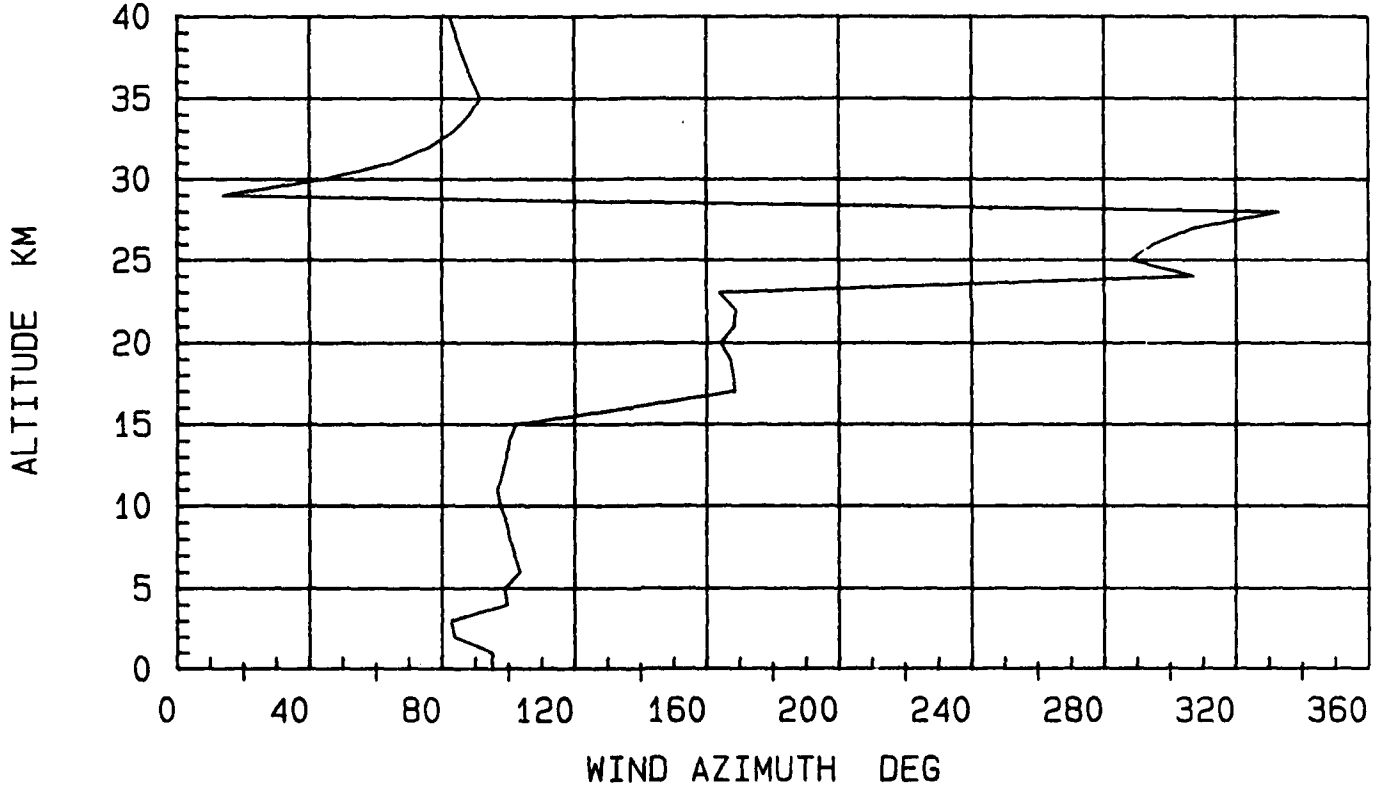

Figure 2.3–31. Wind Azimuth Profile in Mediterranean Sea in January

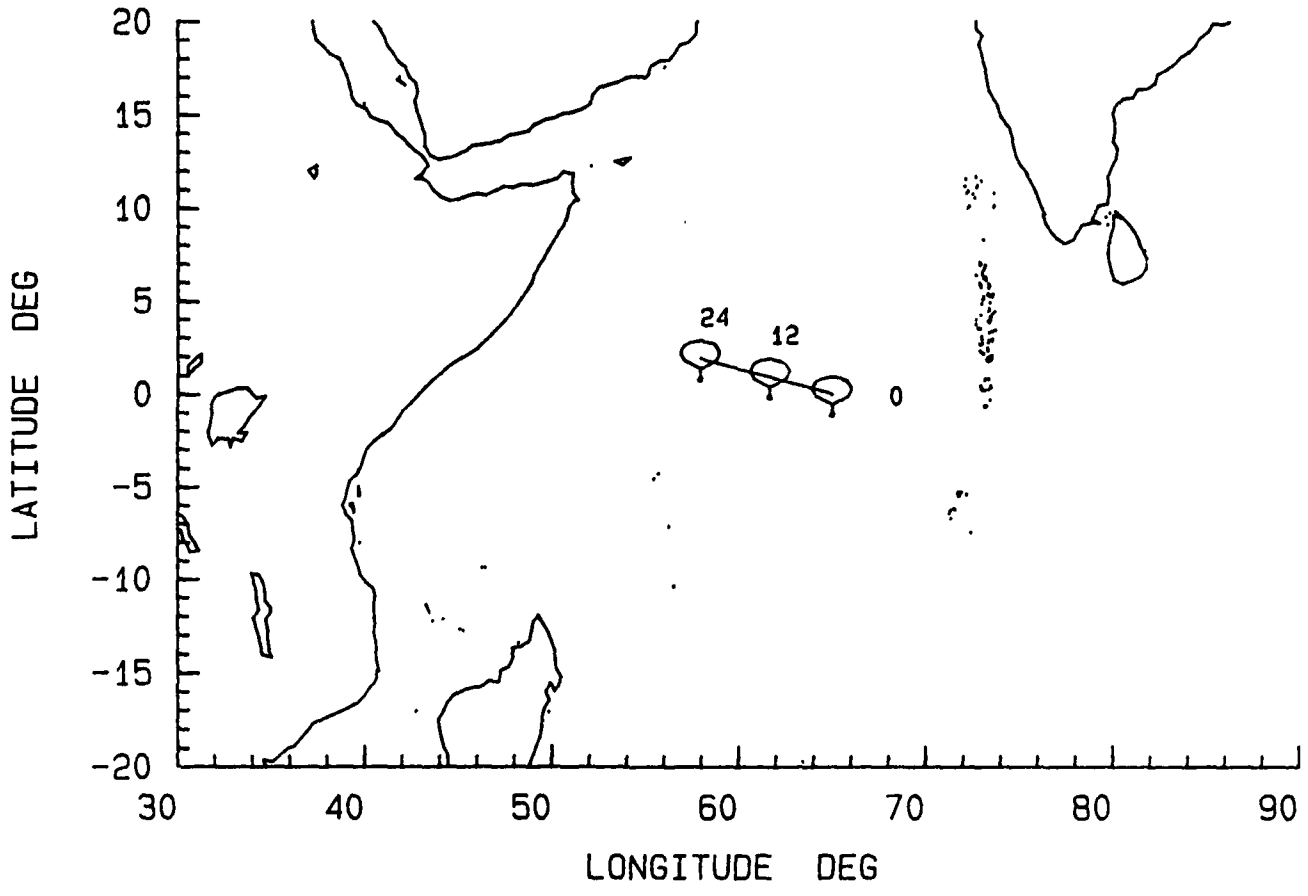

Figure 2.3–32. 24-Hour Drift Pattern for Indian Ocean Flight

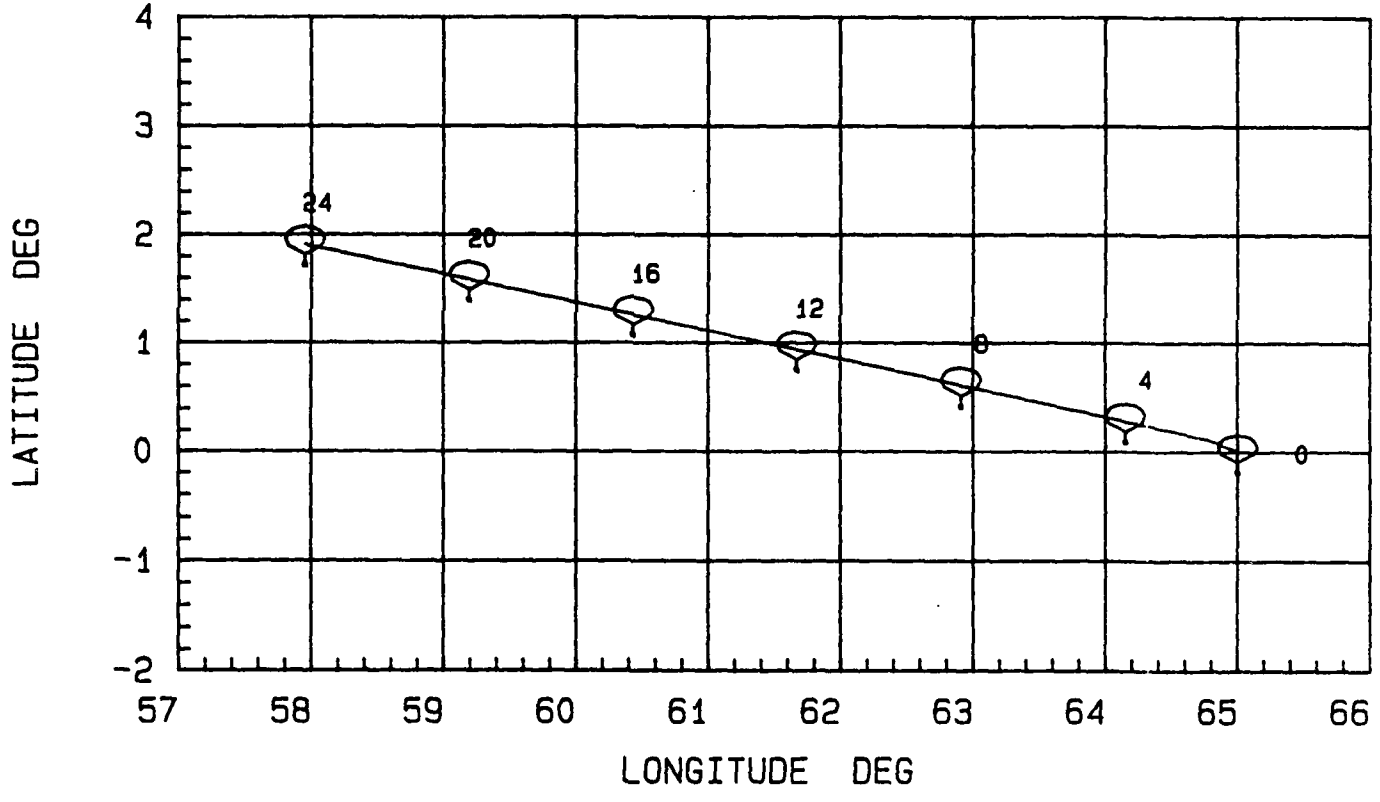

Figure 2.3–33. 24-Hour Drift Pattern for Indian Ocean Flight

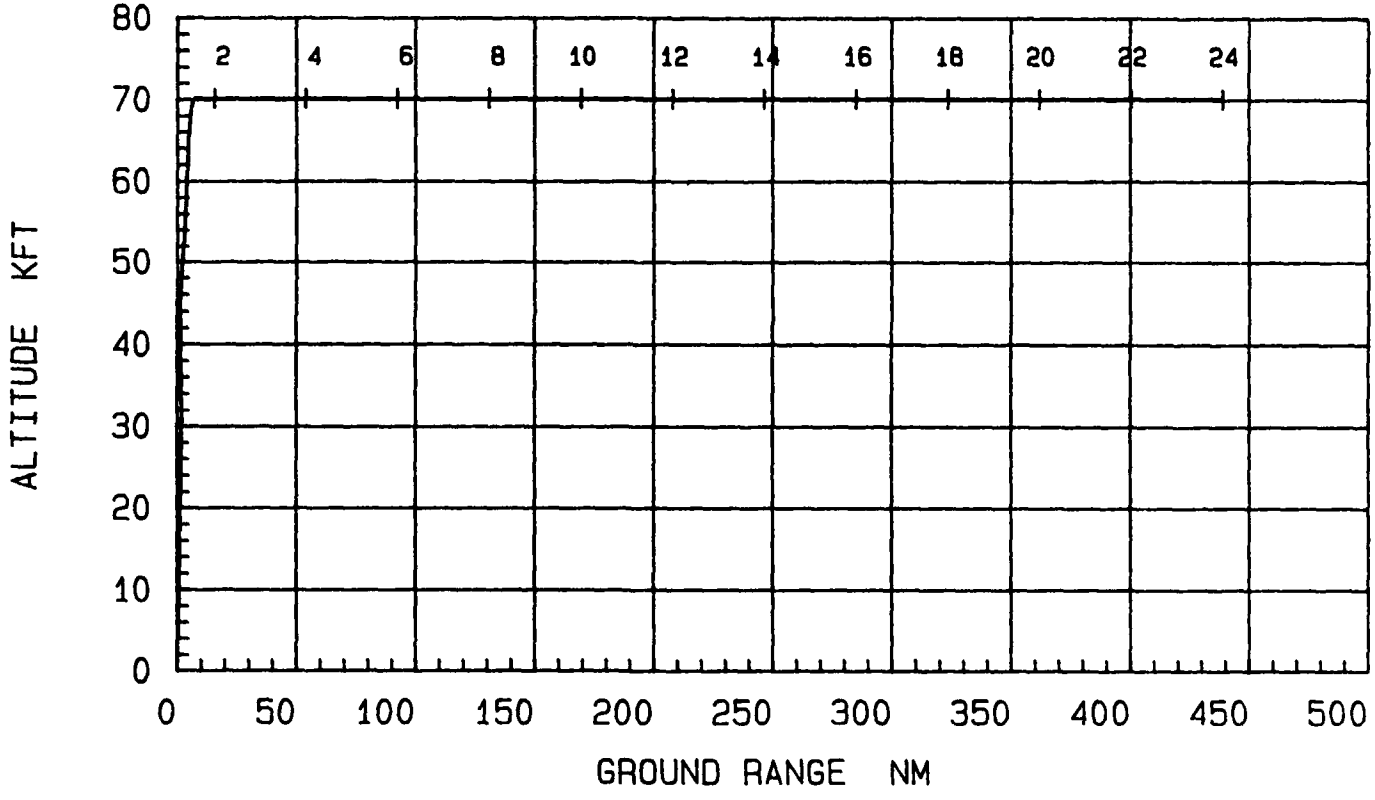

Figure 2.3–34. Altitude Versus Ground Range for 24-Hour Indian Ocean Flight

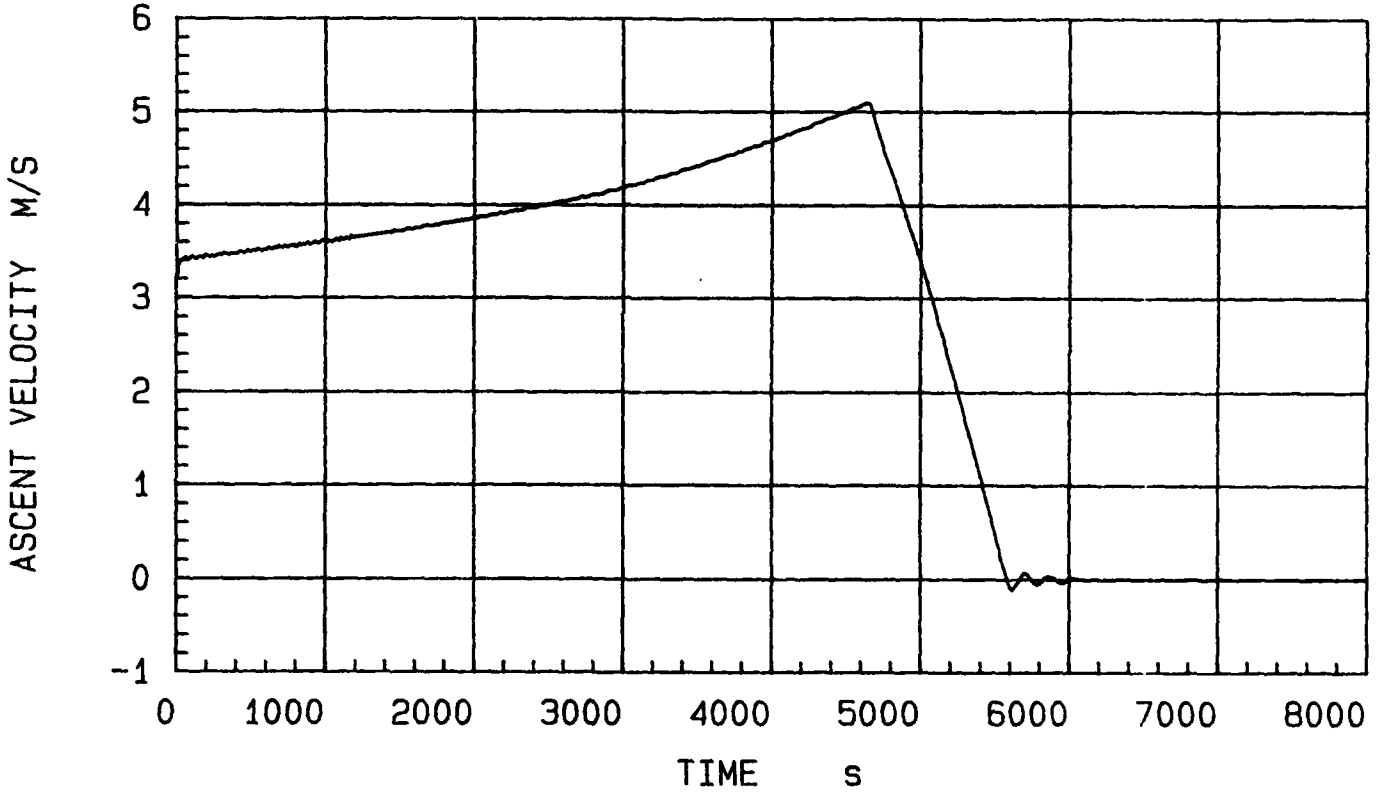

Figure 2.3–35. Ascent Velocity History for 24-Hour Indian Ocean Flight

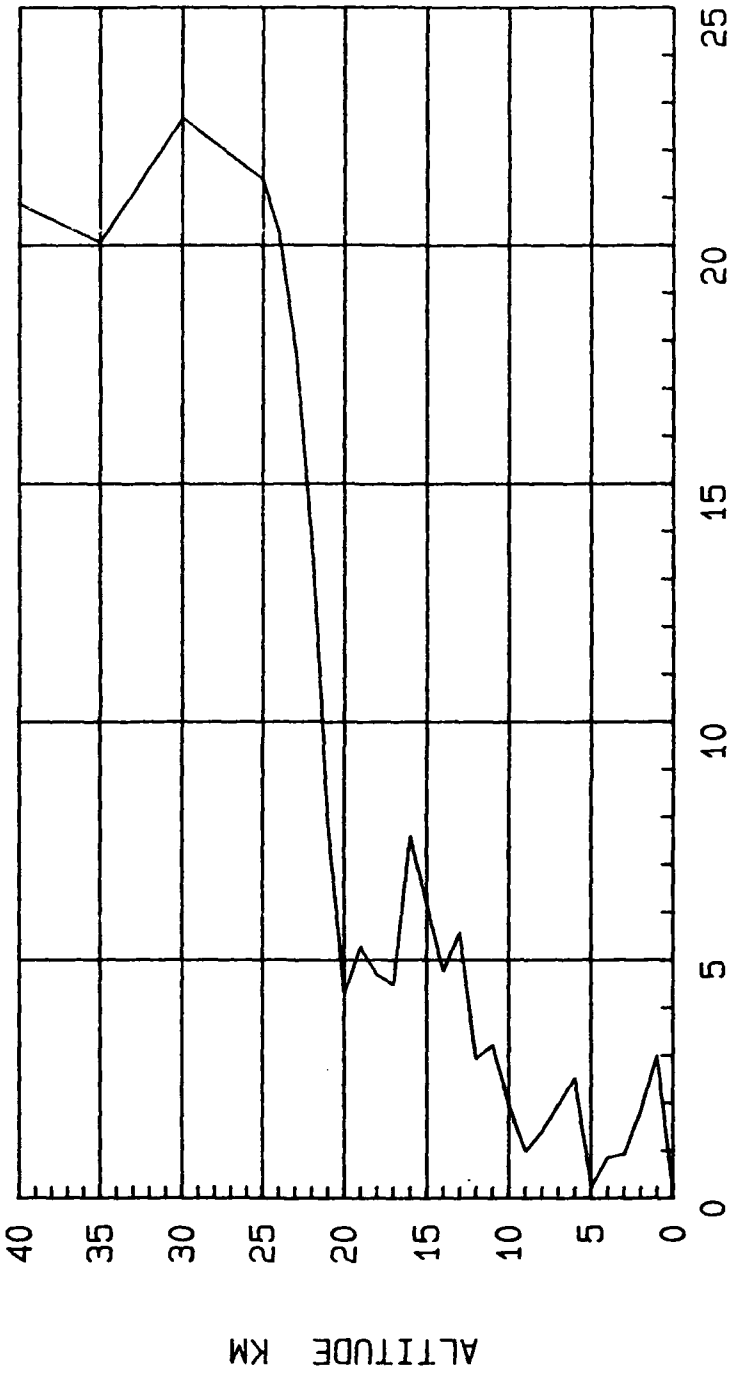

Figure 2.3–36. Wind Speed Profile in Indian Ocean in January

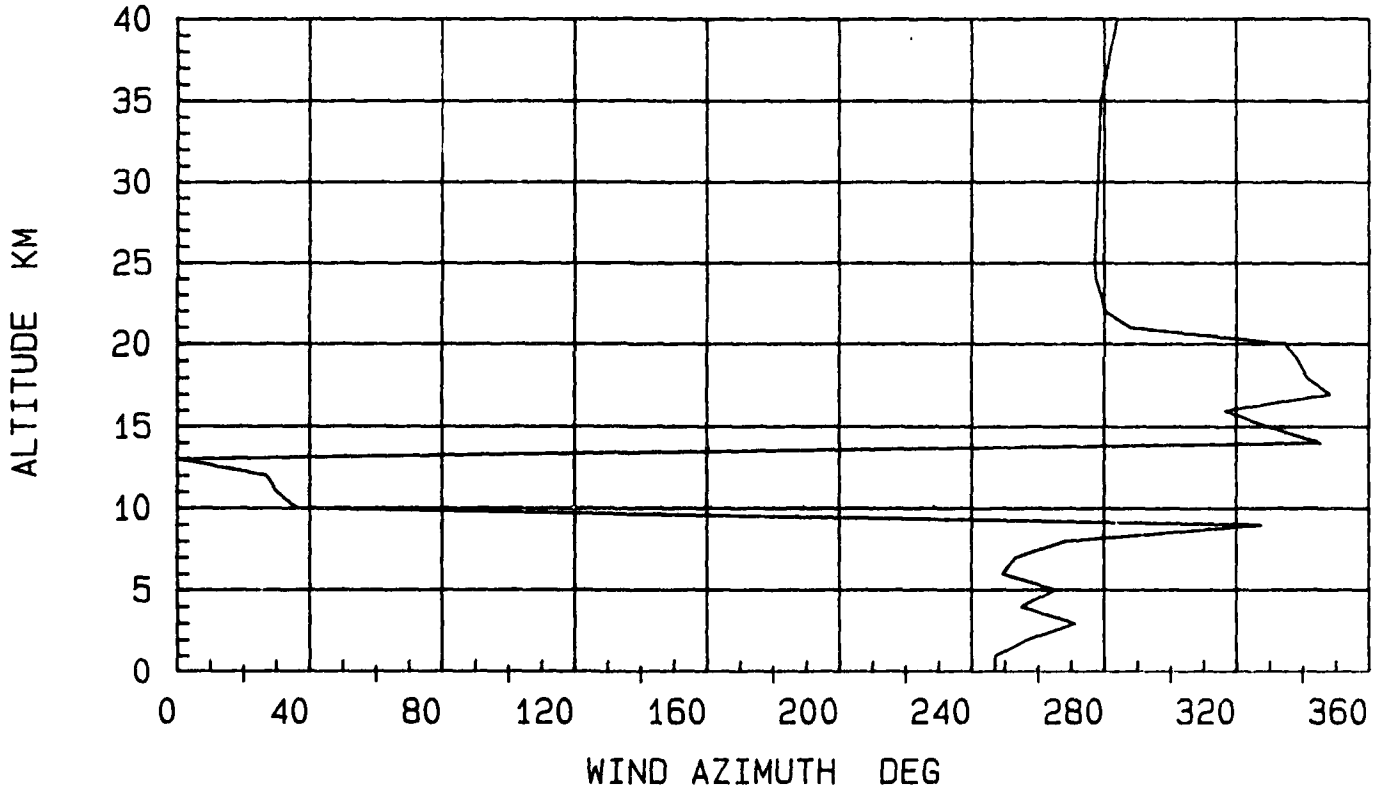

Figure 2.3–37. Wind Azimuth Profile in Indian Ocean in January

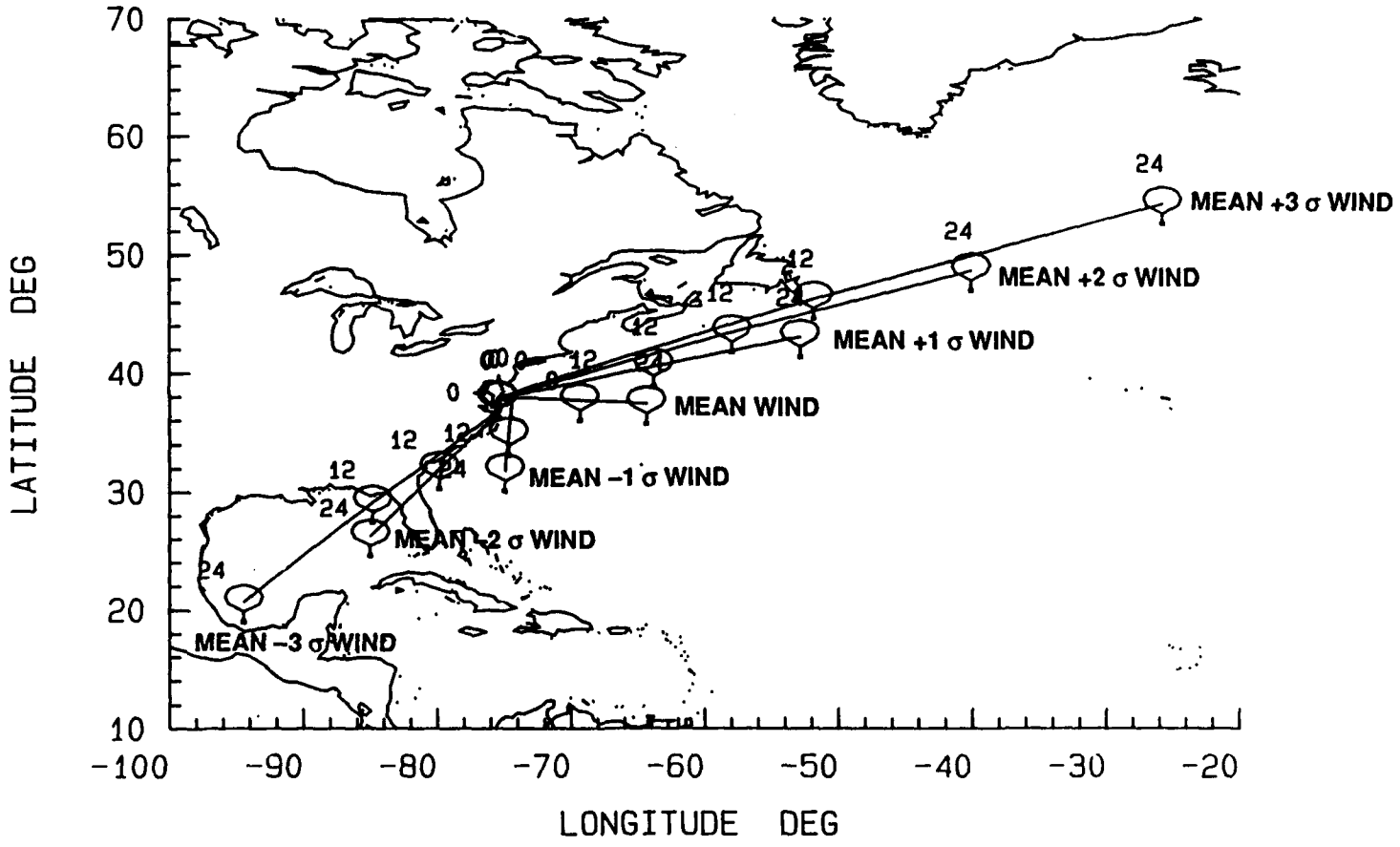

Figure 2.3–38. 24-Hour Drift Patterns for Wallops Island Flight with Statistical January Winds

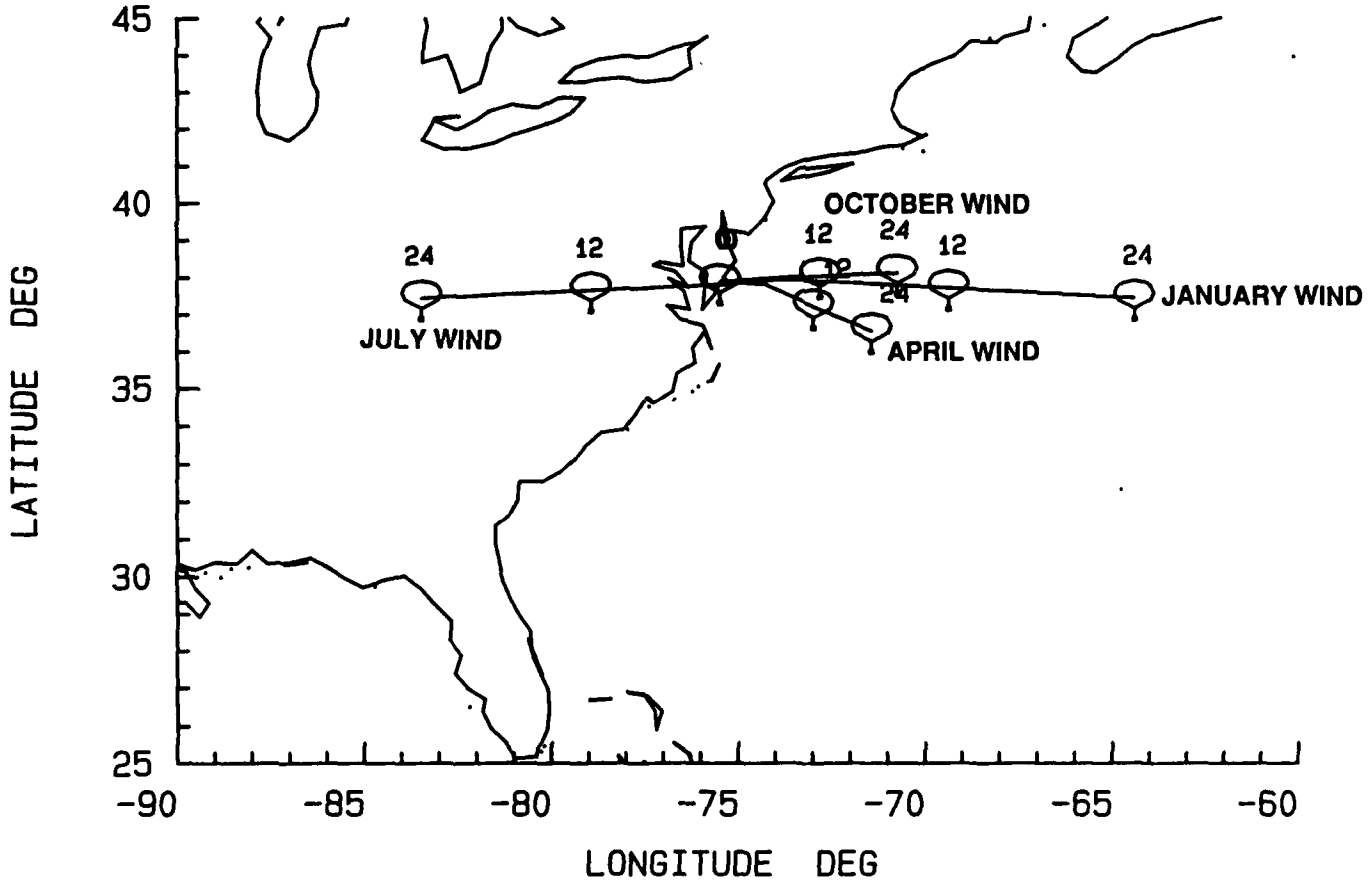

Figure 2.3–39. 24-Hour Drift Patterns for Wallops Island Flights Showing Effects of Seasonal Wind Variations

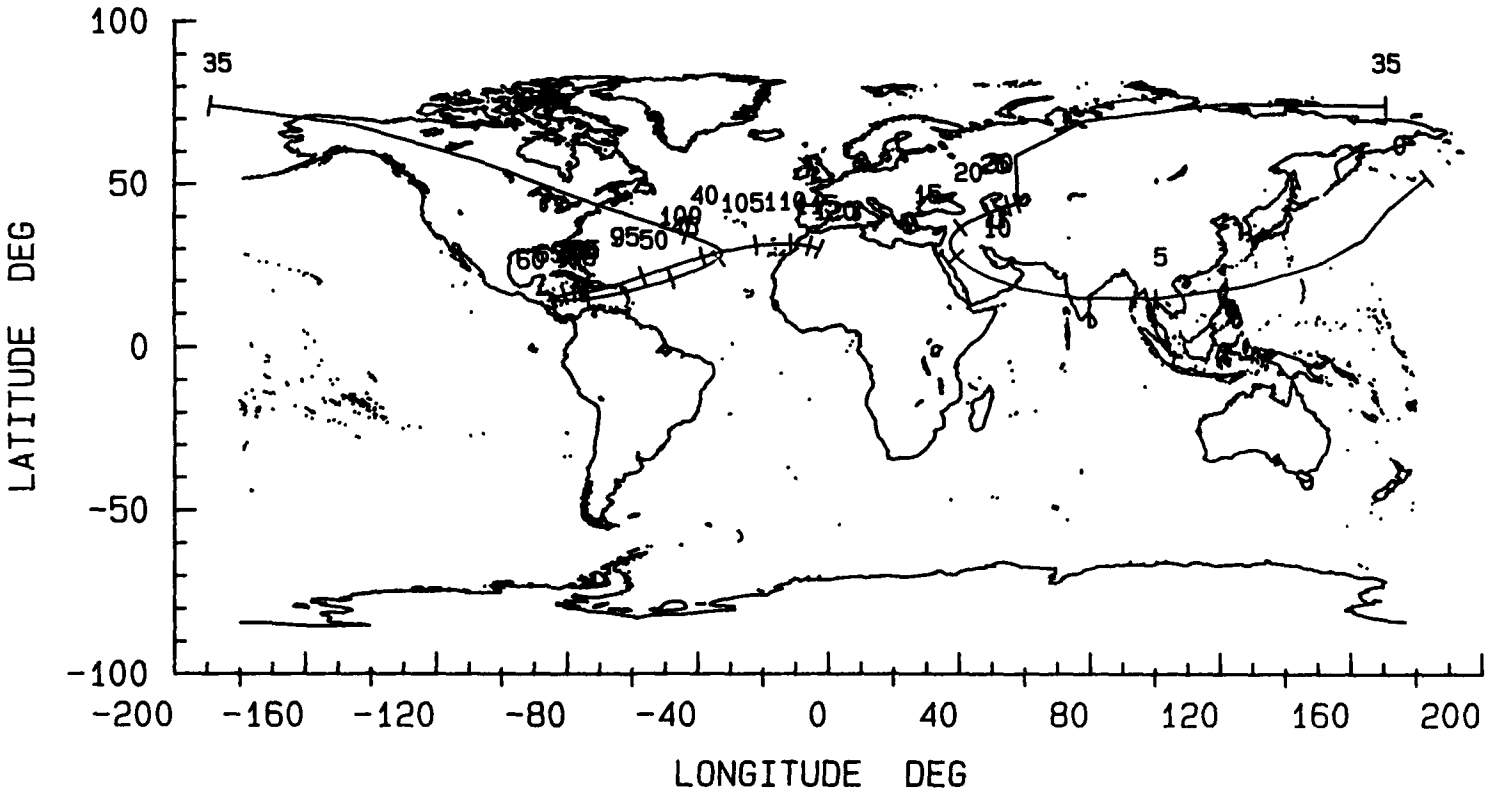

Figure 2.3–40. Super-Pressure Balloon Drift Pattern at 120,000 ft Altitude: Day 1 through Day 120 (Jan 1 — Apr. 30)

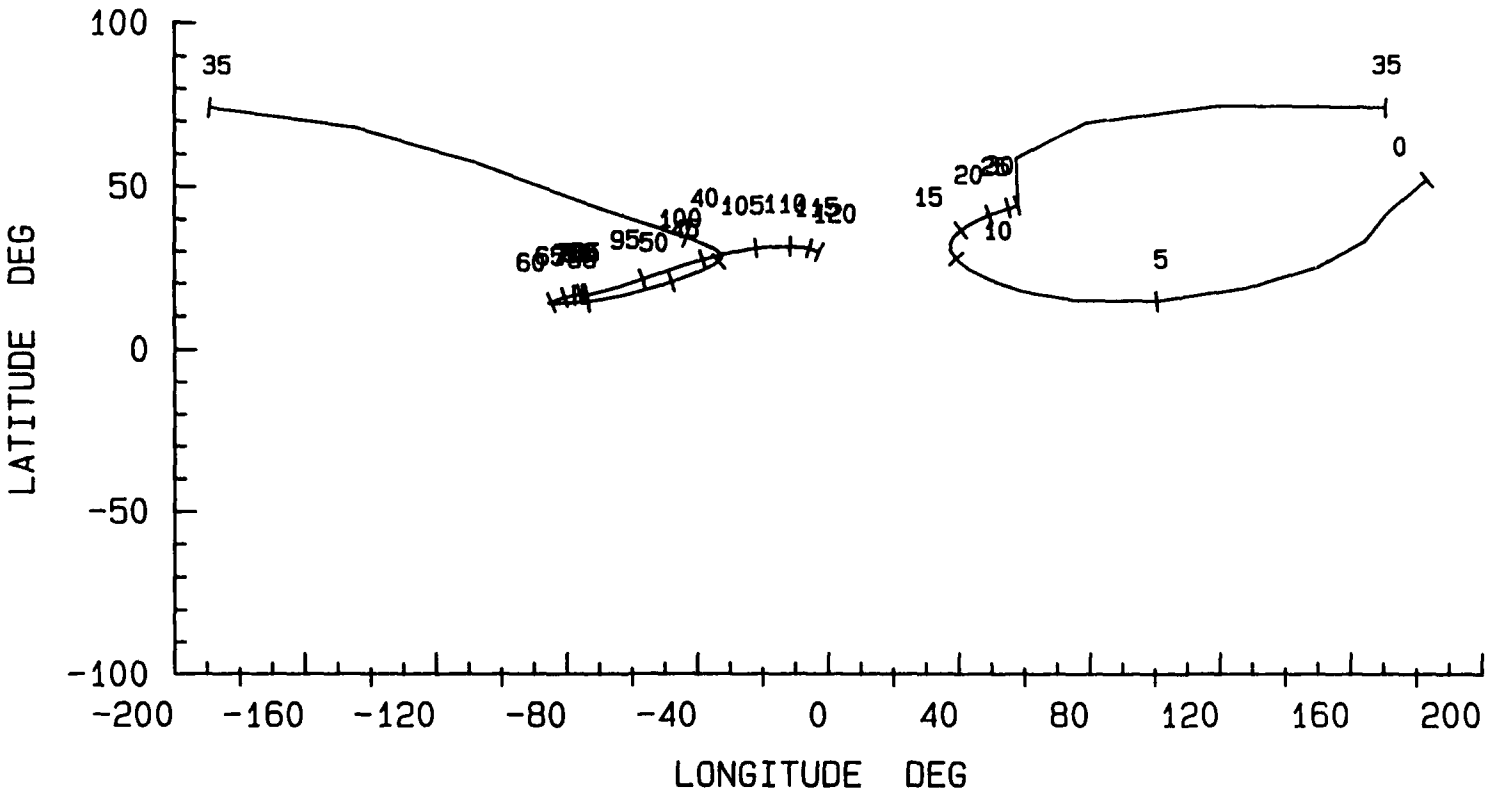

Figure 2.3–41. Super-Pressure Balloon Drift Pattern at 120,000 ft Altitude: Day 1 through Day 120 (Jan 1 — Apr. 30)

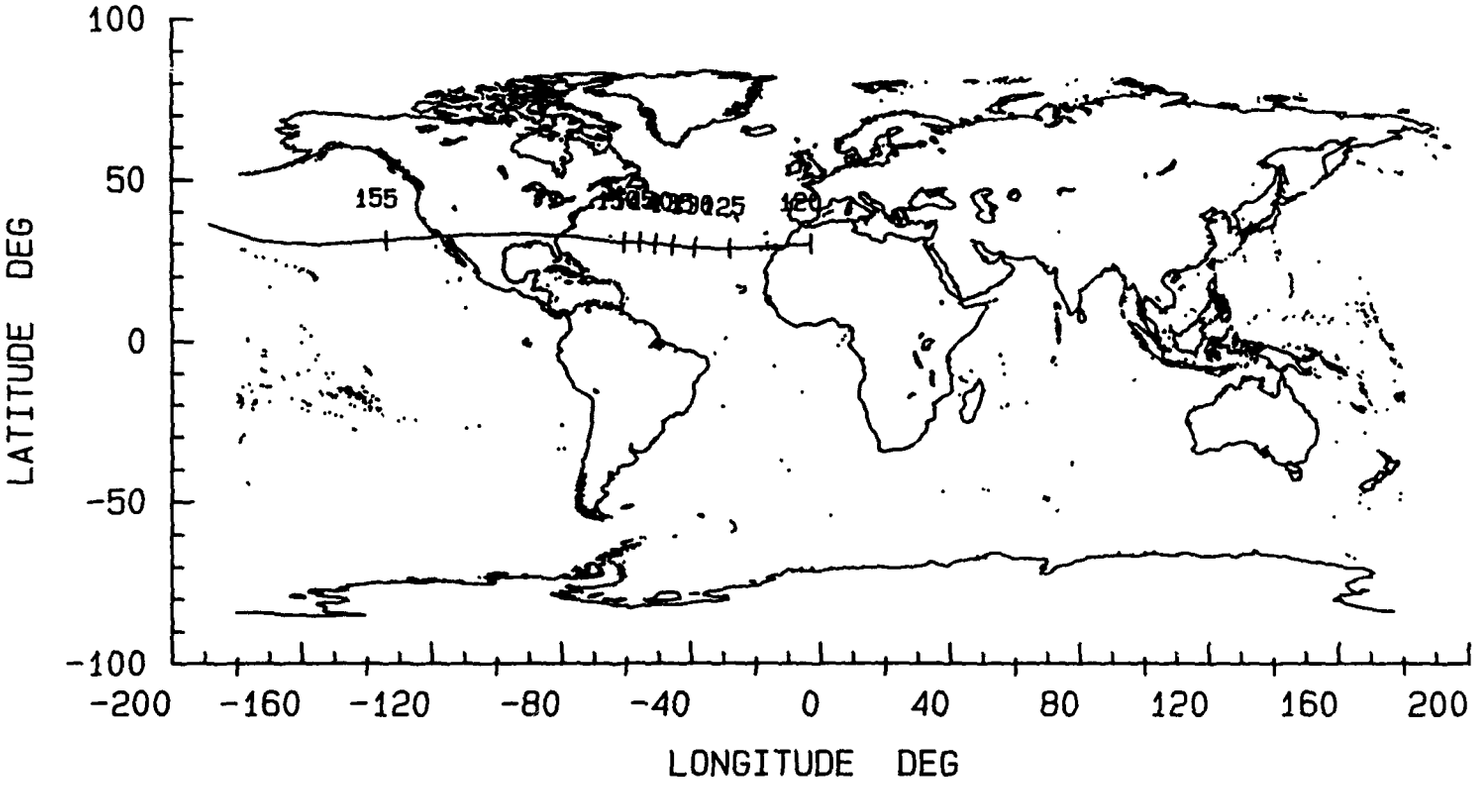

Figure 2.3–42. Super-Pressure Balloon Drift Pattern at 120,000 ft Altitude: Day 120 through Day 158 (Apr. 30 — Jun. 7)

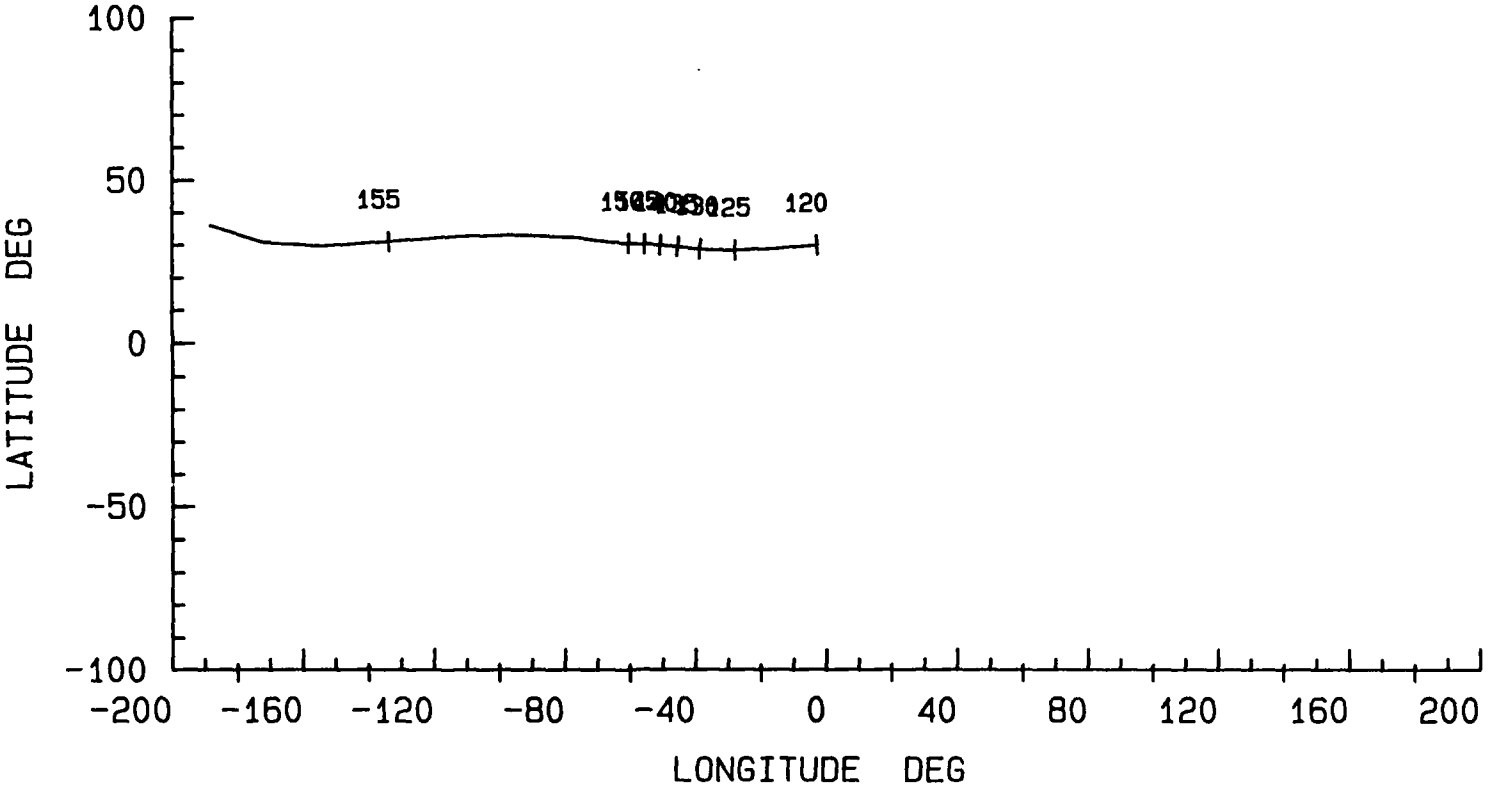

Figure 2.3–43. Super-Pressure Balloon Drift Pattern at 120,000 ft Altitude: Day 120 through Day 158 (Apr. 30 — Jun. 7)

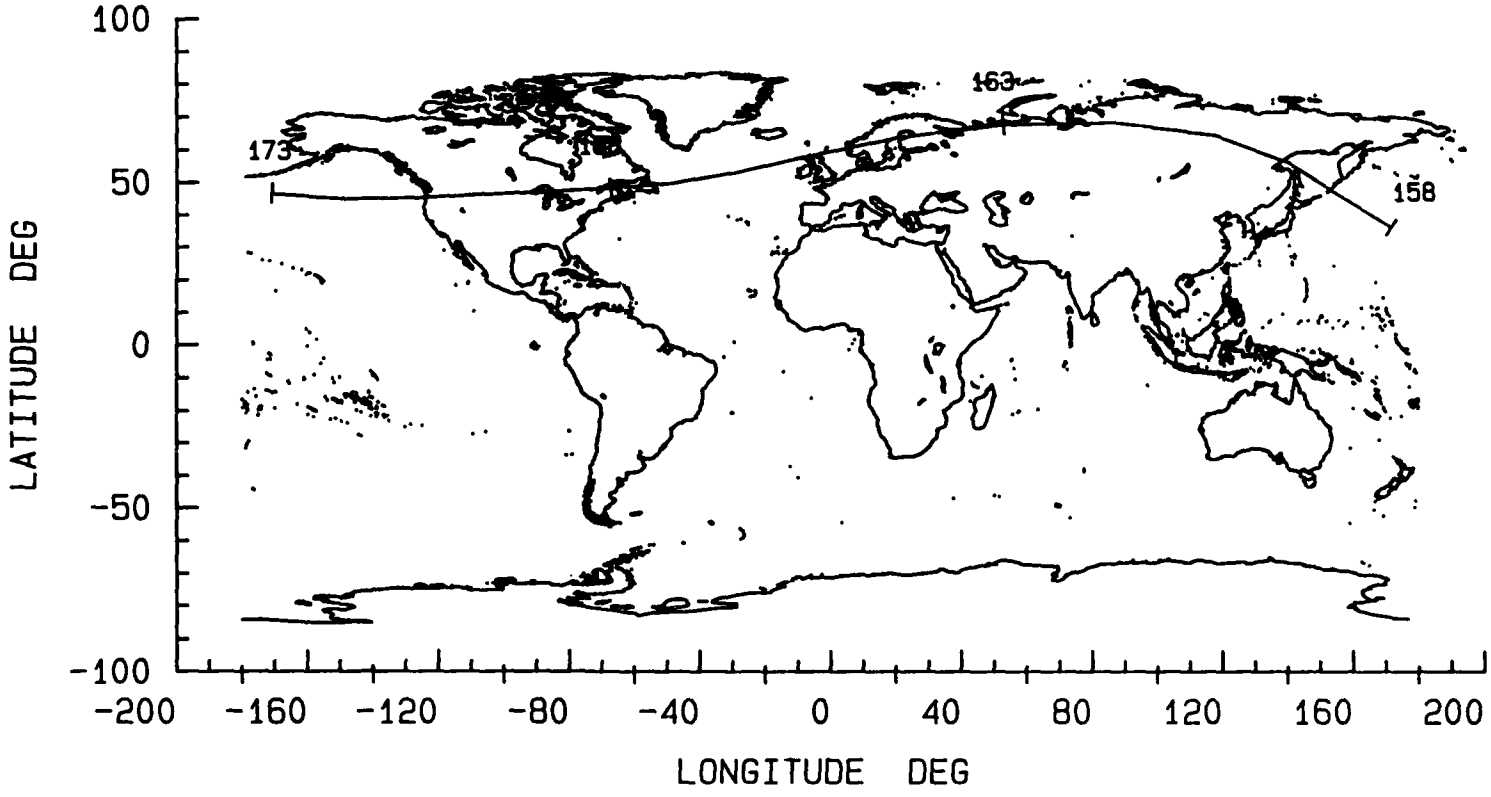

Figure 2.3–44. Super-Pressure Balloon Drift Pattern at 120,000 ft Altitude: Day 158 through Day 173 (Jun. 7 — Jun. 22)

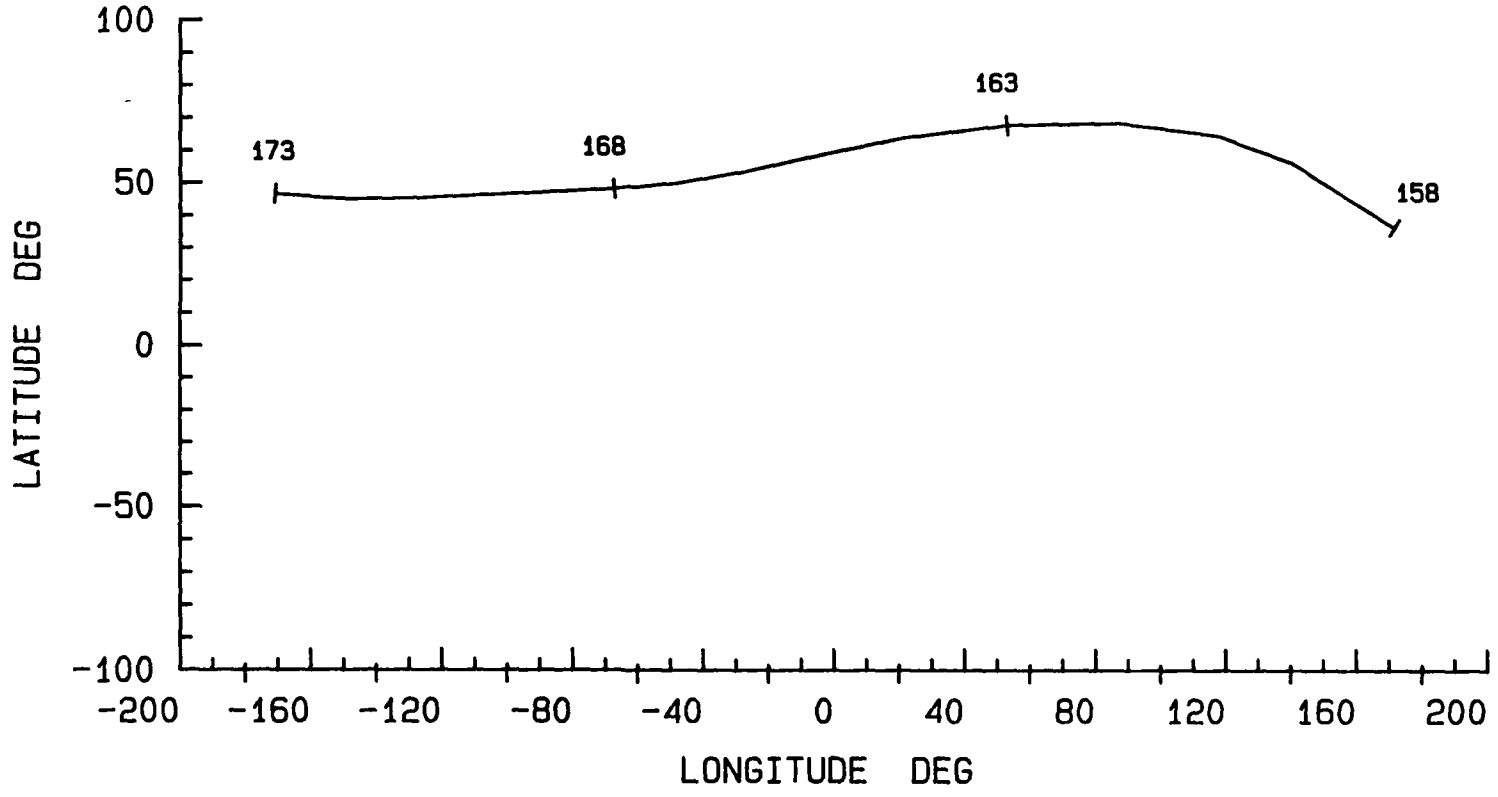

Figure 2.3–45. Super-Pressure Balloon Drift Pattern at 120,000 ft Altitude: Day 158 through Day 173 (Jun. 7 — Jun. 22)

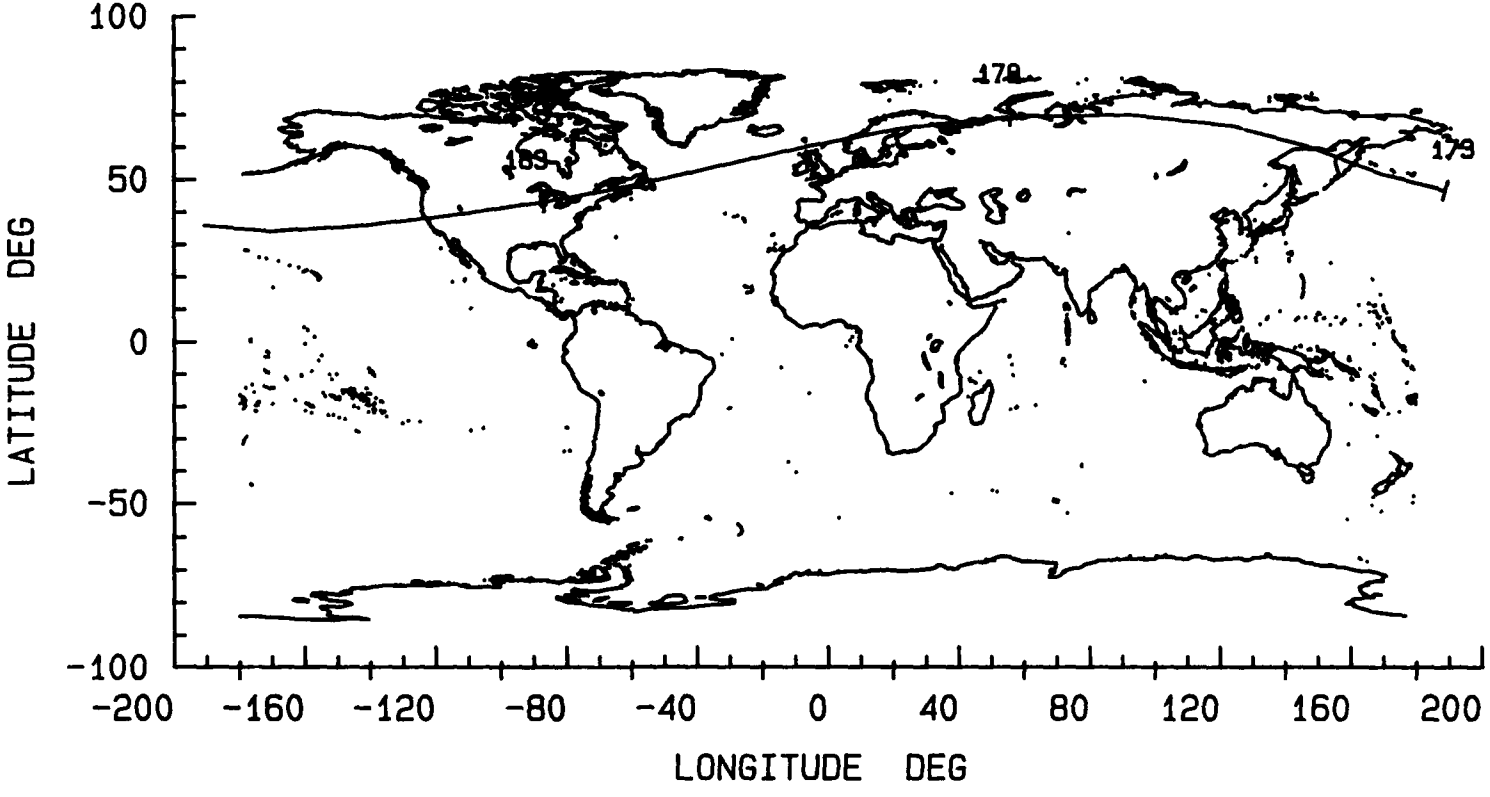

Figure 2.3–46. Super-Pressure Balloon Drift Pattern at 120,000 ft Altitude: Day 173 through Day 187 (Jun. 22— Jul. 6)

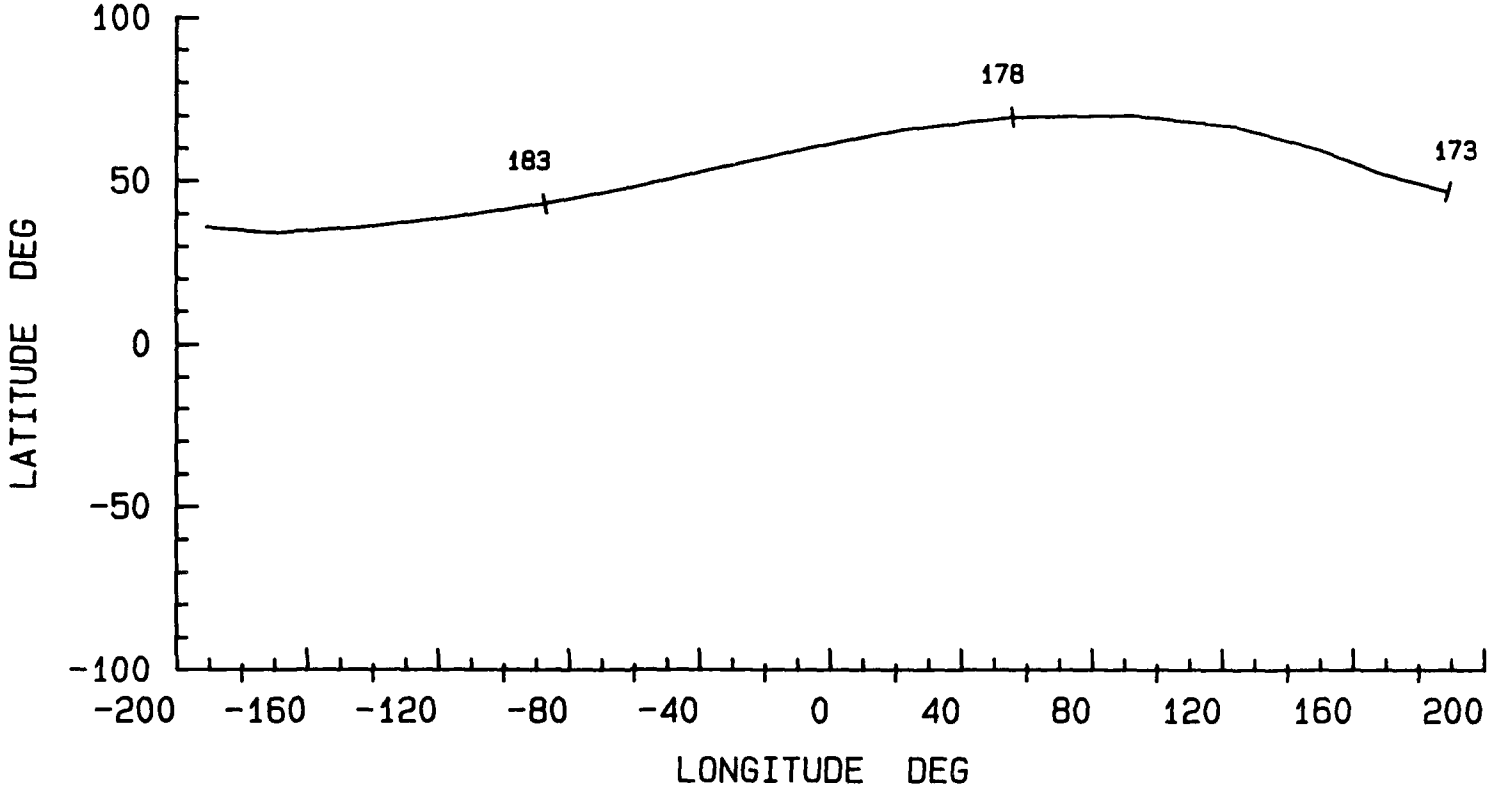

Figure 2.3–47. Super-Pressure Balloon Drift Pattern at 120,000 ft Altitude: Day 173 through Day 187 (Jun. 22— Jul. 6)

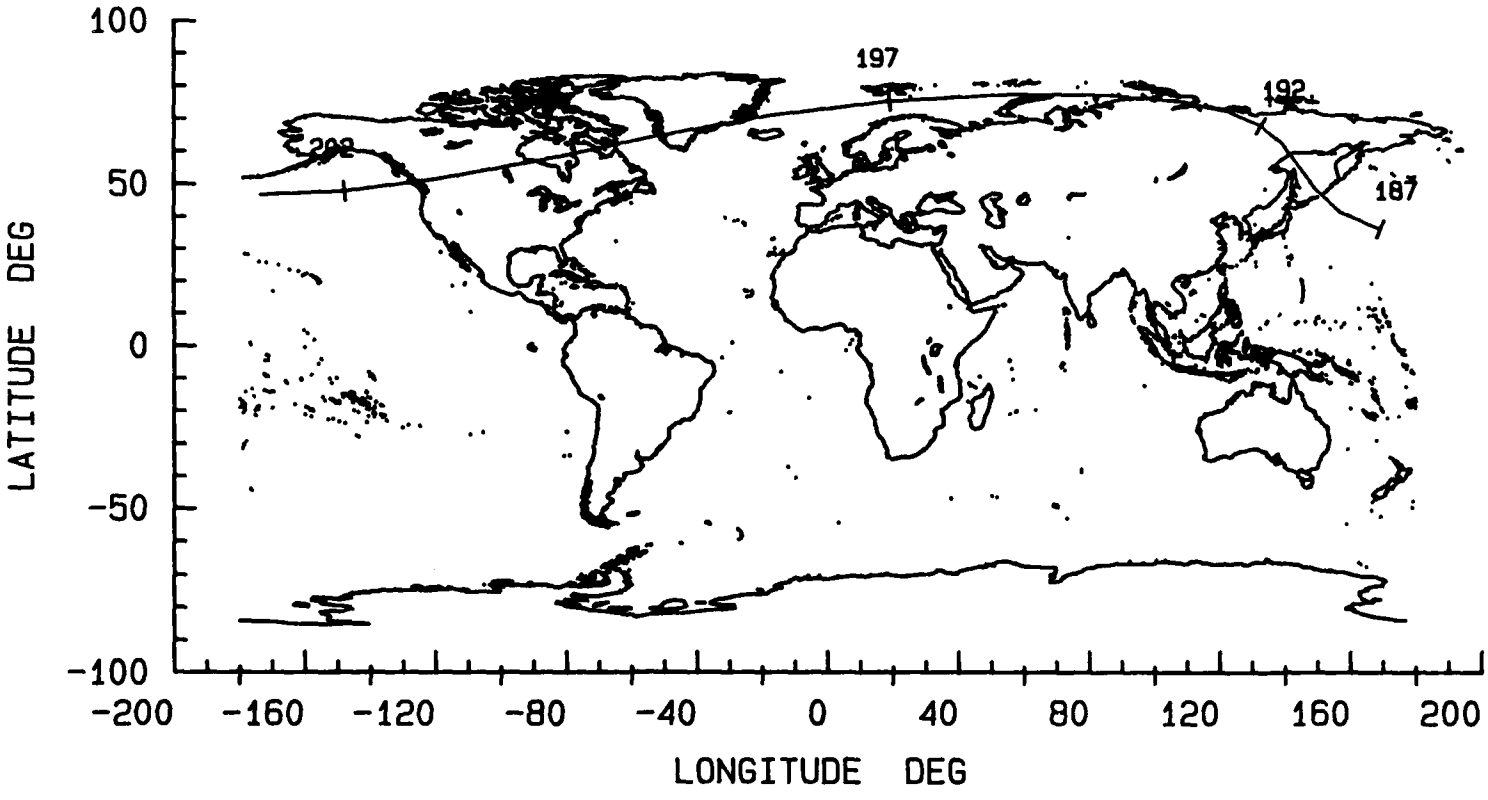

Figure 2.3–48. Super-Pressure Balloon Drift Pattern at 120,000 ft Altitude: Day 187 through Day 203 (Jul. 6— Jul. 22)

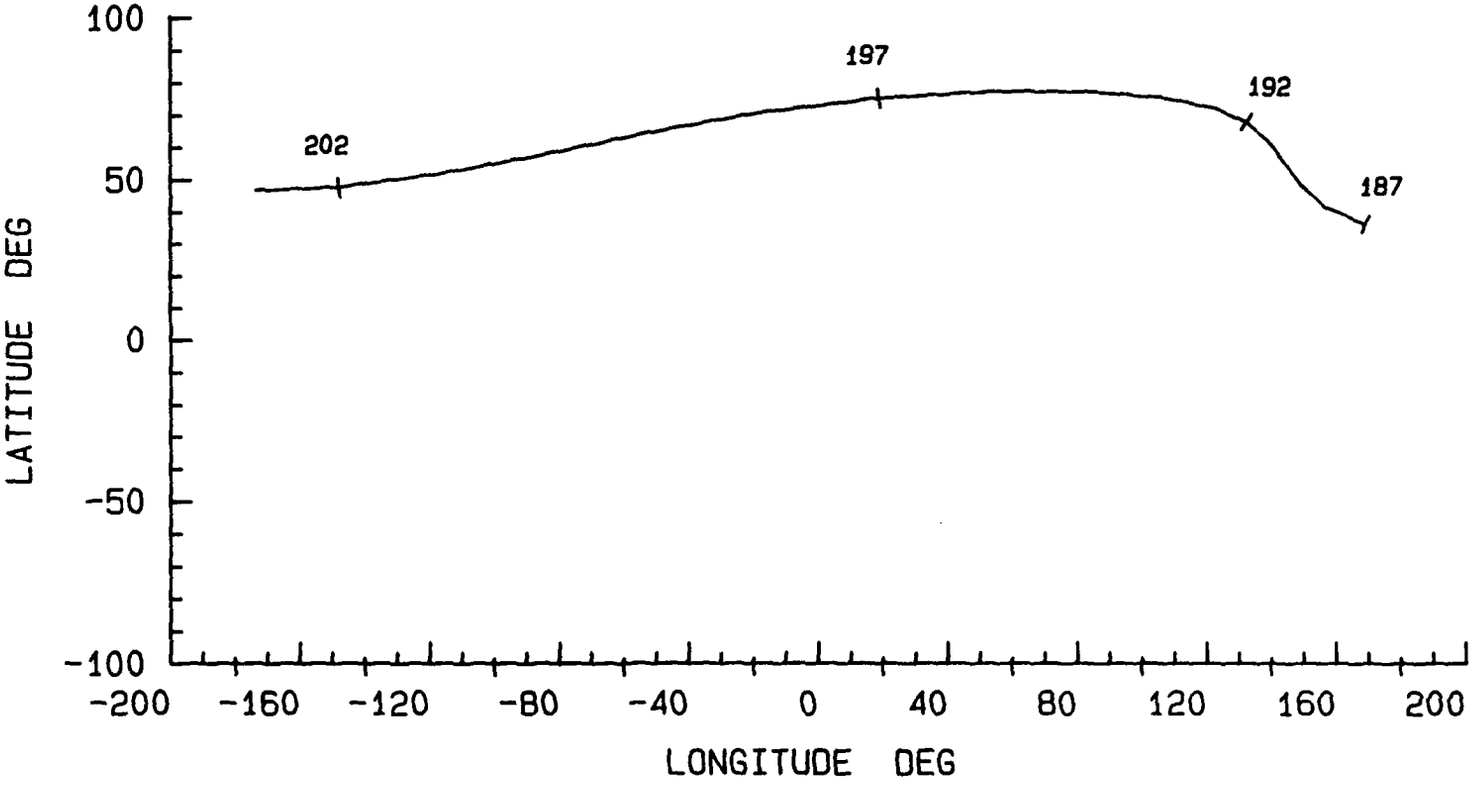

Figure 2.3–49. Super-Pressure Balloon Drift Pattern at 120,000 ft Altitude: Day 187 through Day 203 (Jul. 6— Jul. 22)

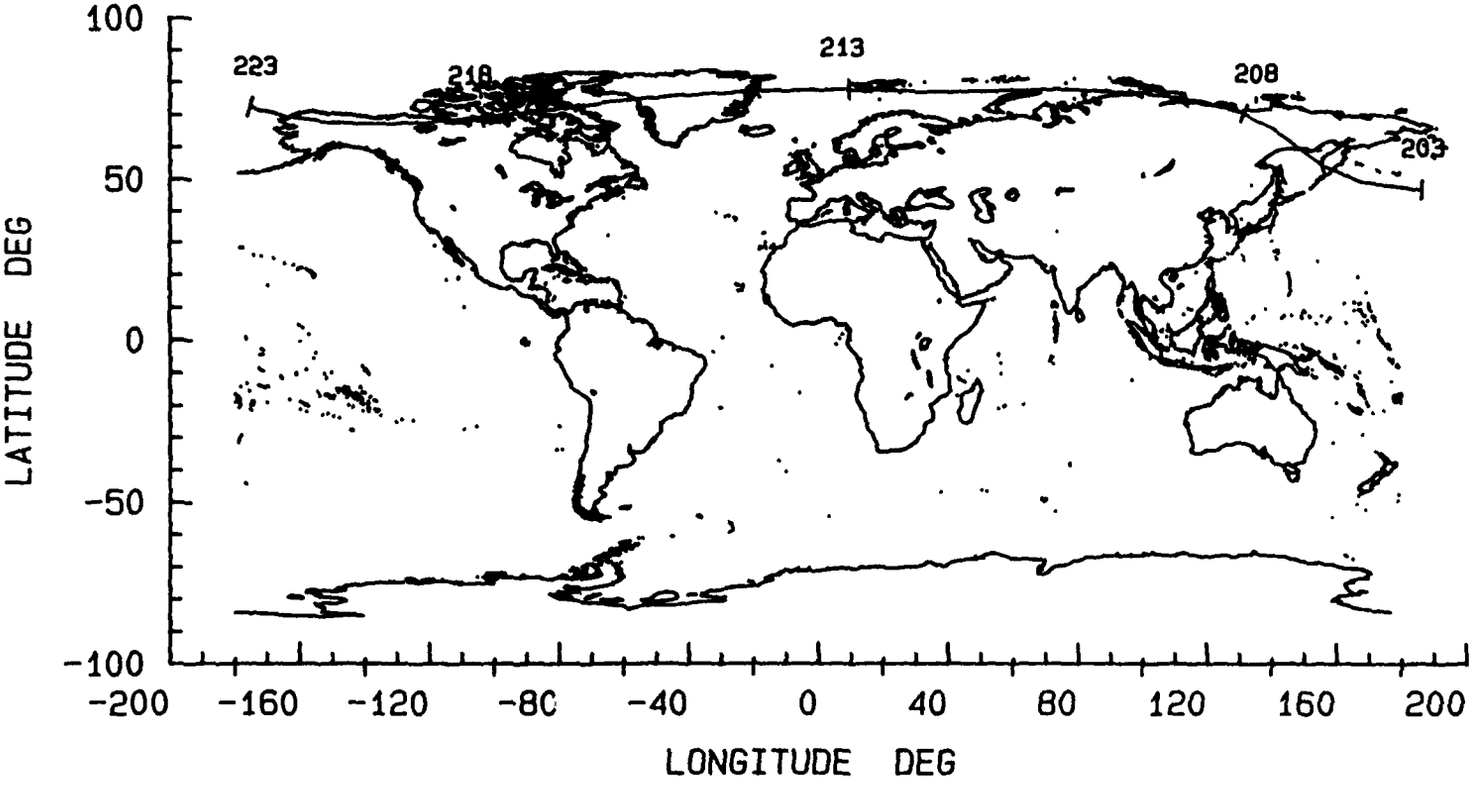

Figure 2.3–50. Super-Pressure Balloon Drift Pattern at 120,000 ft Altitude: Day 203 through Day 223 (Jul. 22— Aug 11)

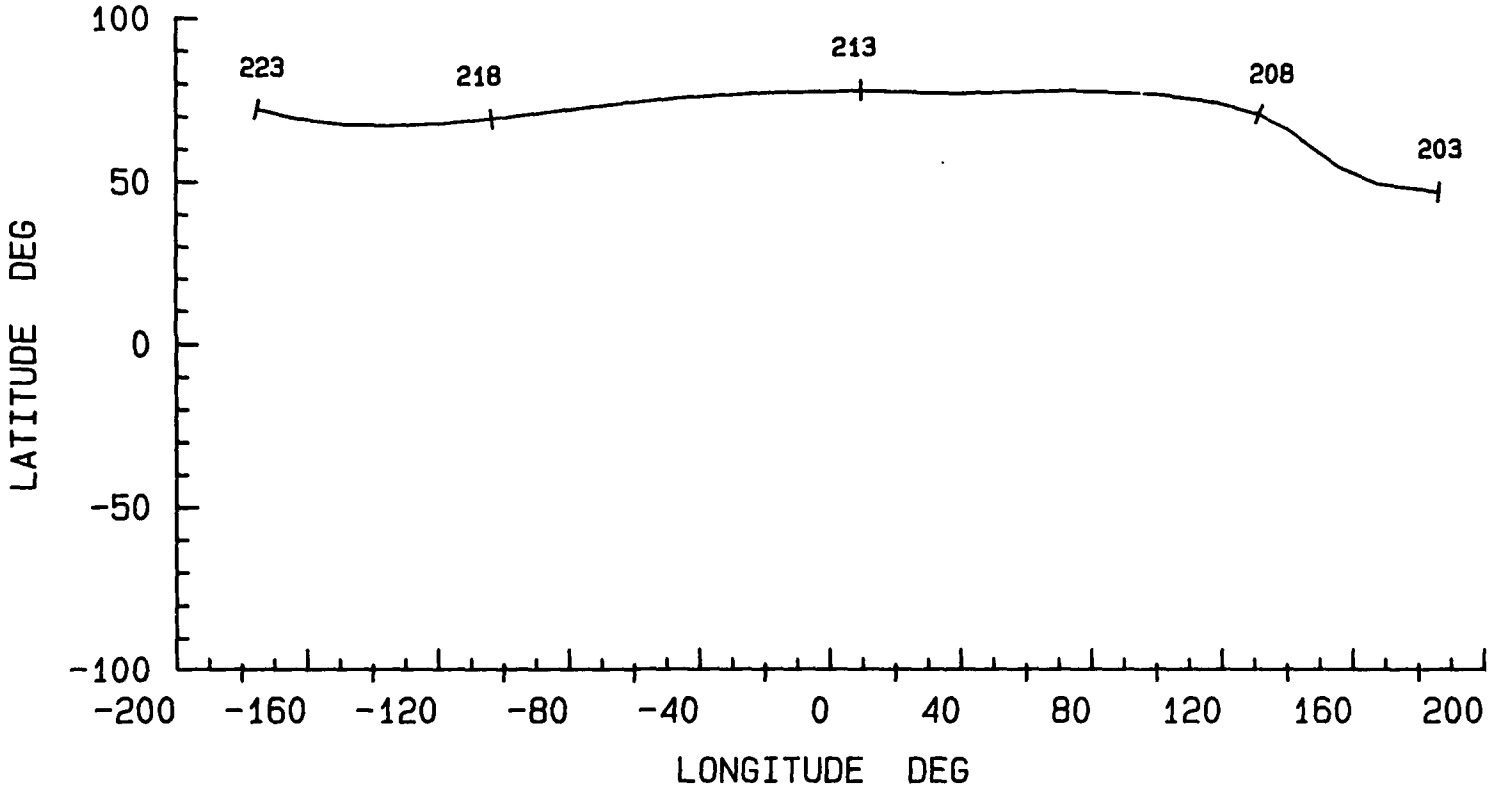

Figure 2.3–51. Super-Pressure Balloon Drift Pattern at 120,000 ft Altitude: Day 203 through Day 223 (Jul. 22— Aug 11)

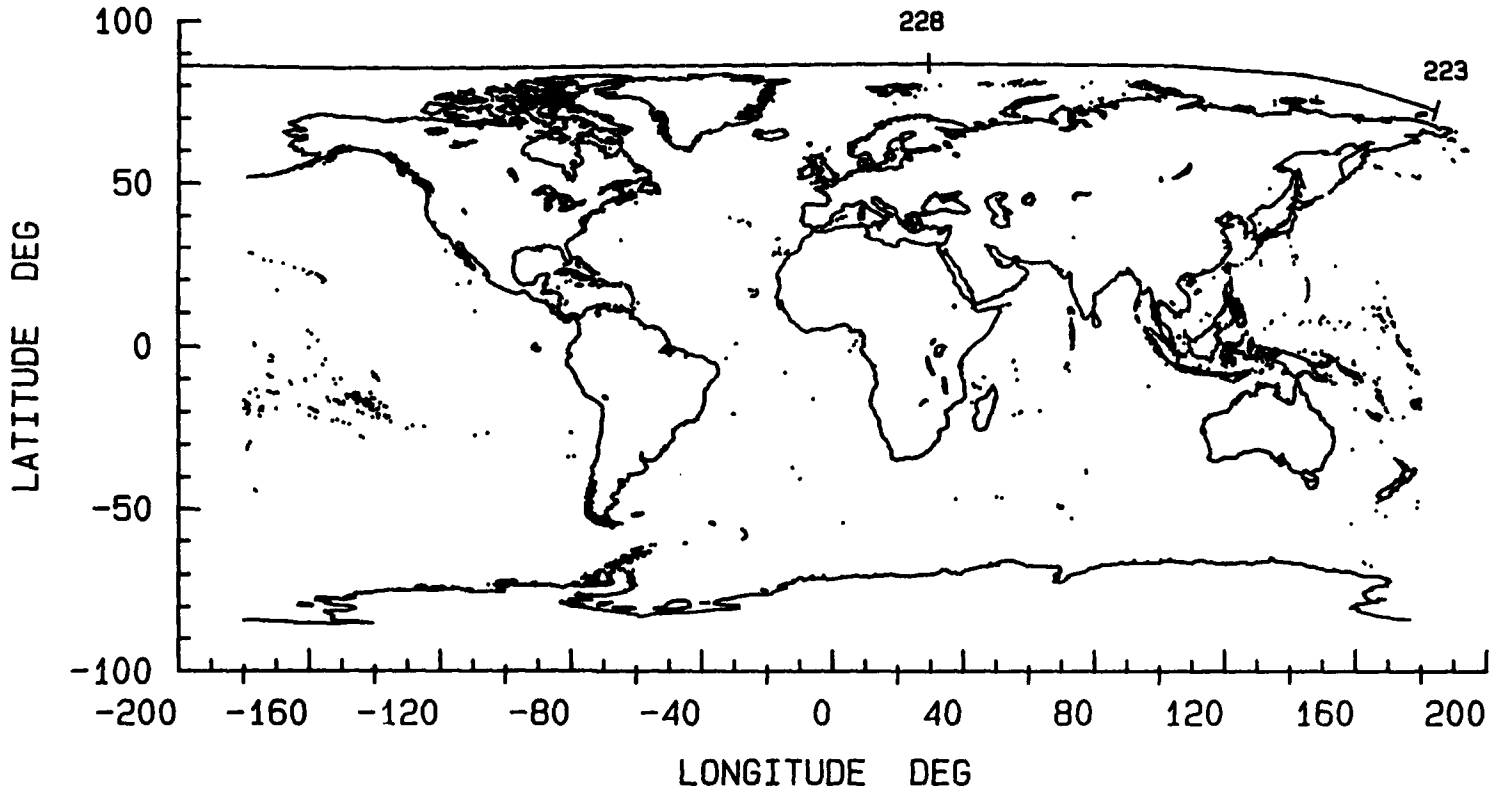

Figure 2.3–52. Super-Pressure Balloon Drift Pattern at 120,000 ft Altitude: Day 223 through Day 232 (Aug 11 — Aug 20)

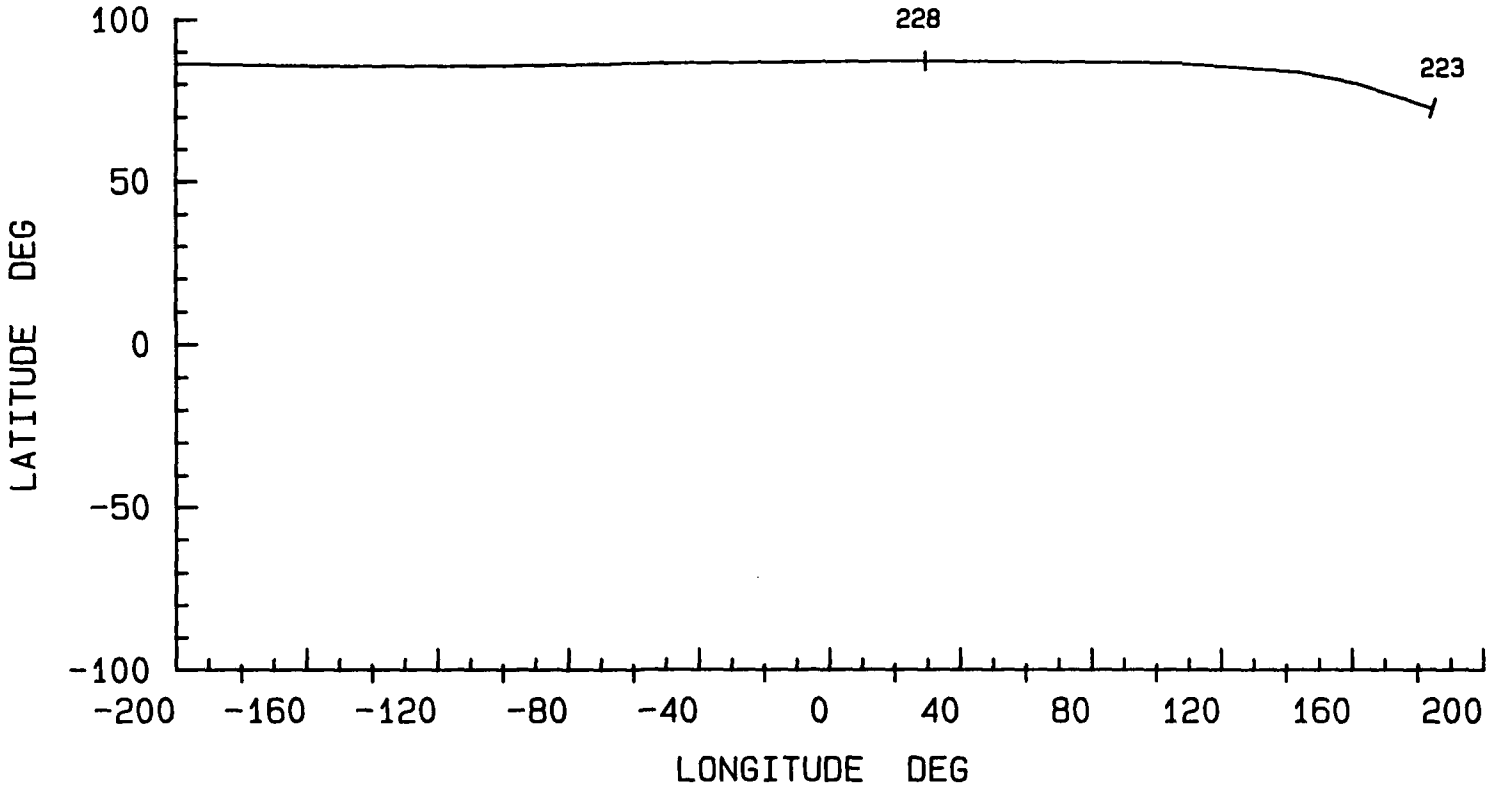

Figure 2.3–53. Super-Pressure Balloon Drift Pattern at 120,000 ft Altitude: Day 223 through Day 232 (Aug 11 — Aug 20)

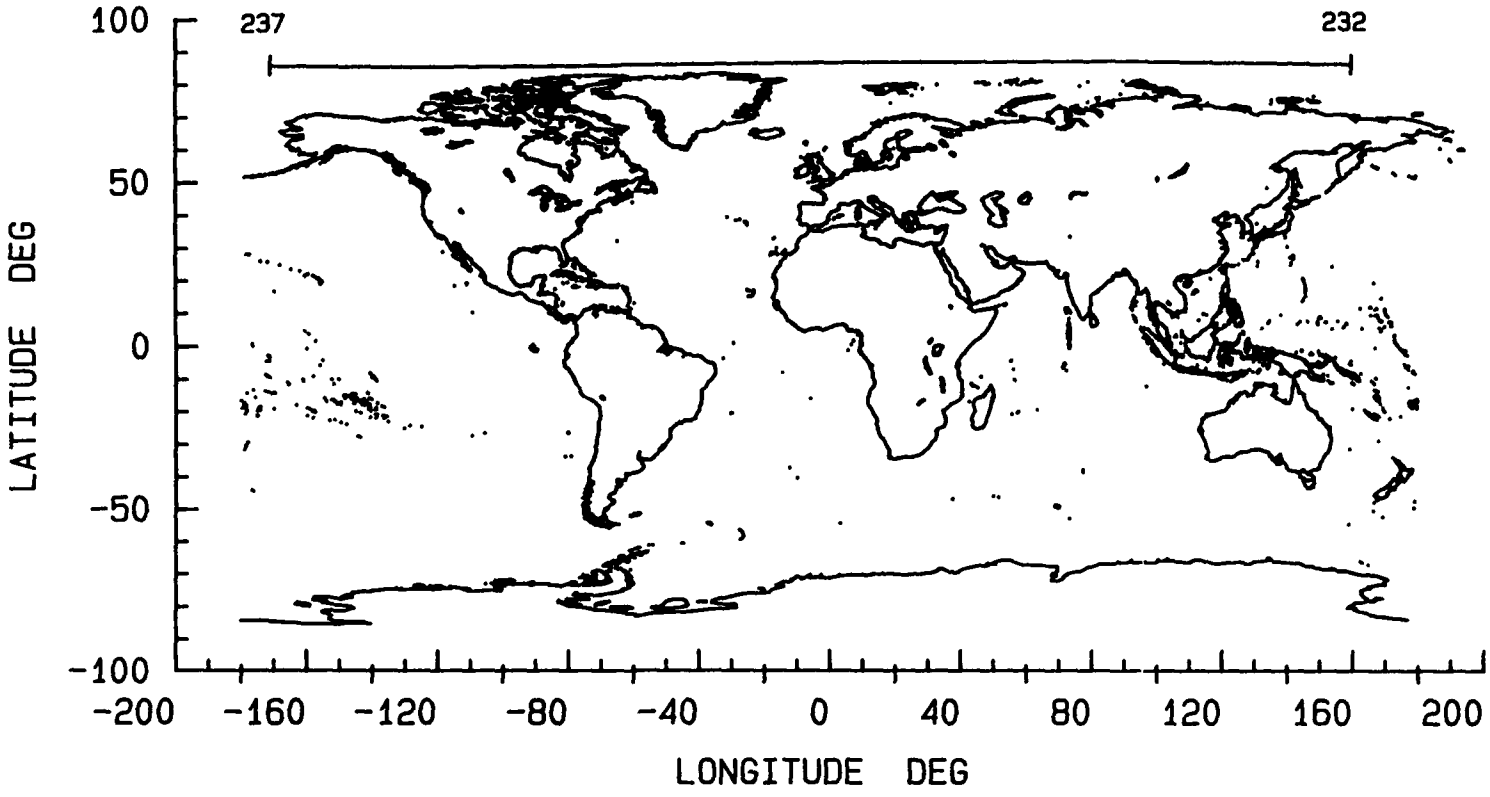

Figure 2.3–54. Super-Pressure Balloon Drift Pattern at 120,000 ft Altitude: Day 232 through Day 237 (Aug 20 — Aug 25)

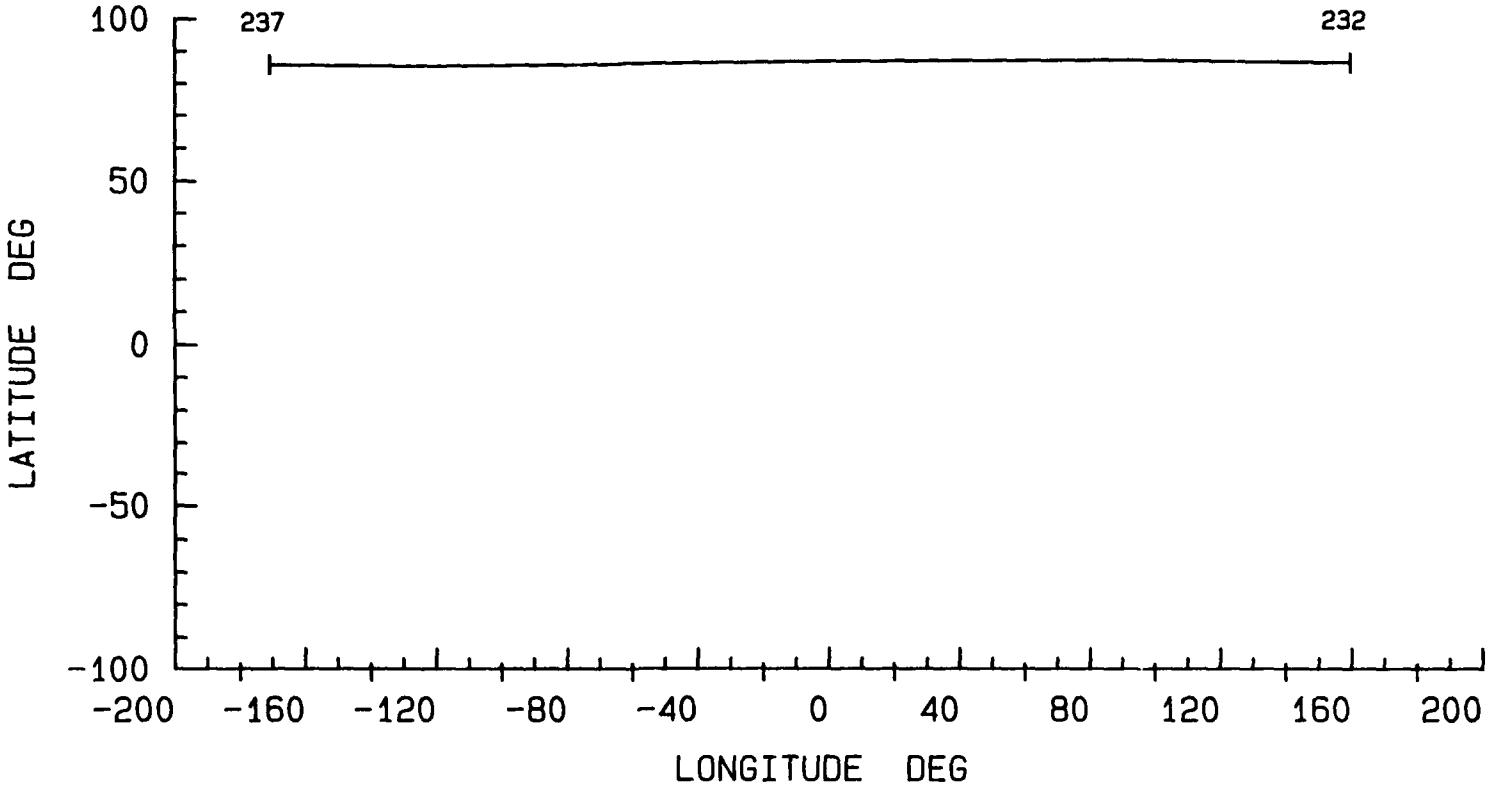

Figure 2.3–55. Super-Pressure Balloon Drift Pattern at 120,000 ft Altitude: Day 232 through Day 237 (Aug 20 — Aug 25)

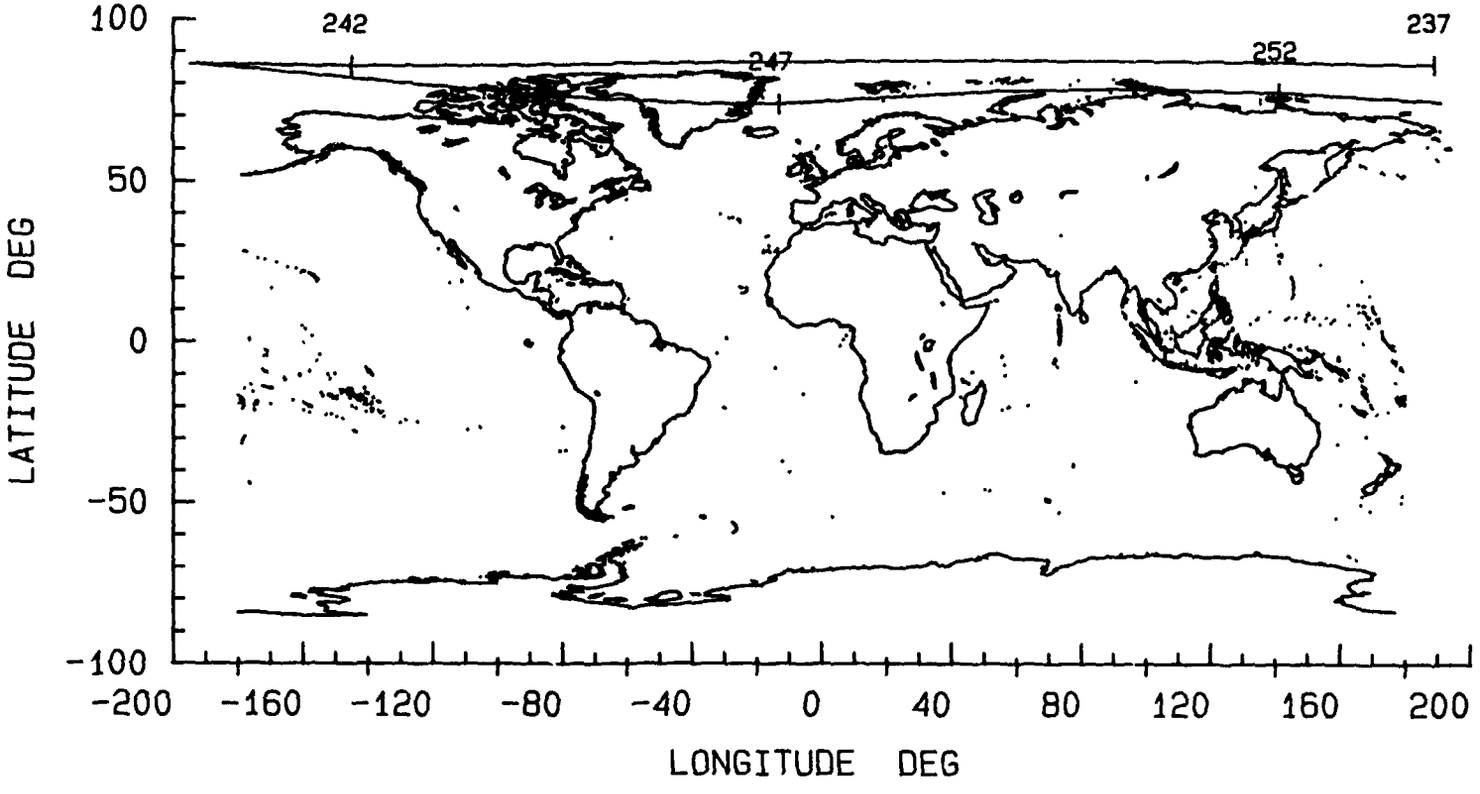

Figure 2.3–56. Super-Pressure Balloon Drift Pattern at 120,000 ft Altitude: Day 237 through Day 253 (Aug 25 — Sep 10)

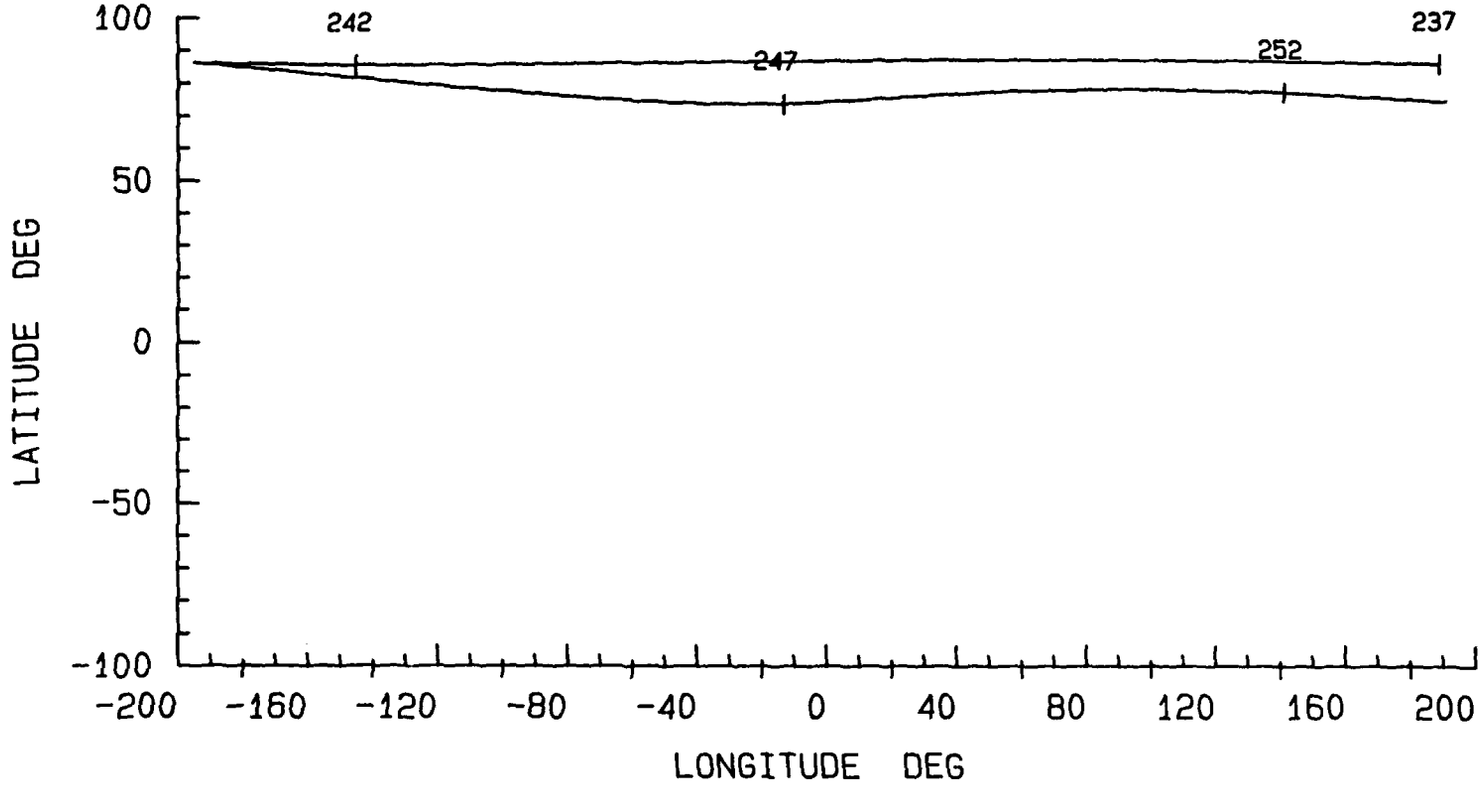

Figure 2.3–57. Super-Pressure Balloon Drift Pattern at 120,000 ft Altitude: Day 237 through Day 253 (Aug 25 — Sep 10)

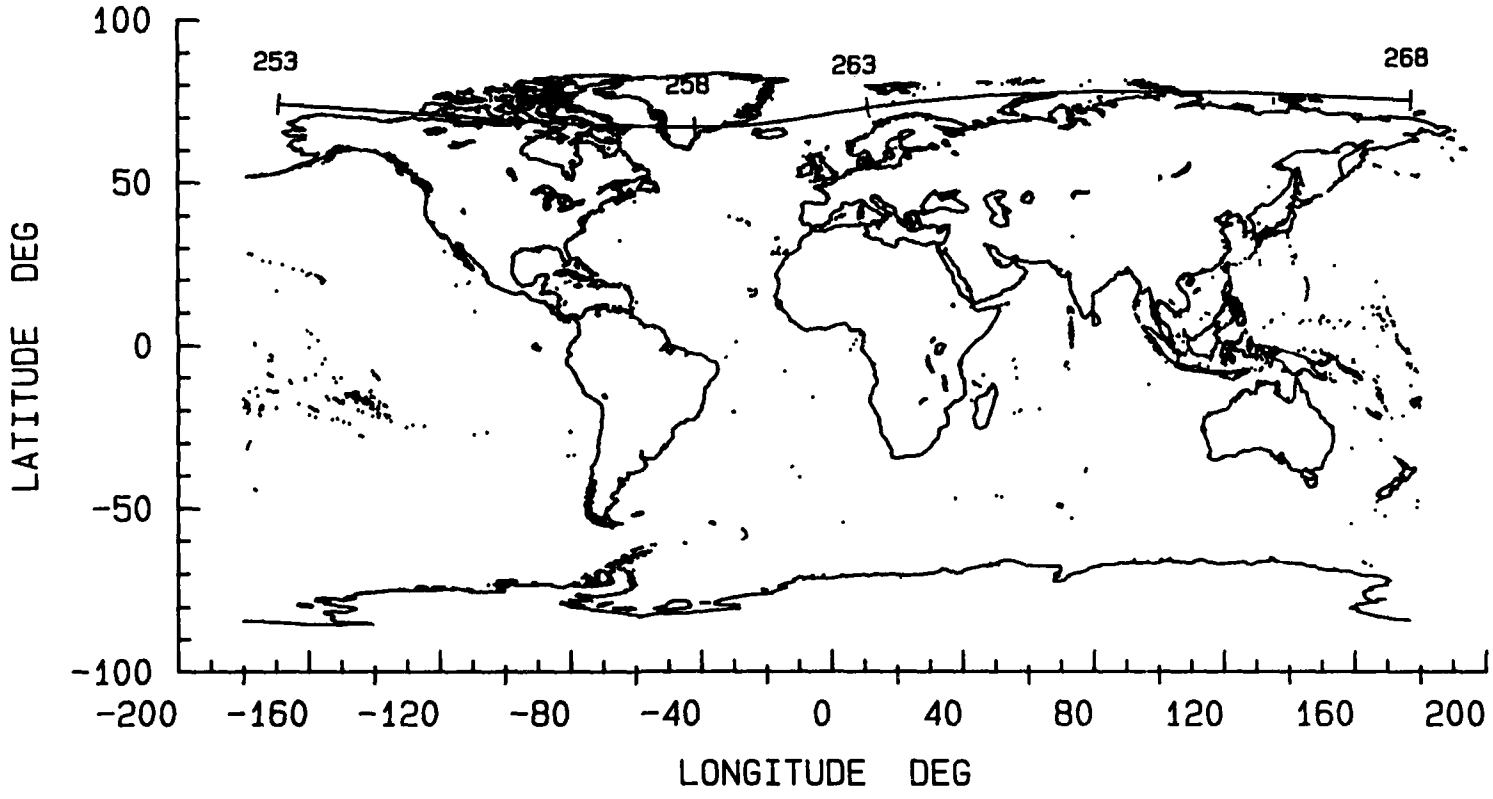

Figure 2.3–58. Super-Pressure Balloon Drift Pattern at 120,000 ft Altitude: Day 253 through Day 268 (Sep 10 — Sep 25)

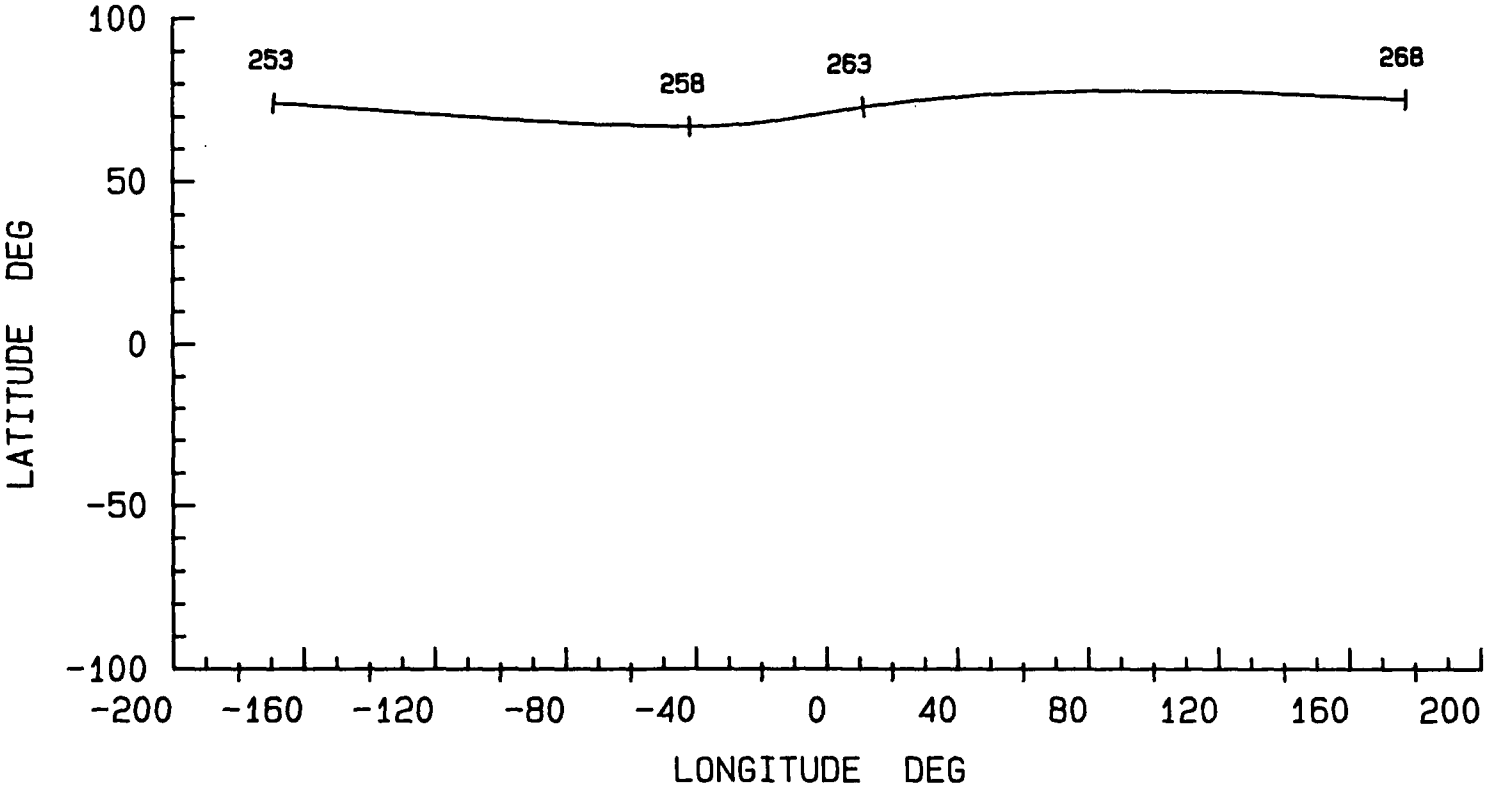

Figure 2.3–59. Super-Pressure Balloon Drift Pattern at 120,000 ft Altitude: Day 253 through Day 268 (Sep 10 — Sep 25)

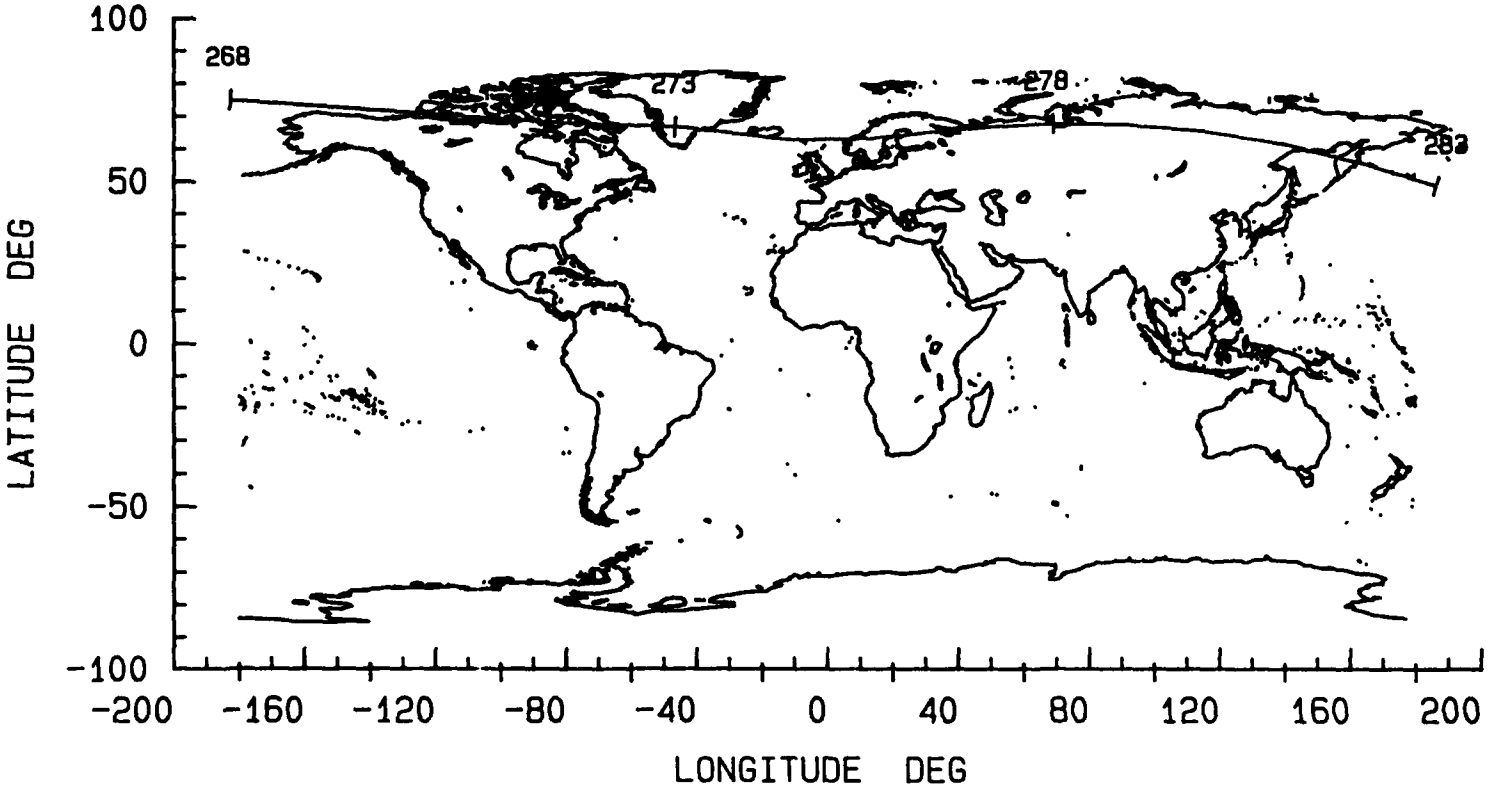

Figure 2.3–60. Super-Pressure Balloon Drift Pattern at 120,000 ft Altitude: Day 268 through Day 283 (Sep 25 — Oct 10)

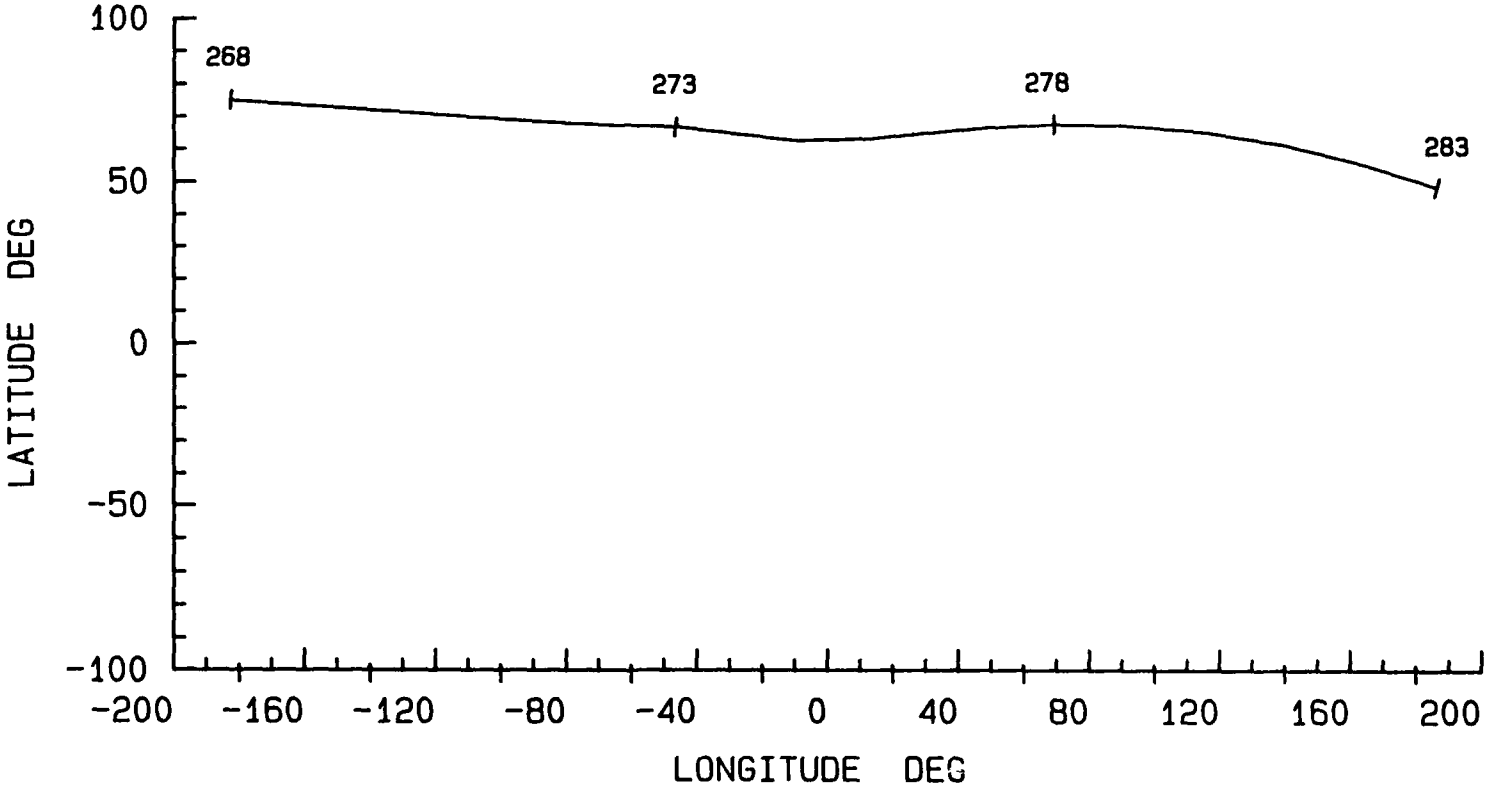

Figure 2.3–61. Super-Pressure Balloon Drift Pattern at 120,000 ft Altitude: Day 268 through Day 283 (Sep 25 — Oct 10)

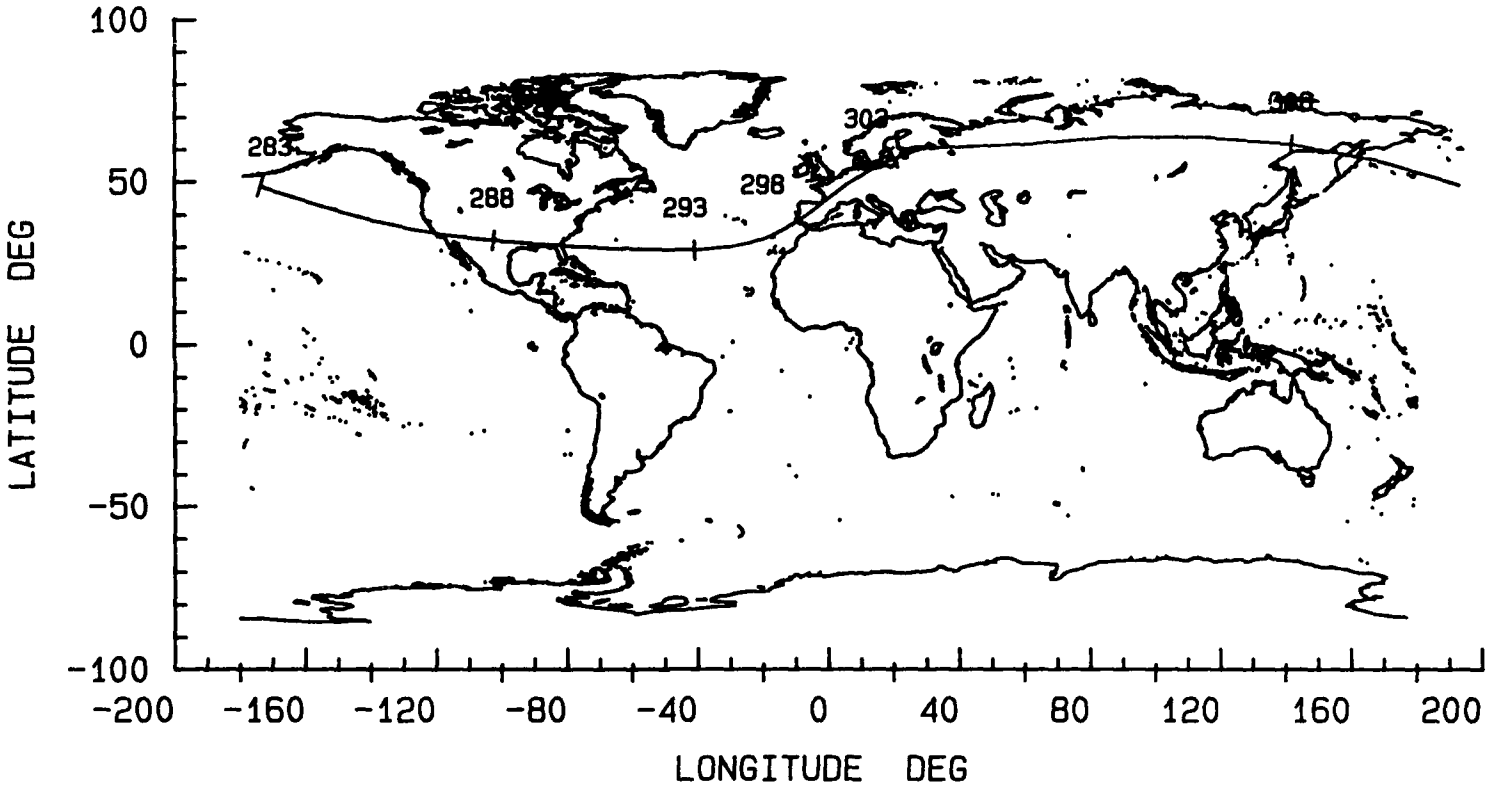

Figure 2.3–62. Super-Pressure Balloon Drift Pattern at 120,000 ft Altitude: Day 283 through Day 310 (Oct 10 — Nov 6)

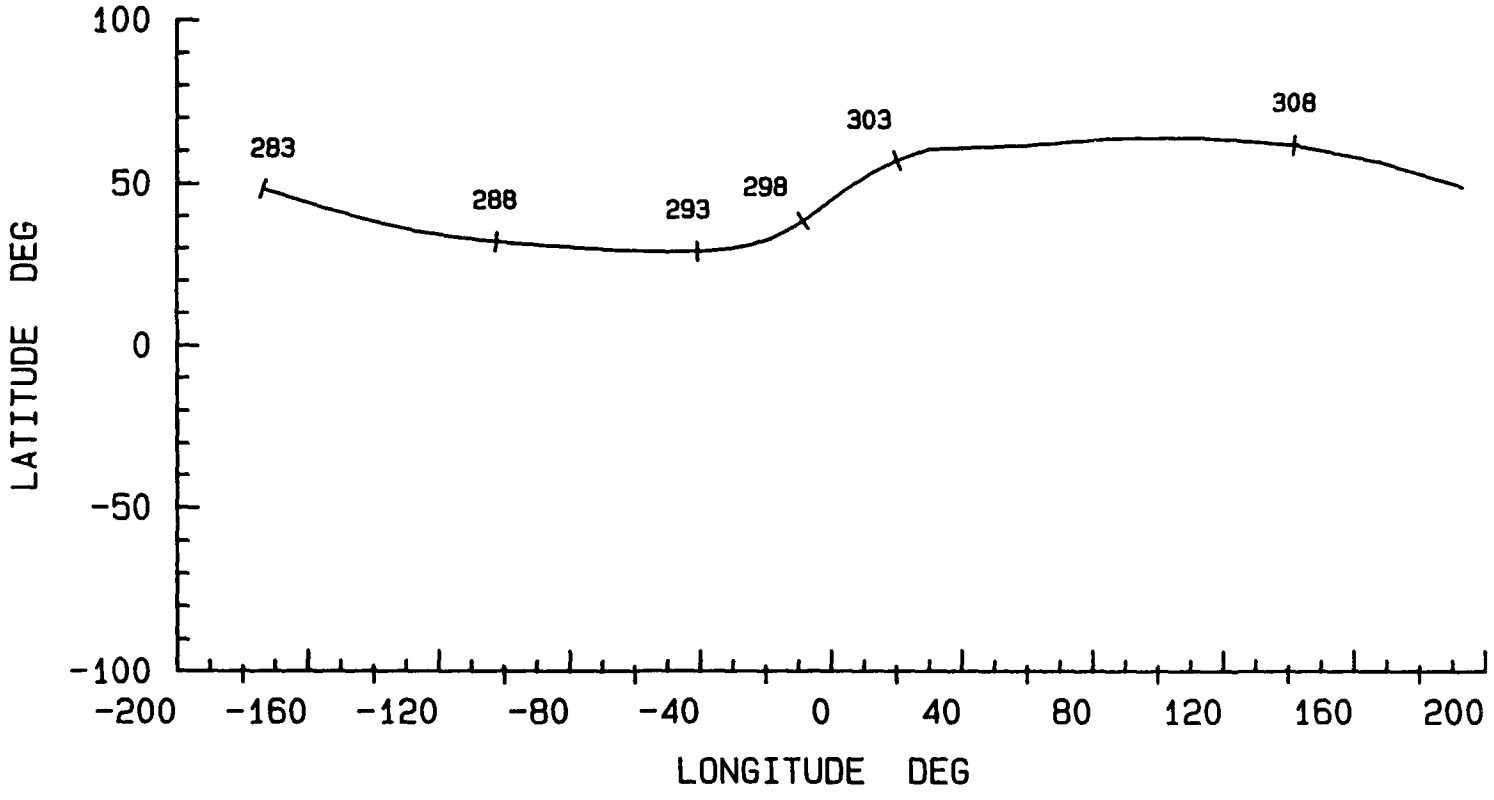

Figure 2.3–63. Super-Pressure Balloon Drift Pattern at 120,000 ft Altitude: Day 283 through Day 310 (Oct 10 — Nov 6)

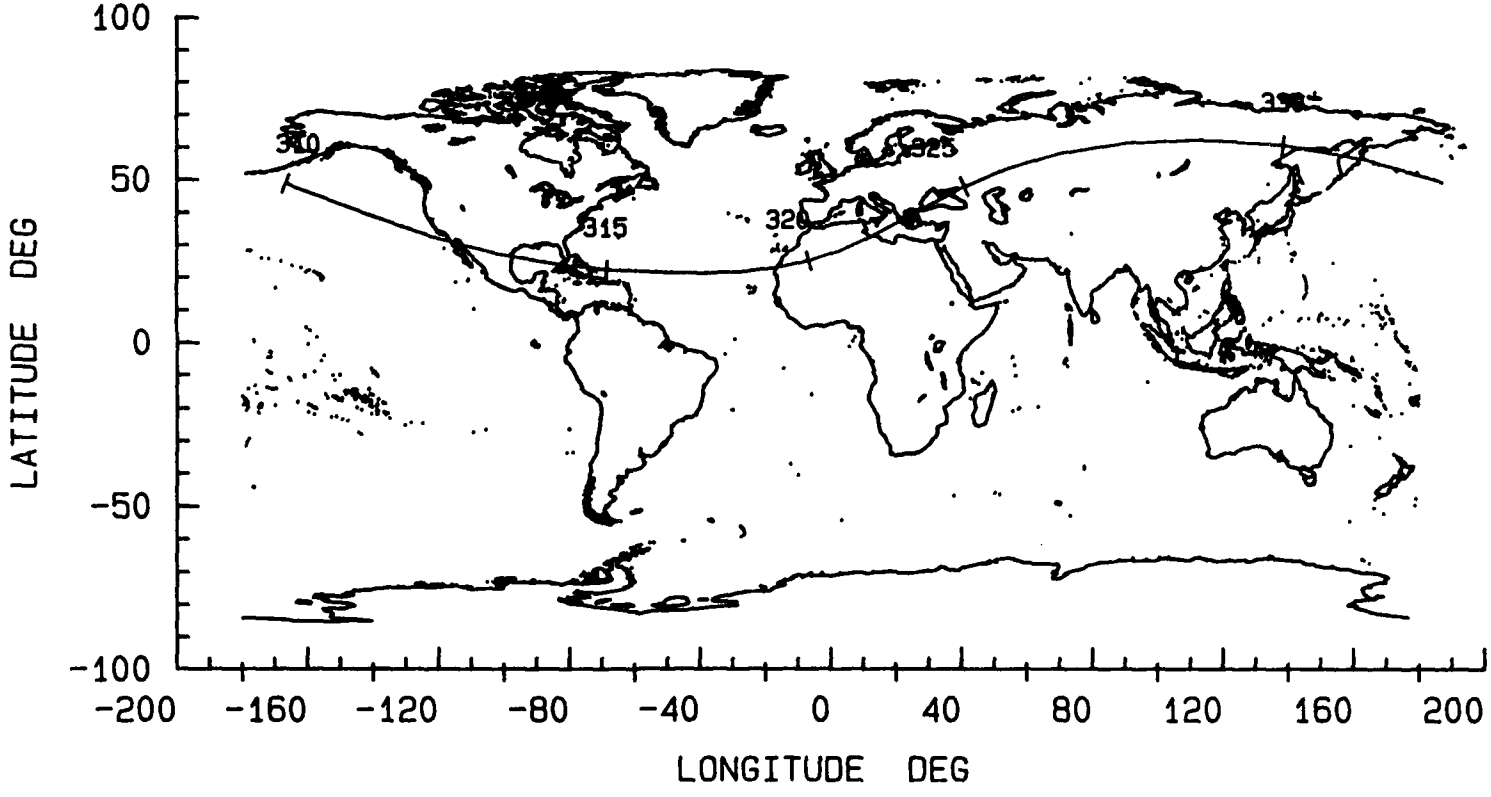

Figure 2.3–64. Super-Pressure Balloon Drift Pattern at 120,000 ft Altitude: Day 310 through Day 332 (Nov 6 — Nov 28)

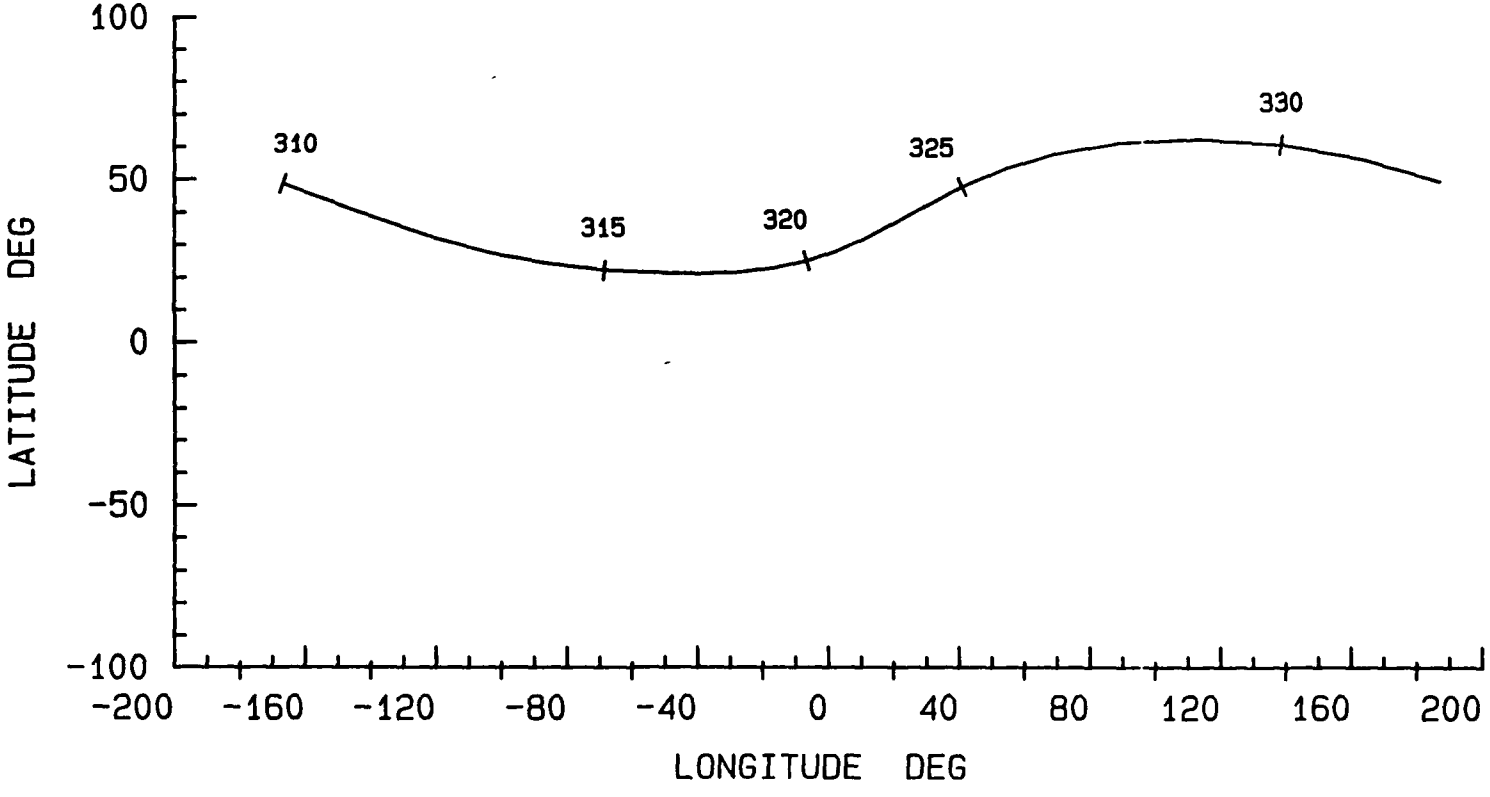

Figure 2.3–65. Super-Pressure Balloon Drift Pattern at 120,000 ft Altitude: Day 310 through Day 332 (Nov 6 — Nov 28)

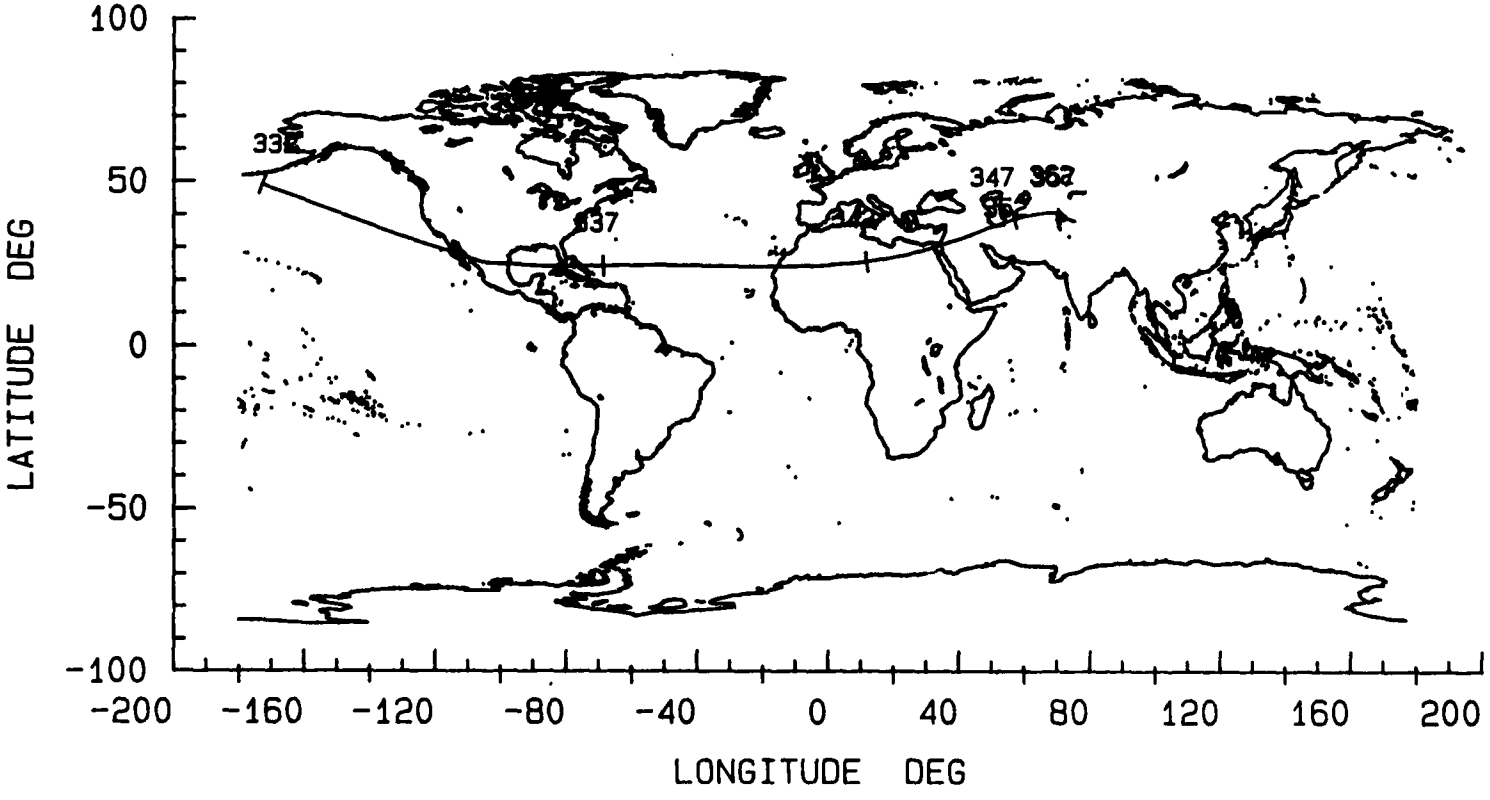

Figure 2.3–66. Super-Pressure Balloon Drift Pattern at 120,000 ft Altitude: Day 332 through Day 365 (Nov 28 — Dec 31)

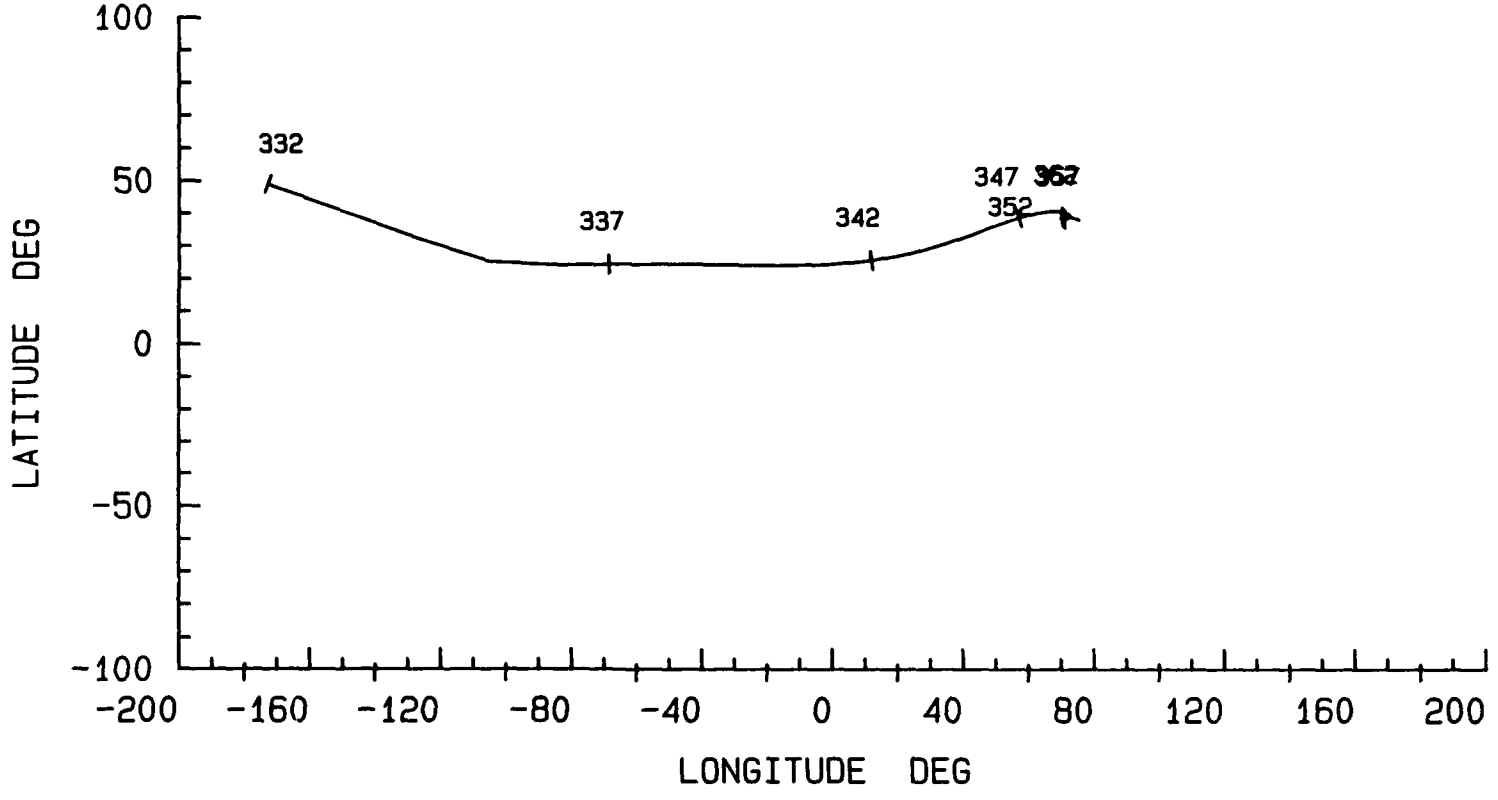

Figure 2.3–67. Super-Pressure Balloon Drift Pattern at 120,000 ft Altitude: Day 332 through Day 365 (Nov 28 — Dec 31)

3.0 CONCLUSIONS

CRC has demonstrated a capability to produce simulated balloon drift patterns using digital computer simulation techniques. Where possible, available balloon flight test data was used for comparison with the simulation results, showing similar trends with reasonable agreement.

The models used and developed for this effort proved adequate but not optimal. A particular need exists for a closer coupling between GRAM and MDOF in order to reduce potential inaccuracies which may arise from using a single wind profile over the extent of a balloon's drift. More tightly integrated BPDS models would also serve to reduce the effort associated with the production of a single drift pattern, whether it is a 24-hour or 1-year mission.

4.0 REFERENCES

1. Morris, A.L., Scientific Ballooning Handbook, NCAR-TN/IA-99, May, 1975.

2. Kreith, F., "Thermal Design of High-Altitude Balloons and Instrument Packages," Journal of Heat Transfer, Trans. ASME, Series C, Vol. 92, Aug. 1970, pp. 307-332.

3. Carlson, L.A, and Horn, W.J., "A Unified Thermal and Vertical Trajectory Model for the Prediction of High Altitude Balloon Performance," Texas Engineering Experiment Station Report TAMRF-4217-81-01, June, 1981.

4. Horn, W.J., and Carlson, L.A, "THERMTRAJ: A FORTRAN Program to Compute the Trajectory and Gas and Film Temperatures of Zero Pressure Balloons," Texas Engineering Experiment Station Report TAMRF-4217-81-02, June, 1981.

5. Dwyer, J.F., "Factors Affecting the Vertical Motion of a Zero-Pressure, Polyethylene, Free Balloon," AFGL-TR-85-0130, May, 1985.

6. Justus, C.G., Fletcher, G.R., Gramling, F.E., and Pace, W.B., "The NASA/MSFC Global Reference Atmosphere Model - MOD 3 (with Spherical Harmonic Wind Model)," NASA CR-3256, 1980.

7. Hoerner, S.F., Aerodynamic Drag, published by the author, 1965.

APPENDIX A

BALLOON MODEL FORTRAN SOURCE CODE

```
001       SUBROUTINE BUOY
002 C
003 C=================================================================C
004 C                                                                 C
005 C                                        REVISION DATE - 16-JAN-1989  C
006 C                                        -------------------------  C
007 C         PURPOSE                                                 C
008 C         . BUOYANT FORCE MODEL                                   C
009 C                                                                 C
010 C         PROGRAM ROUTINES                                        C
011 C         . NONE                                                  C
012 C                                                                 C
013 C         UTILITY ROUTINES                                        C
014 C         . TLU1EI - SINGLE VARIABLE TABLE LOOK-UP                C
015 C         . VMAG3  - VECTOR (3) MAGNITUDE                         C
016 C                                                                 C
017 C         SYSTEM LIBRARIES                                        C
018 C         . (NONE)                                                C
019 C                                                                 C
020 C=================================================================C
021 C
022       DIMENSION ID ( 9999 )
023 C
024       PARAMETER ( AIRMW = 28.97 )
025 C
026 C:::::::::::::::::::::::::::::::::::::::::::::::::::::::::::::::::C
027 C
028 C**  SIMULATION  COMPUTATIONAL  COMMON   * * * *
029 C
030       COMMON / DCOM   /  D ( 9999 ),  V ( 5000 ),  C ( 100 ), JD ( 800 )
031 C
032 C**  UPDATE  COMMON  * * * * * * * * * * * * * * *
033 C
034       COMMON / UCOM   /  UP ( 200 )
035 C
036 C:::::::::::::::::::::::::::::::::::::::::::::::::::::::::::::::::C
037 C
038       EQUIVALENCE ( D(   1),ID(1) )
039 C
040       EQUIVALENCE ( D(  66),RGAS  ),( D(  67),DIAMAX),( D(  68),GASMW )
041       EQUIVALENCE ( D(  69),GSFACT)
042 C
043       EQUIVALENCE ( V(   2),DT    ),( V(   5),TABS  ),( V(   7),X3600 )
044       EQUIVALENCE ( V(  51),GXI   ),( V(  52),GYI   ),( V(  53),GZI   )
045       EQUIVALENCE ( V(  69),PRESS ),( V(  70),DENS  ),( V(  71),DYNP  )
046       EQUIVALENCE ( V(  96),AREF  ),( V( 101),TDATA ),( V( 115),TTLU  )
047       EQUIVALENCE ( V( 126),QS    ),( V( 214),TSUBA )
048       EQUIVALENCE ( V( 243),XDWT  ),( V( 244),XDTWT )
049       EQUIVALENCE ( V( 246),FBUOYX),( V( 247),FBUOYY),( V( 248),FBUOYZ)
050       EQUIVALENCE ( V( 245),FBUOYT)
051       EQUIVALENCE ( V( 267),BPRESS),( V( 268),SPDIAM),( V( 269),GASWT )
052       EQUIVALENCE ( V( 270),FLIFT )
```

```
053 C
054       EQUIVALENCE ( C(   1),PI    ),( C(  65),GO    )
055       EQUIVALENCE ( C(  81),GMASS ),( C(  82),DEXPEL),( C(  83),VOLUME)
056       EQUIVALENCE ( C(  84),VOLMAX),( C(  85),GIMAG ),( C(  86),TMP6  )
057       EQUIVALENCE ( C(  87),WEIGHT),( C(  88),WGHTO ),( C(  89),GASOUT)
058       EQUIVALENCE ( C(  90),GMAX  )
059 C
060       EQUIVALENCE (ID(   2),IBUOY )
061 C
062       EQUIVALENCE (JD(  55),IRWGT ),(JD( 438),ICWGT )
063 C
064       SAVE
065 C
066 C-----------------------------------------------------------------------C
067 C
068 C     CALCULATE MAGNITUDE OF INERTIAL GRAVITY VECTOR
069 C
070       CALL VMAG3 ( GXI, GIMAG, TMP6 )
071 C
072 C     FIND VOLUME OF LIFTING GAS AT CURRENT AMBIENT PRESSURE AND
073 C     TEMPERATURE USING IDEAL GAS LAW: V = MRT/P
074 C
075       GMASS  = GASWT / GO
076       VOLUME = GMASS * RGAS * TSUBA / PRESS
077 C
078 C     SET INTERNAL BALLOON PRESSURE EQUAL TO AMBIENT PRESSURE
079 C
080       BPRESS = PRESS
081 C
082 C     CALCULATE CURRENT DIAMETER ASSUMING SPHERICAL SHAPE
083 C
084       SPDIAM = ( 6.0 * VOLUME / PI ) ** 0.333333
085 C
086 C     IBUOY=1 -> ZERO-PRESSURE BALLOON
087 C
088       IF (IBUOY.EQ.1) THEN
089 C
090 C        CALCULATE FREE LIFT FOR ZERO-PRESSURE BALLOON; FIRST,
091 C        COMPUTE INDEPENDENT VARIABLE FOR TABLE LOOK UP TO GET
092 C        CURRENT WEIGHT EXCLUDING WEIGHT OF LIFTING GAS
093 C
094          TTLU = TABS - TDATA
095          TMP6 = TTLU*XDIWT
096          CALL TLU1EI (TMP6, D(IRWGT), ICWGT, WGHTO)
097          WEIGHT = WGHTO*XDWT/GO
098 C
099          FLIFT = 100.0 * ((GMASS * (AIRMW/GASMW - 1.0)) / WEIGHT -1.0 )
100 C
101 C        COMPARE THE IDEAL-GAS/SPHERICAL DIAMETER TO THE MAXIMUM
102 C        EFFECTIVE SPHERICAL DIAMETER
103 C
104          IF (SPDIAM.GT.DIAMAX) THEN
105             VOLMAX = ( PI / 6.0 ) * DIAMAX**3
106             GMAX   = (PRESS * VOLMAX) / (RGAS * TSUBA)
```

```
C
            IF (GMASS.GT.(GMAX*GSFACT)) THEN
C
C           CALCULATE THE MASS EXPULSION RATE FOR EXCESS LIFTING GAS
C
               DEXPEL = (GMASS - GMAX*GSFACT) / (DT * 8.0)
               GASOUT = DEXPEL * DT
               GMASS  = GMASS - GASOUT
               GASWT  = GMASS * GO
            ENDIF
C
            VOLUME = VOLMAX
            BPRESS = GMASS * RGAS * TSUBA / VOLUME
         ENDIF
C
C     IBUOY=2 -> SUPERPRESSURE BALLOON
C
      ELSE IF (IBUOY.EQ.2) THEN
C
C        COMPARE THE IDEAL-GAS/SPHERICAL DIAMETER TO THE MAXIMUM
C        EFFECTIVE SPHERICAL DIAMETER
C
         IF (SPDIAM.GT.DIAMAX) THEN
            SPDIAM = DIAMAX
            VOLUME = ( PI / 6.0 ) * SPDIAM**3
            BPRESS = GMASS * RGAS * TSUBA / VOLUME
         ENDIF
C
      ENDIF
C
C     COMPUTE TOTAL BUOYANT FORCE (WEIGHT OF THE DISPLACED FLUID)
C
      FBUOYT = VOLUME * DENS * GIMAG
C
C     COMPUTE AERODYNAMIC REFERENCE AREA AND QS PRODUCT
C
      AREF = ( PI / 4.0 ) * SPDIAM**2
      QS   = DYNP * AREF
C
C     DECOMPOSE TOTAL BUOYANT FORCE INTO BODY-REFERENCE COMPONENTS GIVEN
C     THAT BALLOON X-AXIS IS FORCED TO BE ORIENTED ALONG GRAVITY VECTOR
C
      FBUOYX = FBUOYT
      FBUOYY = 0.0
      FBUOYZ = 0.0
C
      RETURN
      END
```